UNIVERSITY OF CALABRIA
Department of Civil Engineering
MIUR - Ministero dell'istruzione, dell'Università e della Ricerca

PhD Thesis in Materials and Structures Engineering of

ROSAMARIA CODISPOTI

MECHANICAL PERFORMANCE OF NATURAL FIBER-REINFORCED COMPOSITES FOR THE STRENGTHENING OF ANCIENT MASONRY

Section: Materials and Structures Engineering
XXVI Cycle (2010 - 2013) - S.S.D. ICAR 08 - Structural Mechanics

Coordinator: Prof. Renato S. Olivito
Tutor: Prof. Renato S. Olivito
Prof. Daniel V. Oliveira

CONTENTS

ABSTRACT

The present PhD Thesis was developed thanks to the collaboration between the Civil Engineering Departments of University of Calabria (Italy) and University of Minho (Portugal). The main topic of this work concerned the study of natural fiber-reinforced composites. The study is composed of a vast experimental part, carried out in the Civil Engineering Laboratory and Fibrous Materials Laboratory at University of Minho, and a numerical part, with the purpose of analyzing the performance of natural fiber-reinforced polymer (NFRP) and grout (NFRG) applied to ancient masonry structures.

Why to use natural fiber based-composites? Why to strengthen ancient masonry structures with NFRP/NFRG? These two questions were the basis of this research project. First of all, the sustainable development, the renewable technologies and the low environmental impact represent key factors of the building system, especially regarding the production of construction materials. But the most important aspect is that this trio can be obtained at low cost, by using eco-friendly materials. Secondly, masonry is a material with a very low tensile strength, consequently also natural materials can increase its performance. The common carbon and glass fibers would increase greatly the tensile strength of masonry structures, but they present many disadvantages related to environmental pollution during their manufacture or a high energy consumption, necessary for disposal at the end of their life cycle.

After a preliminary study about the classification of all natural fibers and their origins, it was possible to identify flax, hemp, jute and sisal fibers as the natural fibers most utilized in civil engineering applications.

The experimental part of the work was organized in two main parts: experimental tests on composites and their components, and experimental tests on masonry elements strengthened with NFRP and NFRG.In the first part of the experimental program, mechanical characterization tests of matrixes and fibers was done, carrying out compressive and three point bending tests on mortar and tensile tests on resin and fibers. In fact, three different types of matrixes were used to produce composite materials: two thermosetting matrixes, epoxy and polyester resin (NFRP), and a mortar matrix(NFRG). To manufacture the three composites materials, three different manufacturing methods were used: manual lay-up to produce NFRP epoxy-based matrix, vacuum infusion process for NFRP polyester-based matrix and in order to obtain NFRG, some special formworks were used. Moreover, in order to analyze the performance of natural fiber-reinforced composites in terms of maximum load capacity, tensile strength, and Young's modulus, tensile tests were carried out in laboratory.

In the second part of the experimental plan, the bond behavior between composite materials (NFRP-NFRG) and masonry was investigated. For this purpose, pull-out tests, three point bending tests, and single-lap shear bond tests were carried out on masonry clay bricks reinforced externally with natural fiber-based composites. Finally, to get feedback with the current standards, a comparison with the theoretical approach provided by the Italian technical document (DT-200 R1/2012) was made. In addition to the characterization of mechanical properties of NFRP, also physical properties were calculated in terms of weight per unit area (GSM) and density.

In the last part of the research project, a numerical analysis was carried out. In particular three point bending tests were modelled in FE code DIANA, in order to simulate the behavior of unreinforced clay brick and reinforced clay brick with NFRP. The numerical analysis was compared with the experimental results with particular reference to stiffness, maximum load, and failure modes obtained from both cases.

A new fiber placement technology has been studied, the so-called "braiding technology", in order to increase the mechanical properties of the natural non-impregnated fabrics and also of the composite produced with natural fibers.

Keywords: Natural Fibers, Composites, Strengthening, Ancient Masonry, Experimental tests, Numerical models

SOMMARIO

Il lavoro riportato in questa tesi di dottorato è stato sviluppato grazie alla collaborazione tra i dipartimenti di Ingegneria Civile dell'Università della Calabria e dell'University of Minho (Portogallo). L'argomento principale di questo lavoro di tesi è relativo allo studio dei compositi a base di fibre naturali. Il lavoro comprende un'ampia parte sperimentale eseguita presso i laboratori Civil Engineering e Fibrous Materials dell'University of Minho e una parte numerica, sviluppati entrambi allo scopo di analizzare le prestazioni degli NFRP e NFRG applicati, anche, alle strutture in muratura.

A giorno d'oggi, e già da molti anni, sono diversi i campi di applicazione dei materiali compositi costituiti dalle ormai comuni fibre di carbonio e vetro. Allo scopo di questa tesi, l'attenzione è stata focalizzata al campo dell'ingegneria civile, con particolare riguardo all'uso dei materiali naturali in questo settore.

Perché produrre ed usare i materiali compositi a base di fibre naturali? e perché usare questi compositi per rinforzare costruzioni in muratura? Queste sono le due domande alla base del progetto di ricerca. Ciò che risponde a queste domande è principalmente il fatto che, attualmente, lo sviluppo sostenibile, le tecnologie rinnovabili e il ridotto impatto ambientale costituiscono le parole chiavi del sistema costruttivo, specialmente in relazione alla fase di produzione dei materiali edilizi. Ma ciò che risulta, maggiormente, rilevante è che questo trio di fattori può essere

esplicato ed ottenuto a dei costi molto passi, utilizzando materiali ecosostenibili. Un secondo punto non meno importante, anzi fondamentale, è che la resistenza a trazione della muratura come materiale da costruzione, assume dei valori molto bassi rispetto a quelli relativi alla resistenza a compressione. Conseguentemente a ciò anche l'uso dei compositi a base di fibre naturali potrebbe incrementare, è non di poco, le prestazioni meccaniche delle costruzioni in muratura. I comuni materiali compositi realizzati con fibre di carbonio e vetro incrementano di molto le performance di queste strutture, ma a fronte di una serie di svantaggi relativi all'inquinamento ambientale durante la loro fabbricazione o all'impiego di energia non trascurabile, necessaria per lo smaltimento al termine del loro ciclo di vita.

Dopo uno studio preliminare riguardo le origini delle fibre naturali e la loro classificazione, è stato possibile identificare le fibre di lino, canapa, juta e sisal come le fibre maggiormente utilizzate nel campo dell'ingegneria civile. Queste sono fibre di origine vegetale, più in specifico fibre di rafia, le quali sono state largamente esaminate nella parte sperimentale di questo lavoro di tesi.

La parte sperimentale di questo progetto di ricerca è stato suddiviso in due macro fasi: prove sperimentali sui compositi e sui loro componenti, e prove sperimentali su macro-elementi in muratura rinforzati con NFRP e NFRG.

Nella prima parte del programma sperimentale, sono state svolte in laboratorio prove di caratterizzazione meccanica sulle matrici e sulle fibre/tessuti naturali, eseguendo prove di compressione e flessione su tre punti sulla malta e prove di trazione sulla resina. Infatti, sono state utilizzate tre tipologie differenti di matrici: due matrici termoindurenti, resina epossidica e poliestere, e una matrice di origine naturale, malta cementizia. Per produrre le tre tipologie di materiali compositi, sono stati considerati tre differenti metodi di produzione: manual lay-up per produrre NFRP a base di resina epossidica, vacuum infusion process per produrre NFRP a base di poliestere epossidico e sono state utilizzate particolari casseforme in acciaio per costruire i compositi NFRG a base di malta cementizia. Inoltre, allo scopo di analizzare le proprietà meccaniche dei compositi prodotti, in termini di capacità massima di carico, resistenza a trazione e modulo elastico, sono state svolte delle prove sperimentali di trazione in laboratorio.

Nella seconda parte del piano sperimentale, è stato studiato il comportamento dei compositi in relazione al materiale muratura, specialmente la tensione di aderenza tra i due materiali. A tal proposito sono state eseguite prove di pull-out, prove di flessione su tre punti e prove di delaminazione su mattoni in laterizio, comunemente utilizzati nel capo dell'ingegneria civile, rinforzati con NFRP and NFRG. Infine per

avere un riscontro con la normativa vigente, è stato effettuato un confronto con l'approccio teorico proposto dal documento tecnico italiano DT-200 R1/2012.

In aggiunta alle proprietà meccaniche dei compositi NFRP, sono state calcolate anche le loro proprietà fisiche, in termini di peso per unità di superficie (GSM) e densità.

Nell'ultima parte del progetto di ricerca è stata elaborata una parte numerica, anche se in parte minore rispetto a quella sperimentale. In particolare è stato proposto un modello numerico che rappresentasse le prove di flessione su tre punti dei provini rinforzati con NFRP e non rinforzati, utilizzando il codice di calcolo agli elementi finiti DIANA. L'analisi numerica è stata confrontata con i risultati ottenuti sperimentalmente, con particolare riferimento alla rigidezza, al carico massimo e al modo di rottura osservati in entrambi i casi.

In fine è stata studiata una nuova tecnologia di intreccio dei tessuti, la cosidetta "braiding technology", allo scopo di produrre dei tessuti in fibre naturali che aumentino le proprietà meccaniche non soltanto nel loro stato naturale ma anche sotto forma di compositi.

Parole Chiavi: Materiali naturali, Compositi, Rinforzo, Muratura antica,
Prove sperimentali, Modelli numerici

RESUMO

A presente tese de doutoramento foi desenvolvida graças à colaboração entre os Departamentos de Engenharia Civil da Universidade da Calábria (Itália) e da Universidade do Minho (Portugal). O tema principal desta tese focou-se no estudo de compósitos de fibras naturais. O estudo é composto por uma vasta campanha experimental, realizada nos Laboratórios de Estruturas e Textil da Universidade do Minho, e por uma parte numérica, com a finalidade de analisar o desempenho dos compósitos de polímeros e argamassa reforçados com fibras naturais (NFRP e NFRG, respetivamente) quando aplicados a estruturas antigas de alvenaria.

Porquê a utilização de compósitos com base em fibras naturais? Porquê reforçar estruturas antigas de alvenaria com NFRP/NFRG? Estas duas perguntas são a base deste tópico de pesquisa. Em primeiro lugar, o desenvolvimento sustentável, as tecnologias renováveis e o baixo impacto ambiental representam fatores-chave do setor da construção, especialmente em relação à produção de materiais de construção. O mais importante é que este trio pode ser obtido a um custo baixo, através do uso de materiais "amigos do ambiente". Em segundo lugar, a alvenaria é um material com uma resistência à tração muito baixa, logo os materiais naturais podem melhorar o seu desempenho. As fibras de carbono e de vidro comummente aplicadas aumentam bastante a resistência à tração das estruturas de alvenaria, mas apresentam muitos inconvenientes relacionados com a poluição do meio ambiente

durante o seu fabrico ou uma elevada utilização de energia, necessária para a eliminação no fim do seu ciclo de vida.

Depois de um estudo preliminar sobre a classificação de todas as fibras naturais e as suas origens, foi possível identificar o linho, o cânhamo, a juta e o sisal como as fibras naturais com maior potencial de utilização na engenharia civil

A campanha experimental deste trabalho foi organizada em duas partes principais: ensaios em compósitos e seus componentes, e ensaios em elementos de alvenaria reforçados com NFRP e NFRG.

Na primeira parte da campanha experimental foi realizada a caracterização mecânica de matrizes e fibras, através de ensaios de compressão e flexão em três pontos da argamassa e ensaios de tração da resina e das fibras. Foram utilizadas três tipos diferentes de matrizes para produzir os materiais compósitos: duas matrizes termo-endurecíveis, de resina epoxi e de resina de poliéster (NFRP), e uma matriz de argamassa (NFRG). Para fabricar os três materiais compósitos, foram utilizados três métodos de fabrico diferentes: aplicação manual para produzir a matriz à base de epóxi NFRP, processo de infusão em vácuo para a matriz à base de poliéster NFRP e por fim, para obter a NFRG foram usadas cofragens especiais. Além disso, com o objetivo de analisar o desempenho de compósitos reforçados com fibras naturais, em termos de capacidade de carga máxima, resistência à tração e módulo de Young, foram realizados ensaios de tração em laboratório.

Na segunda parte da campanha experimental, foi investigado o comportamento da aderência entre materiais compósitos (NFRP-NFRG) e alvenaria. Para este efeito, foram realizados ensaios de arrancamento, ensaios de flexão em três pontos e ensaios de aderência em corte simples em tijolos cerâmicos para alvenaria reforçados externamente com compósitos à base de fibras naturais. Finalmente, estabeleceu-se uma comparação com a abordagem teórica de dimensionamento fornecida pelo documento técnico italiano (DT -200 R1/2012). Além das propriedades mecânicas do NFRP, também as propriedades físicas foram determinadas em termos de peso por unidade de área (GSM) e densidade.

Na última parte da pesquisa efetuada foi realizada uma análise numérica. Em particular, para os ensaios de flexão em três pontos foi desenvolvido um modelo de elementos finitos, no software TNO DIANA, com o objetivo de simular o comportamento do tijolo cerâmico não reforçado e reforçado com NFRP. A análise numérica foi comparada com os resultados obtidos experimentalmente, em termos de rigidez, carga máxima e modo de rotura obtido nos dois casos.

Com a finalidade de melhorar as propriedades mecânicas dos tecidos não impregnados naturais, foi estudada a tecnologia de colocação da fibrabaseada no entrançamento.

Palavras-chave: fibras naturais, compósitos, reforço, alvenaria antiga,
Ensaios experimentais, modelos numérico

1

INTRODUCTION

The analysis of historic masonry buildings presents even bigger difficulties when compared to ordinary modern concrete or steel buildings. The first cause is due to the artistic and cultural value of masonry buildings, that, often built hundreds of years ago, still characterize the historical centers of most of the Italian and European cities. It is important that historical architecture is protected, but to ensure their static security state and choose suitable strengthening techniques is quite complex.

Besides this first difficulty encountered operating with masonry constructions, the second one is connected to the mechanical properties of the masonry material. Masonry is a composite material, not homogeneous, with strength and deformation characteristics that highly depend its components: elements in natural or artificial stone of various sizes, and mortar. A simple model of the masonry material, frequently used in the study of the behavior of historic masonry structures is that of the so-called "*rigid non-reactive to traction*". This one, according to the fact that the tensile strength of the masonry shows smaller values (20-25 times less) than the compressive strength, due to the low tensile strength of the mortar but especially to the low adhesion strength between mortar and substrate .

The last difficulty is caused by the properties of the substrate. The masonry variety that can be found in the historic buildings is extremely wide. It is possible to distinguish the presence of irregular elements, in the case of poor construction, or regular elements built in a regular or irregular way. There are also mixed masonries, in which, apart from the stone elements, pebbles or tuff are present. When studying these structures, the choice of the materials that have to be used as reinforcement, is very important because they must be compatible with the substrate.

Because of the complexity of masonry buildings, is the choice of choose the consolidation techniques, that are able to cope with all these difficulties and at the same time be effective and long-lasting is important, yet very difficult. In Addition attention should be focused on limiting interventions to a minimum, avoiding unnecessary strengthening. This goal is clearly in agreement with the principles of sustainable development.

1.1 Objectives

The principal purpose of this PhD research thesis is focused on the study of composite materials based on natural fibers used as reinforcement of the historic masonry buildings, from an experimental and numerical point of view.

The aim of this research project are developed and compared to what is mentioned above, and are the following:

- To manufacture natural fibers-based composite materials (NF) using both polymer matrices based on thermosetting resins (NFRP) and matrix-based mortar (NFRG). To analyze the fiber reinforced composite materials and their components through a set of experimental tests, in order to research their mechanical properties and to categorize the natural materials that are stronger and more suitable for the production of composites, but especially compatible with the masonry substrate.
- To analyze the adhesion behavior between the composite materials based on natural fibers and the masonry system. For this purpose, the study and experimental analysis is based on macroelements in masonry strengthened with natural fibers-based composite (NFRP), built in the laboratory.
- To compare the results obtained experimentally with an appropriate numerical model that should be able to provide a good agreement in terms of ultimate load, global behavior and failure mode of the specimens built and tested in laboratory.

Common composite materials (with glass and carbon fibers) have numerous advantages when compared to traditional materials, but at the same time they present some disadvantages that cannot be avoided. In fact, these materials cause environmental pollution during their manufacture, but also a high use of energy, necessary for disposal at the end of their life cycle. The availability, renewability, low density, and price as well as the mechanical properties on NFRP make them an attractive alternative to glass, carbon and other man-made fibers used for the manufacturing of composites. Natural fiber-based composites are more environmental friendly, and used in many fields like transportation (automobiles, railway coaches, aerospace), building and construction industries (ceiling paneling, partition boards).

To sum up, these three objectives, described above, which are closely connected to each other, are presented as innovation elements in the field of civil construction. Sustainable development, renewable technologies and low environmental impact represent, nowadays, the key factors in the building system, especially in relation to the phases of the production of building materials. The most important thing is that this trio can be obtained at very low costs, by using eco-friendly materials.

1.2 Outline of the thesis

The following PhD thesis is organized in six chapters with a final appendix that regards a new technology studied to improve the mechanical properties of the natural material.

In Chapter 2, a general review about the strengthening techniques usually used in case of masonry structures is given. Attention was focused on the use of fiber-reinforced composites as a way to strengthen masonry construction with the description in different application sectors. Afterwards, natural fiber-based composites were illustrated as an alternative solution to reinforce the ancient masonry, due to their advantages compared to the common carbon or glass fibers. Moreover, natural fibers were classified in function of their origin, performance and textile structure. Finally, after the description of the different manufacturing methods of the natural fiber-based composites, the chapter was concetrated on the research of the use of the natural fiber in the civil engineering field and the natural materials mostly utilized in the same sector.

In Chapter 3, the properties and performance of the natural fibers and matrices have been studied. Initially, the mechanical and physical properties of the natural materials were mainly unknown, some, among the best known natural materials have been taken in account and mechanical characterization tests have been carried out on them. In particular, seven different types of bi-directional natural fabrics have been analyzed and tested in the laboratory, two of which are mixed fabrics. The wide experimental investigation has dealt with the use of flax, hemp, jute, sisal and coir fibers. In the first part of the research plan, single yarns and fabrics have been tested, carrying out tensile tests in the laboratory, in order to assess the mechanical behavior of the materials in terms of tensile strength and failure modes. to conclude the first part of the experimental plan, three types of matrices have been used and investigated: two thermosetting matrices, epoxy resin and polyester resin, and a natural matrix- based mortar. Tensile tests on resin and compressive and three point bending tests on mortar have been carried out, in order to calculate the tensile, compressive and flexural strength of the matrixes used.

In Chapter 4, mechanical testing and the performance of natural fiber-based composites have been discussed. The second part of the experimental program has been organized in two sections: in the first natural fiber-based composites have been manufactured in the laboratory distinguishing three types of composites: NFRP-based epoxy resin, NFRP-based polyester resin and NFTG. Tensile tests on NFRP and NFRG have been carried out in the laboratory, for the purpose to investigate on the different levels of strength of the composites produced. In the last section, masonry macro-elements have been built in the laboratory in order to analyze the adhesion strength between NFRP composites and the masonry system. Pull-out tests, three point bending tests and single-lap shear bond tests have been carried out on masonry clay brick externally strengthened with natural fiber-reinforced polymer sheets. Furthermore, a comparison between the experimental results achieved, in terms of the maximum load capacity, and that one proposed by Italian design code CNR 200 R1/2012 has been performed picking out some relevant aspects about design procedures. Finally, the density of the NFRP composites has been calculated.

In Chapter 5, numerical analysis of the three point bending tests on NFRP-strengthened masonry clay brick have been presented. In the first part of the chapter a brief reference to solution procedures used in non-linear finite element formulations has been described. Afterwards, the analysis of two numerical models was performed. The first model has concerned the unreinforced brick and the second

model, on the other hand, concerning the reinforced brick, with flax fibers and hemp fibers. All the geometric and mechanical properties used to develop the numerical models were those obtained experimentally, described in Chapter 4. Basically, a comparison between the experimental and numerical results has been done in order to countercheck with what was experimentally evaluated in the laboratory. Lastly, an evaluation in terms of the max load capacity, deformed mesh and failure pattern has been analyzed in order to appraise the quality of the numerical results.

Finally, in Chapter 6, an extended summary and final conclusions, which can be drawn out from this research, has been given, with some suggestions for future work.

In appendix A, a new fiber placement technology has been explained, the so-called "braiding technology", in order to increase the mechanical properties of the natural non-impregnated materials.

2

STATE OF THE ART

2.1 Applications field of fibrous material

There are several application areas in which the fiber-reinforced polymer composite (FRP) are used. Some of them are describes following, with reference to the *Fibrenamics group*[1].

Sport field

Fibrous materials are used in almost all kinds of sports, both in equipment and clothing for sports. These materials offer several advantageous properties such as reduced weight, better mechanical performance, durability, elasticity and others, tending to increase athlete's performance.

The fibers used in most sports applications are: polyester, polyamide, polypropylene, acrylic, spandex, carbon, aramid and high performance fibers. These materials are used due to their good tactile properties, low moisture absorption,

[1] The FIBRENAMICS project aims at developing various contents for dissemination in the media, about the latest developments in the field of fiber-based materials, with special focus on advanced applications in medicine, construction, architecture, personal protection, transport and sports.

ability to transport perspiration outside of the body, design and color variety, thermal insulation and, therefore, comfort.

The main applications of these materials are in sportswear with functions such as moisture management, temperature control, water repellency, breathability and monitoring of vital signs. In addition, fibrous materials are used in sports equipments in the form of composites to provide strength, durability, weight reduction as well as ease of maintenance and transportation (fig.2.1).

Figure 2.1: FRP applications in Sport field

Medicine field:

Fibrous materials for medical applications are used in products specially designed to meet specific needs in health-care and well-being areas, being suitable for medical, surgical and post-surgical treatments. The materials applied in this area possess properties such as: flexibility, strength, biocompatibility, and porosity, among other characteristics.

The fibers used in most medical applications include: cotton, polyurethane, polypropylene, polyester, alginate and also bio-absorbable fibers such as chitin and collagen.

In medical applications, fibrous materials can be grouped: implantable surgical materials (artificial tendons, stents, artificial heart valves, prosthetics, etc.), non-implantable surgical materials (gauze, cotton, dressings, etc.), extra-body devices (kidney, liver and artificial lung) and healthcare/ hygiene products (coats, hats, drapes, etc.) (fig.2.2).

Figure 2.2: FRP applications in Medicine field

Personal protection:

Fibrous materials are used in personal protection to protect the user from dangerous environmental effects that may result in damage or even lead to death.

These materials have applications in many other professional activities such as military, police, firefighters, welders, biologists, gardeners, electricians and workers from oil platforms, representing real benefits such as greater comfort, wellbeing and safety.

The most used fibers in protection include: polyester, polyamide, aramid, acrylic, polyethylene and elastane that may present various functional features such as thermoregulation, flame resistance, impact and perforation resistance, and anti-microbial protection.

Fibrous materials provide protection in several areas, including thermal protection (firefighter suits and protection against extreme cold), chemical protection (protection against harmful agents), mechanical protection (protection against cutting, drilling, abrasion and ballistic) and biological protection (protection against micro-organisms) (fig.2.3).

Figure 2.3: FRP applications in Personal Protection field

Transport field:

Fibrous materials are used in various transport systems to promote comfort (insulation and interior lining of cars, planes, trains, etc.), improve safety (example: air

bags, belts, tire reinforcement, etc.), weight reduction and, consequently, reduction of CO2 emissions (example application of composite materials as supports for instrument panels, airframes, hulls, boat propellers, etc.).

These materials are used in air transportation systems (such as aircraft and helicopters), ground systems (cars, buses, trucks and trains) as well as marine systems (boats and ships). Polyester and polyamide fibers are widely used in order to improve the safety in case of seat belts and airbags.

For the weight reduction and consequent reduction of CO2 emissions, carbon, aramid and natural fibers (flax, hemp and coconut) are used in combination with polymeric matrices, such as epoxy or polyester.

The use of polypropylene, wool, polyester and viscose fibers is very common in the elements of transport vehicles to provide comfort (fig.2.4).

Figure 2.4: FRP applications in Transport field

Building field:

Fibrous materials offer very interesting solutions for the construction industry in applications such as concrete reinforcement, soil stabilization, and thermal and acoustic insulation. Fibrous materials used in construction include glass, carbon, aramid, basalt and natural fibers. The advantages of these materials are:

- Excellent relation between weight and strength, possessing higher mechanical properties than steel for a reduced weight;
- Good relation between thermal resistance and thickness (good thermal insulation);
- Good behavior as an acoustic insulator;
- Resistance to chemical / biological; (corrosion, microorganisms, etc.);
- Good interaction with the ground (geotextiles);
- High possibility of structuring fibers (textiles, nonwovens and composites) allowing to design materials that adjust to the application requirements;
- Ability to be intelligent (monitoring).

One of the major advantages of their use in buildings is the huge reduction in weight as compared to the conventional materials (fig.2.5).

Figure 2.5: FRP applications in Building field

Architecture field:

In architecture, fibrous materials offer very interesting degrees of freedom with respect to their properties such as ease of handling, lightness and flexibility, giving the opportunity to an architect for taking an innovative approach. Over the past few years, the use of fibrous materials in architectural membranes resulted in the construction of public buildings, such as airports and sports stadiums, much lighter and functional. On the other hand, in terms of pneumatic structures, architectural membranes have allowed stable and lasting solutions addressing the inherent needs of temporary buildings. Also as functional elements and partitions, fibrous materials provide several interesting properties such as self-cleaning, odor control, thermal insulation and lightness.

With regard to the fibrous materials applied in architecture, the most used are polyamide, polyethylene, polyester, glass, and optical fiber. For achitectural membranes, fibrous structures are impregnated with polymers such as polyvinyl chloride and silicone.

The polymers confer increased mechanical strength, protection against UV rays, impermeability and other properties. Fibrous based materials provide additional liberties to the architects when compared to conventional materials such as steel, wood or concrete (fig.2.6).

Figure 2.6: FRP applications in Architecture field

2.2 Natural composite materials as an alternative solution

Nowadays, natural fibers represents an alternative reinforcement in polymer composites, indeed many researchers and scientists have attracted their attention, due to the advantages over conventional glass and carbon fibers [1]. These natural fiber include flax, hemp, jute, sisal, coir, kefal, banana and many others [2]. The various advantages of natural fibers over man-made glass and carbon fibers are low cost, low density, comparable specific tensile properties, non-abrasive to the equipments, non-irritation to the risk, renewability, recyclability and biodegradability [3].

Table 2.I and table 2.II [4] shows a comparison between natural fibers (NF) and glass fibers (GF) highlighting clearly the advantages of the NF respect the GF.

Table 2.I
Advantages of natural fibers (NF) than glass fibers (GF)

	Natural Fibers (*NF*)	**Glass Fibers (*GF*)**
Density	Lower	Double than *NF*
Cost	Lower	Double than *NF*
Renewability	Yes	No
Recyclable	Yes	No
Energy production	Lower	High
Marketing	Vast	Vast
CO_2 emission	Neutral	No-neutral
Abrasion	No	Yes
Chemical risk	No	Yes
Waste	Biodegradable	Non biodegradabili

The neutrality of carbon dioxide from natural fibers is a particularly significant as regards the reduction of pollution. In fact, the combustion of fossil-derived

products, such as those produced from synthetic fibers, requires significant quantities of energy and involves in the emission of CO2 into the atmosphere; phenomenon, the latter regarded as the main cause of the greenhouse effect.

In addition, natural fiber-based composites, given their low density, have a higher fiber content for equivalent performance, thus reducing the content more pollutants of the base polymer, if it deals of traditional-based matrix composite. To get an idea of the extent of the savings that would occur using a natural fiber-based composite, it is possible to compare glass fibers and some of the mostly natural fibers used (table 2.II)

Moreover, the glass fiber has a density of about 2,6 g/cm3 and it costs between 0,90 and 1,50 € / kg, on the other hand, flax fiber has a density of 1,5 g/cm3 and costs between 0,15 and 0,80 € / kg) [5].

Table 2.II
Comparison of properties between natural fibers (NF) and glass fibers (GF)

Properties	***GF***	**Hemp**	**Jute**	**Flax**	**Cotton**	**Coir**
Density (g/cm^3)	2.55	1.48	1.46	1.4	1.51	1.25
Tensile strength (MPa)	2400	550-900	400-800	800-1500	400	220
Young's Modulus *E* (GPa)	73	70	10-30	60-80	12	6
Peak deformations (%)	3	1.6	1.8	1.2-1.6	3-10	15-25
Umidity (%)	-	8	12	7	8-25	10

There are many factors that can be influence the performance of the natural fiber reinforced composites, such as for example their hydrophilic nature or fiber content/amount to filler. The effect of the fiber content on the mechanical properties of the natural fiber reinforced composites is particularly significance. Another important factor is the processing parameters used to manufacture the composite, they significantly influences the properties and interfacial characteristics [6].

Regarding the disadvantages of natural fibers reinforced composites is connected with the incompatibility between the hydrophilic natural fibers and the hydrophobic thermoplastic matrices and the relative high moisture sorption. This leads to undesirable properties of the composites. Consequently of this, it is necessary to modify the fiber surface by employing chemical modifications to improve the adhesion between fiber and polymer matrix. Chemical treatments also reduce the water absorption of composites and improve their mechanical performance [7].

In addition to the chemical treatments can be used physical treatments. They include stretching, calendaring, thermo-treatment and the production of hybrid yarns for the modification of natural fibers. Physical treatments change structural and surface properties of the fiber, influencing the mechanical bonding of polymers [8].

A brief review on the mostly readily utilized natural fibers and biopolymer is concerned in the follow section. The overall characteristics of reinforcing fibers used in biocomposites, including source, type, structure, composition, as well as mechanical properties and applications field are discussed.

2.2.1 Reinforced natural fibers

Natural fibers are classified in three big category according to their origin: vegetable fibers, animal fibers and mineral fibers [9-10].

Vegetable fibers

The plant that produce natural fibers, are classified as primary and secondary depending on their utilization. Primary plants are those grown for their fiber content while the secondary plants are plants in which the fibers are produced as a by-product. There are six basic types of natural fibers:

- *Seed fiber*: coir, cotton and kapok fibers collected from the seeds;
- *Leaf fiber*: abaca, sisal and pineapple fibers collected from leaves;
- *Bast fiber*: jute, flax, hemp, ramie and kefal fibers collected from the skin or bast surrounding the stem of their respective plant
- *Core fiber*: kenaf, hemp and jute extracted from the core of the plant;
- *Stalk fiber*: wheat, corn and rice fibers; they are essentially the stalk of the plant; bamboo and grass fiber are including in this group;
- *Other fiber*: wood and roots fibers are considered natural fibers.

Furthermore, vegetable fibers are generally comprised mainly of cellulose.

Animal fibers

Animal fibers are constituted by proteins; these fibers can be further categorized into the following:

- *Animal hairs*: they are fibers taken from animals or hairy mammals, for example cashmere or mohair fibers;
- *Silk fibers*: they are fiber collected from dried saliva of bugs or insects during the preparation of cocoons;

- *Avian fibers*: these fibers derive from feathers of birds.

Mineral fibers

Mineral fibers are fibers that derive from the particular treatment of minerals. They can be divided in three categorize:

- *Asbestos*: serpentine and amphiboles mineral fibers
- *Ceramic fibers*: glass fibers, aluminum oxide, silicon and boron carbode;
- *Metal fibers*: aluminum fibers.

Substantially, there are thousands of different fibers in the nature. Moreover, each fiber is characterized by different properties due to non-uniformity of structure of the fiber. It is results very hard to research on all of the existing natural fibers. Mechanical, physical and geometric properties of natural fibers are influenced by many factors: hydrophilic nature, moisture content, defects, structure, cell dimensions, morphology of the plant . One of the drawbacks for natural products is that the range of the characteristic values is remarkably higher than those of common reinforce fiber, like carbon o glass fibers.

The fiber mostly analyzed and studying as a reinforced fibers are those vegetable, especially the bast fibers. These fibers have higher tensile strength than other fibers and they are used for yarns, fabrics, packaging and paper.

In the vast field of Bio-fibers, those of flax and hemp are particularly suited to be used as reinforcement of composite materials environmentally friendly. Observing the main mechanical characteristics in Table 2.II, you can easily notice that they may be a suitable and realistic alternative to glass fibers.

2.2.2 Textile structures

There are different textile structures that are used in many fields of civil engineering. The main textile technologies to produce fibrous structures for composites are weaving, knitting, braiding and nonwoven production techniques. Each of these technologies can produce conventional structure but also innovative structures. The selection of the appropriate structure depends on the type of application to realize.

The most commonly used classification of the textile structures is done exactly taking into consideration the production technologies, grouping them into woven, knitted, braided or nonwoven fabrics.

This classification is commonly used in conventional textiles where the performance of the fabric itself is, most of the time, less important than the aesthetics Basically, for technical uses, the most suitable classification is that done considering the orientation of the fibers in the structure, giving less importance to the technique used to produce it, classifying the textile structures as

- planar or conventional structures (2D);
- three-dimensional structures (3D);
- directionally oriented structures (DOS);
- hybrid structures.

In the civil application the planar textile structure (2D) are mostly used, especially the woven fabrics. The words "*woven fabrics*" generally used to refer to fabric composed of two sets of yarns, warp and filling, that is formed by wearing, which is the interlacing of these sets of yarns. However, there are woven fabrics in which three sets of yarn are used to give a triaxial weave. In two dimensional woven, there may be two or more warps and filling in the fabrics, depending on the complexity of the construction. The manner in which the two sets of yarns are interlaced determines the weave. By using various combinations of the three basic weaves, plain, twill and satin, it is possible to produce an almost unlimited variety of constructions. Other effects may be obtained by varying the type of yarns, filament or spun, and the fiber types, twist levels, etc [11].

The most common woven structures used in technical applications are plain weave (fig. 2.7a), twill weave (fig. 2.7b) and satin weave (fig. 2.7c).

a) b) c)

Figure 2.7: Main weave structures: a) Plain weave; b) Twill weave; c) Satin weave

The mechanical properties of woven fabrics are very important for composite materials; they depend on different factors, principally by warp[2] and weft[3] linear

[2] The set of yarns in all woven fabrics that runs lengthwise and parallel to the selvage and is interwoven with the filling.

mass, yarn density and weave structure. The strength of the fabric is usually higher in warp direction than weft directions, while the diagonal directions present lower mechanical properties, higher elasticity and lower shear resistance.

In addition considering the direction of the fibers in the fabric, the latter can be classified into three different types:

- *Unidirectional fabrics*: the fibers are all oriented in the same direction (warp 90 °) and are held together by a light weave of non-structural types;
- *Bidirectional fabrics*: the fibers are oriented in two directions (warp 90° and weft 0°) in order to form a weaving weft-warp orthogonal usually balanced (same percentage of fibers in both directions).

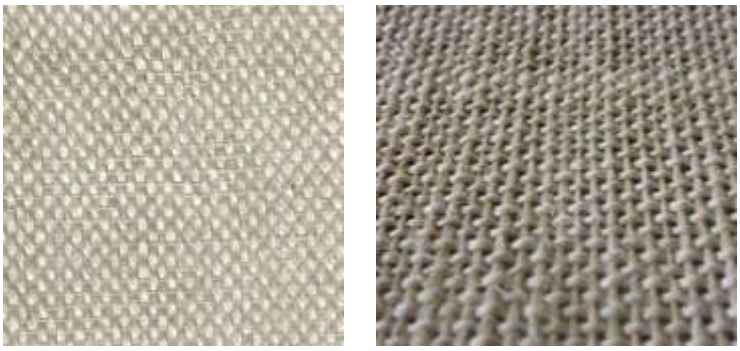

a) b)

Figure 2.8: Orientation of the fibers in the warp and weft direction: a) Unidirectional fabrics; b) Bidirectional fabrics.

2.2.3 Performance of Natural Fiber based Composites

Performance of natural fiber-based composite are closely linked to their tensile, flexural and impact properties. The majority of researchers have focused their studies on these three properties in order to improve the potential of the natural fibers as well as the performance of the composites system.

Mechanical properties of the composites mostly analyzed are those relating to tensile strength. The tensile strength of a fiber depends strongly on the geometrical characteristics of the single fiber, such as the thickness or diameter of the fiber. Regarding the flexural properties of the composite, they are related to the di-

[3] In a woven fabric the yarn running from selvage to selvage at right angles to the warp; weft is the transverse yarns.

mension, not so much of the fibers, but of the specimens used for the experimental test: the surface on which the load is applied plays an important role in this case. Indeed, the ductile or brittle behavior of a specimen depends on the size of the specimen (figure 2.9). Maintaining the same material and geometric shape of the specimens, if the size scale increase, it will find a brittle behavior, with a sudden drop in load and a rapid propagation of a crack. On the contrary, in specimens of relatively small size, it will occurs a ductile behavior with a slow propagation of the crack. Moreover, while during the tensile test, the load is distributed in uniform way along the cross-section of the composite, on the other hand during the bending tests, the composite will be subjected to eccentric load applied on the top and bottom of the specimen figure [12].

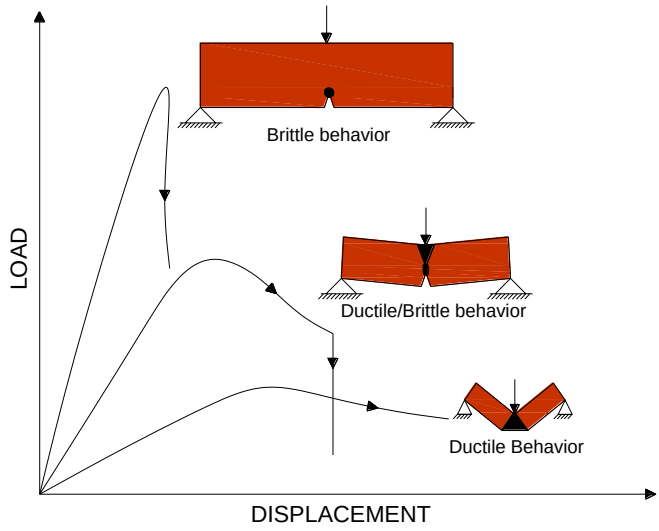

Figure 2.9: Behavior brittle/ductile of different size of specimens

Another important properties of the composites is the Impact strength. It is the ability of a material to resist fracture under stress applied at high speed. It is also expressed as the capacity of the material to absorb energy while it deforms in elastic field.

Recently studies show that impact tests on natural fiber-reinforced composites are comparable with tests on glass-fiber-reinforced composites, characterized by the equivalent fiber volume fraction [13-14]. Impact strength of the material also depends on the adhesion between fiber / matrix. It provides an effective resistance of the crack propagation during the impact tests.

in the last few years, new processing and manufacturing methods have strongly influenced the research of many studious, in order to enhancement of fiber/matrix adhesion.

Anyway, the performance of the natural fiber-reinforced composite are currently underway for many research projects around the world, being numerous the factors to take into account.

2.2.4 Manufacturing process

Nowadays, several methods for manufacturing of composites are available. A first classification can be made considering the matrix used for the production of composites, in fact it have: processing technologies for natural fiber reinforced thermoplastics and processing technologies for natural fiber reinforced thermosetting. Manufacturing methods most commonly used are the following [15]:

Manual lay-up

The simplest technique to manufacture a composite is called lay-up moulding, wet lay-up or laminating. This method is performed by applying (by hand) layer upon layer of fibres (or mats of fibres) with resin in between on a shaped surface. This is repeated until the desired thickness is obtained after which pressure is applied, normally by hand rolling.

Vacuum bagging

A little bit more elaborate than the manual lay-up method, is to impregnate a mat with a resin, (referred to as a prepreg), which is placed on the shaped surface with a bag on top. The pressure is applied either by evacuating the air inside, creating a vacuum, or by pressurising the bag on the outside with compressed air. Both manual lay-up and vacuum bagging are then cured at room temperature or at an elevated temperature.

Sheet moulding compound (SMC)

SMC is a thin mat of short/continuous fibres impregnated by a thermoset resin. The mats are placed in a hot-pressing machine, where heat and pressure is applied which activates the curing process.

Bulk moulding compound (BMC)

BMC is a pre-mix of short/continuous fibers and normally used in case of thermo-setting resin. The mixture is cured under pressure and heat.

Natural fiber mat thermoplastic (NMT)

NMT is a development of GMT, which is a Glass fibre Mat with non-oriented short fibers impregnated by a thermoplastic. The fibres in the NMT are natural fibres such as flax and hemp, thereby the replacement of the G in GMT.
The manufacturing starts out by placing the NMT in an oven. When the matrix starts to melt the NMT is pressed to the desired shape in a hydraulic press. The matrix cools in the press and the matrix solidifies.

Preform sheet resin (PSR)

PSR is similar to the SMC method. A pre-form of fiber is placed in a mould with a sheet of resin on top. Then the mould is closed and curing occurs in vacuum.

Pultrusion

Pultrusion is a continuous manufacturing process for manufacturing long straight profiles with a constant cross sectional area. The process is basically performed by squeezing the mixture of resin and fiber through a heated die, similar to extrusion of aluminum profiles.

In the field of civil applications of the method are usually the manual lay-up, pultrusion and vaccum infusion.

Moreover, in accordance with the Italian standard [16], reinforcement systems can be classified into three categories, depending on the production method used to realize them:

- *Pre-cured systems*: Composites manufactured in various shape by pultrusion or lamination, bonded to the structural element to be reinforced;
- *Wet lay-up systems*: Composite sheets manufactured with unidirectional fibers or fabrics that are multidirectional or impregnated with a resin, which also serves as adhesive with the substrate in question (eg, concrete, masonry);
- *Prepreg systems*: Composite sheets manufactured with unidirectional fibers or multidirectional fiber sheets or fabric pre-impregnated with resin partially polymerized. It can be bonded to the substrate to be reinforced with (or without) the use of additional resins.

2.3 Textile natural fibers used in civil engineering field

The natural fibers mostly used in the civil engineering field are basically the bast fiber, especially three types: flax, hemp, jute. It also used in the engineering applications a leaf fibers, exactly sisal fibers.

In civil engineering applications, the use of natural fibers is constrained by their moderate mechanical properties. However, their low specific weight and their renewable nature make some of these fibers attractive as the reinforcing elements in composites.

The bast or stem fibers are cellulosic fibers that form the fibrous bundles in the inner bark of the stems of dicotyledonous plants, i.e. plants that form two seed leaves. These fibers are constructed of long thick-walled cells that overlap one another. They are connected together by non-cellulosic materials to form continuous strands that may run the entire length of the plant stem. The strands of bast fibers are normally released from the cellular and woody tissue of the stem by a process called retting. Often the strands are used commercially without separating the individual fibers one from another [17]. Some examples of bast fibers are flax, hemp, jute and ramie (fig. 2.8)

Fibre	Tenacity (N/tex)	Tensile strength (GPa)	Extension to break (%)	Young's modulus (N/tex)	Young's modulus (GPa)	Density (g/cm^3)
Natural						
Flax	0.54	0.831	3	18	27.72	1.54
Hemp	0.47	0.705	2.2	21.7	32.55	1.50
Jute	0.31	0.465	1.8	17.2	25.8	1.50
Ramie	0.59	0.885	3.7	14.6	21.9	1.50
Natural polymer						
Tenasco	0.27	0.405	16.9	6	9	1.50
Fortisan	0.59	0.885	6.4	16.1	24.15	1.50
Synthetic						
Nylon 6.6 HT	0.66	0.752	16	4.4	5	1.14
Polyester HT	0.56	0.778	7	13.2	18.35	1.39
Polypropylene	0.65	0.591	17	7.1	6.46	0.91
Para-aramid HM	2	2.88	2.4	80	115.2	1.44
Carbon HM	1.20	2.196	0.7–1.7	256	468.48	1.83
E-glass	0.78	2	4	28	72.24	2.58
Basalt CBF	0.7–0.9	1.8–2.5	3.1	30–35	80–93	2.65
PVA fibres	0.7–1.23	0.91–1.60	7	6.5–17	8.45–22	1.3
SWNTs	10–41	13–53	16	770–3846	1–5 × 10^3	1.3–1.4
Metals						
Stainless steel fibres	0.22–0.28	1.7–2.21	1.5–11	25.19	199	7.9
Steel	–	0.34–2.1	–	–	210	7.8
Aluminium	–	0.14–0.62	–	–	70	2.7

Figure 2.10: Tensile properties and density of typical textile fibers used for technical applications in comparison with metal

Engineering applications of natural fibers-based composite materials are essentially focused on internal reinforcement of concrete structures, as a structural health monitoring, in building applications (as strengthening) and architectural membranes (fig. 2.11).

Reinforcement Concrete

Structural Monitoring

Insulation

Geotextile

Mooring systems for ocean platforms

Partition Panels

Figure 2.11: Different applications field of natural fibers (NF)

2.3.1 Flax fibers

Flax belongs to the family *Linaceae* (fig. 2.10a) and it is one of the oldest fiber crops in the world. The genus *linum* as about 230 species. Linen flax, L. *usitatissimim*, is a annual plant and grows 0,5-1,25m tall with a stem diameter of 16-3,2mm. It grows in temperate climates and the best producing countries are China, France and Belarus. Flax is harvested for fiber production after approximately 100 days or when the base of the plant turns yellow. The plant is grown both for its fiber and for its seeds, which are used to make linseed oil.

The bast fibers are separated from the inner bark by retting. About 0,1-0,25 of the weight of the stalk are bast fibers. The ultimate fiber length averages 33mm and fibers average 19μm in width. The fibers have tapered ends [17]. Under the microscope the cells of flax fiber look like long and transparent cylindrical tubes. The fiber cell has a narrow lumen running through the centre and the cell walls are thick and polygonal in cross-section. Flax has an average tenacity of around 0,57 N/tex, an extension at break of around 1,8% (dry fiber) or 2.2% (wet fiber).

After the fiber processing, which includes the steps of steeping in water, carding, combing and spinning in wet, they present themselves as in figure 2.10.b. Flax fibers can constitute composite systems to be impregnated in situ for the external strengthening of structural elements, in the form of strips or fabrics (fig. 2.10.c) with a different orientation in warp and weft direction.

a) b) c)

Figure 2.12: *Linum usitatissimim*: a) Flax plant; b) Yarns; c) Fabrics.

2.3.2 Hemp fibers

Hemp is the common name for plants belonging to the genus *Cannabis* (fig. 2.11a). It is an annual plant, like flax fibers, it is considered as the oldest cultivated fiber plant in the world. The plant grow up to 4,5m (1,2-5m) in height in approximately 140-145 days with a stem diameter of 4-20mm. the growing of hemp has declined over the past two centuries but it has been a popular fiber because the plant grows fast, producing very strong bast fibers. It has a long traditional uses as a textile fiber and for canvas. Hemp rope is famous for its strength and resistance to rot. the bast fibers are covered by a thick layer of bark, which is removed by retting and represent about 15-25% of the total dry weight of the stalk. The average hemp bast ultimate fiber length is 25mmm with an average fiber width of 25μm. The bast fiber ends are tapered and blunt. Hemp has traditionally been sold by quality, dependent mainly on color and luster, and weight. The cross-section of hemp fiber is cylindrical and thicker than flax, presenting many irregularities on the surface [17].

Processing phases of hemp fibers are the same of those of flax. At the end of the wet spinning hemp appears as in figure 2.11b, instead figure 2.11c shows the image of a hemp fabric designed to be impregnated in situ as structural reinforcement by means of an epoxy/polyester resin or cement mortar.

a) b) c)

Figure 2.13: *Cannabis*: a) Hemp plant; b) Yarns; c) Fabrics.

2.3.3 Jute fibers

Jute is one of the most affordable natural fibers and is second only to cotton in amount produced and variety of uses of vegetable fibers. Jute fibers are composed primarily of the plant materials cellulose and lignin. Jute is produced from plants in the genus *Corchorus* which has about 100 species. Two different types of jute is possible to distinguishing: *Corchorus Capsularis* (known as white jute - fig. 2.12a) and *Corchorus Olitorius* (nown as Tossa jute - fig. 2.12b). Tossa jute fiber is softer, silkier, and stronger than white jute. The growing cycle for jute is 120-150 days with an average yield of 1700Kg/ha in warm and wet climates. The plant grows 2,5-3,5m in height. Jute bast fiber are 1-4m long and are separated from the stalk by retting. The ultimate fibers have an average length of 2m and an average width of 20μm. the fibers are short and narrow with think cell walls [17].

The cross-section of the single yarns of jute is polygonal with thick walls and irregular along the length (fig. 2.12c). Due to the irregular thickness of the single yarns, jute is not as strong or durable as flax or hemp.

a) b) c)

Figure 2.14: *Corchorus*: a) White jute; b) Tossa jute; c) Jute fabric.

2.3.4 Sisal fibers

Sisal, *Agave sisalana*, is an agave that yields a stiff fiber traditionally used in making twine and rope, and also dartboards. These types of fibers which grow with sword-shaped leaves about 1,5-2m tall. The name comes from the Yucatan port of sisal from which the fiber was first exported. The sisal plant has a 7-10 year lifespan and typically produces 100-250 dark to pale green leaves in the formed ina rosette on the trunk. each leaf is approximately 1-2m long, 10-15cm wide and 6mm thick and contains an average of 1000 fibers. The fiber element, which accounts for only about 4% of the plant by weight, is extracted by a process known as decortication. The plant grows to a height of 2m with a short trunk 0,15-0,23m in diameter. The sisal leaf fibers are bundles as long as the leaf, 1-2m long. the ultimate fibers of sisal average 3mm long and 20μm wide [17].

a) b) c)

Figure 2.15: *Agave sisalana* : a) Sisal plant; b) Sisal fibers; c) Sisal fabric

3

PROPERTIES AND PERFORMANCE OF NATURAL FIBERS AND MATRIX

3.1 Natural fibrous materials

Textile materials in form of fibers, yarns and fabrics, are used in different civil engineering applications. A fiber is a unit of matter characterized by flexibility, fineness and a high ratio of length to thickness. As fibers have a high surface to volume ratio, they can be extremely strong materials. Fibers are normally made up of by long and chain-like molecules known as macromolecules or polymers, which may have an organic or inorganic nature. According to their origin, textile fibers may be classified as *natural fibers*, when they appear in nature in that form, and *man-made fibers*, when they do not appear in nature in fibers form. Keeping in mind the purpose of this thesis, mainly the production of natural fiber-reinforced composites, only natural fibers were taken into consideration [18].

In fiber-reinforced composites, fibers perform the role of bearing elements both in terms of resistance and stiffness. The matrix, as well as protecting the fi-

bers, acts as a means of transfer of efforts between the fibers and possibly between the latter and the structural element that has to be reinforced.

In this chapter, mechanical characterization tests on components of the natural fiber-based composites have been carried out in the Civil Engineering Laboratory and Fibrous Materials Laboratory at University of Minho; in particular tensile tests, compressive tests and flexural tests have been performed. For this purpose, the experimental investigation was organized in three different parts: tests on single yarns, tests on non-impregnated fabrics and tests on matrix, in order to analyze the constitutive laws of the single components and the laws between them and the corresponding composite materials.

3.1.1 Natural fiber-based yarns

The composite materials normally used for reinforcement of the structures are made from long fibers, namely that they extend throughout the length of the building. It can be observed how the FRP made from long staple represent an element of substantial innovation and development in structural materials, unlike the short fiber composites. Essentially, the latter have the aim of achieving an improvement in the performance and properties of existing materials. The composites made of long fibers have high tensile strength and stiffness especially in the direction of the fibers. They are the actual reinforcement of structural elements and is therefore of technical interest the tensile constitutive relationship.

This section concerns the study of the tensile constitutive relationship of single yarns. After a description of the natural materials selected, the preparation specimens and set-up procedure were described. Finally, the results achieved and the failure modes observed from tensile tests are shown in detail.

3.1.1.1 Material / Types of yarns

In order to fulfill the aim of this thesis, five types of natural materials have been used: flax, hemp, sisal, jute and coir. Different types of yarns, for density and diameter, have been experimentally-tested, in figure 3.1-3.2 some examples of specimens are shown.

Figure 3.1: Specimens of single yarns

3.1.1.2 Specimens preparation

Given the wide variety properties of the natural fibers, a number between 10-15 specimens for each type of yarn, different in diameter and orientation in the fabrics, was taken in account for the experimental tests. Each specimen was cut, measured and weighed, in order to compute the linear density (Tex) and tenacity (N/Tex). The Table 3.I-3.II shows average values of the diameter *d*, cross area *A*, length *L*, weight *W*, linear density, tenacity and coefficients of variation obtained for all yarns prepared in the laboratory.

Table 3.I

Geometrical and physical properties of the single yarns

	FLAX	**HEMP[1]**	**HEMP[2]**	**HEMP[3]**	**COIR**
L	0,43	0,38	0,45	0,39	0,43
[m]	1%	0%	1%	1%	1%
W	0,15	0,13	0,15	0,15	1,25
[g]	4%	8%	3%	6%	4%
d	0,82	0,86	0,83	0,87	3,19
[mm]	10%	4%	8%	11%	6%
A	0,53	0,58	0,54	0,60	8,02
[mm^2]	19%	7%	16%	23%	13%

Linear Density	322,90	330,14	327,26	381,42	2887,37
[Tex]	6%	7%	1%	4%	3%
Tenacity Max	0,29	0,29	0,20	0,2541	0,14
[N/Tex]	5%	4%	8%	6%	9%

Table 3.II

Geometrical and physical properties of the single yarns

	JUTA[1]	**JUTA[2]**	**JUTA[3]**	**SISAL[1a]**	**SISAL[1b]**	**SISAL[2]**
L	0,43	0,44	0,43	0,46	0,46	0,42
[m]	0%	2%	1%	2%	2%	1%
W	0,11	0,12	0,89	1,79	0,65	1,21
[g]	10%	16%	24%	17%	16%	22%
d	0,67	0,74	1,61	3,51	1,57	2,42
[mm]	16%	11%	19%	8%	16%	14%
A	0,36	0,44	2,09	9,72	1,97	4,67
[mm2]	33%	23%	35%	16%	29%	28%
Linear Density	267,44	281,80	2068,79	3927,26	1439,31	2905,37
[Tex]	10%	17%	24%	18%	17%	23%
Tenacity Max	0,12	0,11	0,21	0,08	0,18	0,22
[N/Tex]	14%	15%	12%	17%	7%	11%

3.1.1.3 Test setup and test procedure

The study of the mechanical properties of the single yarns was done by tensile tests, in accordance with the reference standard [19]. In order to obtain 5 good results, with a failure mode in the middle of the specimens, a number between 10-15 specimens, for each type of yarn, were tested. All tests were conducted in a normal atmosphere on specimens previously acclimatized, by means of a high precision universal testing machine (figure 3.2a-3.2b) and conducted under displacement control of the crossbar. Before each tests, a pre-load of a 1,5 N was applied and a crosshead speed equal to 25mm/min was used.

a) b)

Figure 3.2: Tensile tests: (a) Testing machine; (b) Single yarns

3.1.1.4 Test results and failure modes

Analyzing the first results on the single yarns, it is possible to observe several results linked to the different characteristics of the materials used. First of all, flax is the one that presents higher values in terms of tensile strength followed by hemp sisal and jute. Coir fibers are those least suitable in terms of mechanical properties, consequently they have not been considered as reinforced fibers for composite materials in the next steps of the experimental plan. To sum up all the results achieved from tensile tests on single yarns mechanical properties have been shown in the table 3.III-IV, in terms of peak deformation ε_{peak}, tensile strength f_t and modulus of elasticity *E*.

Table 3.III

Mechanical properties of the single yarns (CoV is provided inside parentheses)

	FLAX	**HEMP[1]**	**HEMP[2]**	**HEMP[3]**	**COIR**
$\boldsymbol{\varepsilon_{peak}}$	3,22	3,58	2,94	5,36	0,16
[%]	7%	5%	12%	7%	10%
$\mathbf{f_t}$	198,10	163,98	124,14	166,60	51,83
[MPa]	14%	13%	19%	23%	19%
E	5913,59	4578,41	4236,98	3104,87	322,07
[MPa]	18%	11%	16%	21%	16%

Table 3.IV

Mechanical properties of the single yarns (CoV is provided inside parentheses)

	JUTE[1]	**JUTE[2]**	**JUTE[3]**	**SISAL[1a]**	**SISAL[1b]**	**SISAL[2]**
ε_{peak}	0,02	0,03	0,06	0,38	0,08	0,05
[%]	8%	15%	13%	26%	4%	10%
f_t	101,66	74,84	224,51	31,53	144,18	144,93
[MPa]	46%	20%	36%	16%	46%	24%
E	4460,12	2769,70	3702,47	85,19	1792,17	2814,27
[MPa]	42%	24%	43%	18%	43%	32%

Regarding the failure modes, it has not been easy to obtain good results immediately; some specimens broke near the clamps of the testing machine and because of this the results have been excluded. In order to analyze the correct strength values of the fibers, only the specimens that broke in the middle of the test length (more or less to 100mm from the clamp) have been considered during the data processing.

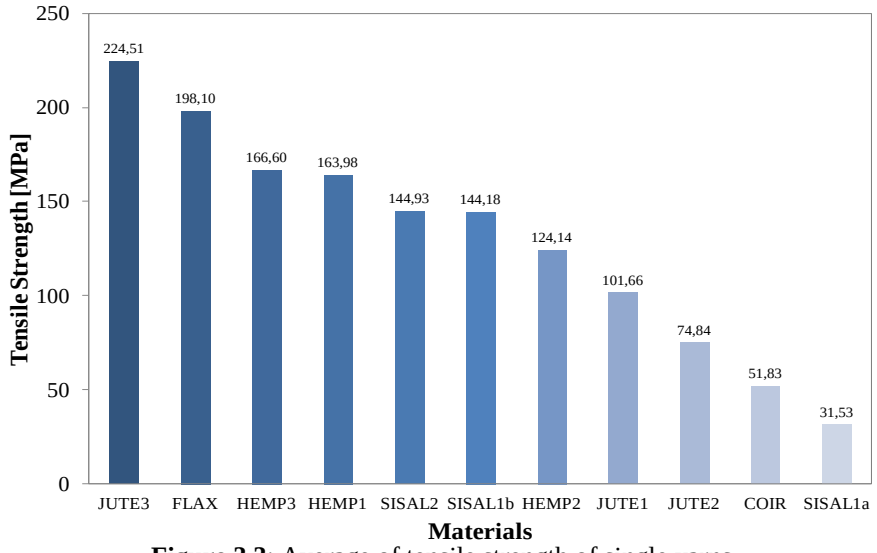

Figure 3.3: Average of tensile strength of single yarns

3.1.2 Fabrics

At the beginning of the research program the specific characteristics of the fabrics in natural fibers were not known, meaning that the more resistant direction of the fabric was indefinite, especially given the presence of various diameters in the two directions of the fabric. Therefore each fabric, both in the weft and warp direction has been studied, by carrying out in the laboratory tensile tests. The non-impregnated fabrics, so called in the first part of the experimental program, are the same ones from which the specimens were taken to carry out tensile tests on single yarns.

3.1.2.1 Materials / Types of fabrics

Four types of natural materials have been considered in this part of the thesis: flax, hemp, jute and sisal. A total of seven kinds of bidirectional fabrics have been put in examination (figure 3.4), different for both density but also in composition, in fact, mixed fabrics, with the presence of different materials in each direction, were tested. The fabrics used, are produced by leading companies in the building and chemical industries, which have been commercializing, for years now, the common carbon and glass fibers.

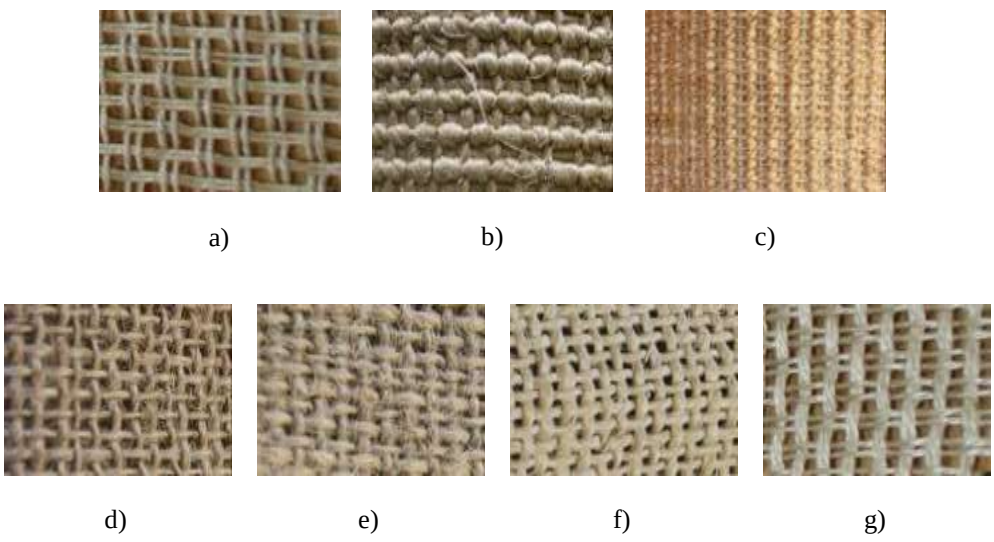

Figure 3.4: Different types of non-impregnated fabrics : Hemp (a); Sisal[1] (b); Sisal[2] (c); Jute[1] (d); Juta[2] (e); Juta[3] (f); Flax (g)

3.1.2.2 Specimens preparation

Specimens cut in the warp direction (90°) and weft direction (0°) were prepared (figure 3.5a), with an equal number of yarns in the direction of load application and with a size equal to 300x50mm^2; being the test length equal to 200mm [20]. In addition each specimen has been equipped with special steel plates on the edges (figure 3.5b), in order to guarantee a uniform distribution of the load and to avoid the specimen from slipping during the test.

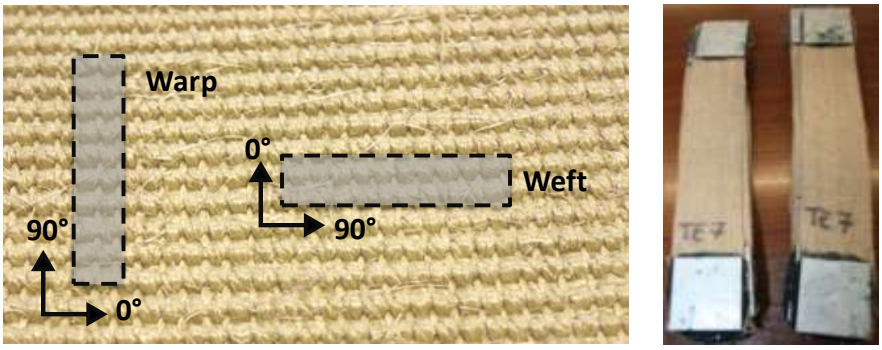

a) b)

Figure 3.5: Preparation of the specimens: with the steel plates:
(a) Cutting direction; (b) Non-impregnated specimens with steel plates.

Moreover, in accordance with standards [21] the mass per unit area was measured; five specimens with circular shape and an area equal to 100cm^2 for each kind of fabric were cut (figure 3.6).

Figure 3.6: Specimens of non-impregnated fabrics

For each specimen, to calculate the mass per unit area GSM, in grams per square meter, the following equation was used:

$$GSM = 10000 \times \frac{w_s}{A} \qquad (3.1)$$

where:

- w_s is the mass, in grams, of the specimen;
- A is the area, in square centimeters, of the specimen.

The values obtained from the average of five specimens considered, in the table 3.V are shown:

Table 3.V

Mass per unit area of the non-impregnated fabrics (CoV is provided inside parentheses)

		JUTE[1]	**JUTE[2]**	**JUTE[3]**	**SISAL[1]**	**SISAL[2]**	**HEMP**	**FLAX**
NON-IMPREGNATED FABRICS	**GSM** [g/m^2]	254,9 (2%)	398,2 (3%)	1099,1 (4%)	1767,6 (4%)	1375,4 (2%)	454,5 (2%)	388,4 (1%)

3.1.2.3 Test setup and test procedure

Tensile tests on specimens taken from non-impregnated fabrics were carried out in accordance with EN ISO 13934-1/2 [20]. All tensile tests were conducted in a normal atmosphere on specimens previously acclimatized, by means of a high precision universal testing machine (figure 3.7), and conducted under displacement control of the crossbar. Before each test, a pre-load of 10N was applied and a crosshead speed equal to 100mm/min was used.

a) b)

Figure 3.7: Tensile tests: (a) Testing machine; (b) Fabrics.

3.1.2.4 Test results and failure modes

The experimental results achieved from tensile tests on non-impregnated fabrics cut at 0º (weft direction) and 90º (warp direction), have shown a clear difference in behavior from the mechanical performance point of view. The main direction of the fabric (90 °) is more strong than the secondary direction (0°); the values of the mechanical characteristics obtained, in terms of peak deformation ε_{peak}, tensile strength f_t and modulus of elasticity E are summarized in the table 3.VI. Regarding hemp and flax fibers, it is possible to note only one value: the fabrics analyzed, are so-called "*balanced fabrics*" because they contain the same number of fibers in both directions [16].

Table 3.VI

Average values obtained from tensile tests on non impregnated fabrics - warp and weft direction (CoV is provided inside parentheses)

		JUTE[1]	JUTE[2]	JUTE[3]	SISAL[1]	SISAL[2]	HEMP	FLAX
ε_{peak} [%]	warp	4,8% (9%)	8,6% (1%)	6% (7%)	4,4% (3%)	4% (7%)	7,5% (2%)	4% (4%)
	weft	3,3% (4%)	6,2% (3%)	1,7% (5%)	7,2% (4%)	54% (2%)		
f_t [MPa]	warp	32,91 (14%)	31,41 (5%)	55,20 (17%)	17,73 (11%)	9,94 (6%)	46,68 (8%)	68,81 (7%)
	weft	22,83 (19%)	34,5 (6%)	30,68 (29%)	7,43 (9%)	15,34 (18%)		
E [MPa]	warp	691,49 (11%)	364,74 (5%)	863,33 (15%)	402 (9%)	239,23 (10%)	618,65 (7%)	1746,91 (10%)
	weft	699,48 (21%)	554,29 (6%)	178,87 (30%)	103,6 (7%)	28,25 (18%)		

It is of particular importance to focus the attention on the failure mode observed during the tests and in the curve tensile strength - strain diagrams obtained. Non-impregnated specimens are characterized by a reduction of the area of the individual yarns that make up the fabric with a softening final part in the diagram, as it is possible to see in the figure 3.8. The fibers with the most effective mechanical properties both in terms of strength and in terms of limited deformation are those of flax, to confirm what obtained by the tensile tests on single yarns. Regarding the

fabrics of jute, it was observed that the fabric jute[3] ensures higher resistance values than jute[1] and jute[2], this is due to the higher density of fibers present in the fabric (see the table 3.I- 3.II). Also the hemp fabric, being a natural material, is suitable as for the production of fiber-reinforced composites; the fabrics of sisal turn out to be less resistant.

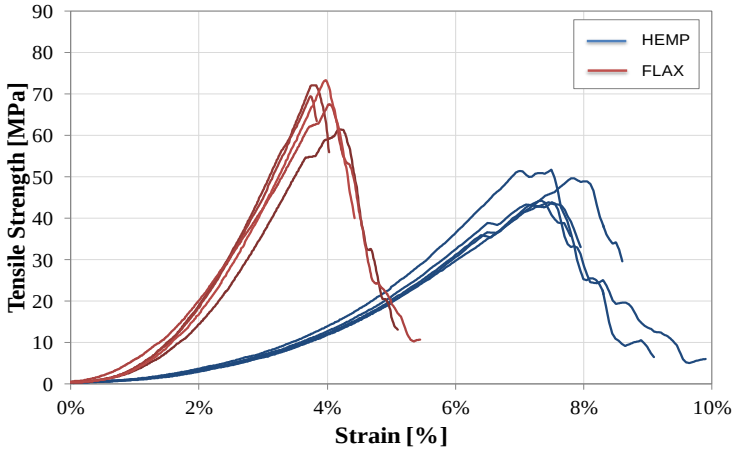

a)

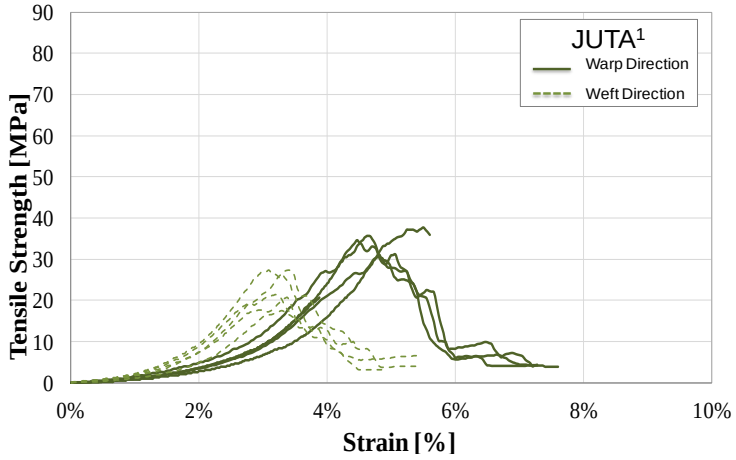

b)

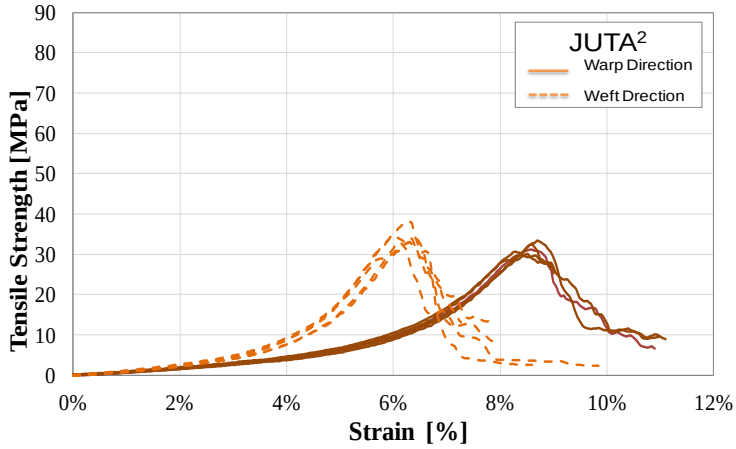
JUTA2
Warp Direction
Weft Drection
Tensile Strength [MPa]
Strain [%]
0
10
20
30
40
50
60
70
80
90
0%
2%
4%
6%
8%
10%
12%

c)

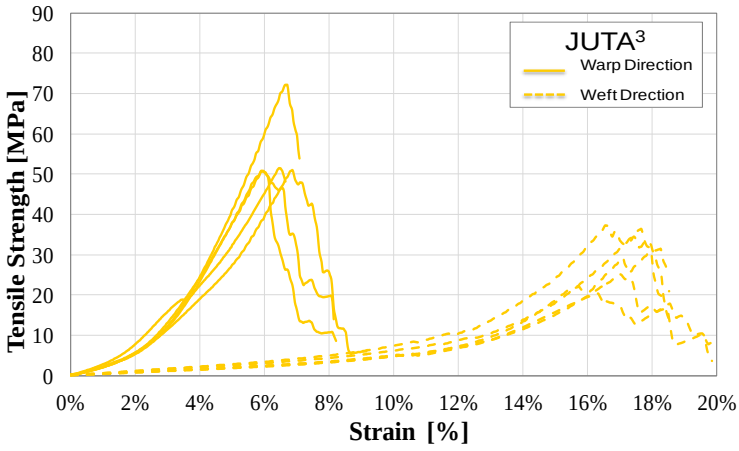
JUTA3
Warp Direction
Weft Drection
Tensile Strength [MPa]
Strain [%]
0
10
20
30
40
50
60
70
80
90
0%
2%
4%
6%
8%
10%
12%
14%
16%
18%
20%

d)

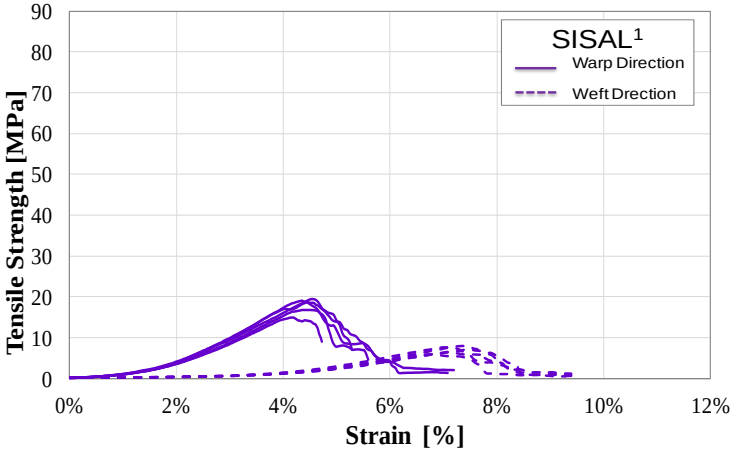
SISAL1
Warp Direction
Weft Drection
Tensile Strength [MPa]
Strain [%]
0
10
20
30
40
50
60
70
80
90
0%
2%
4%
6%
8%
10%
12%

e)

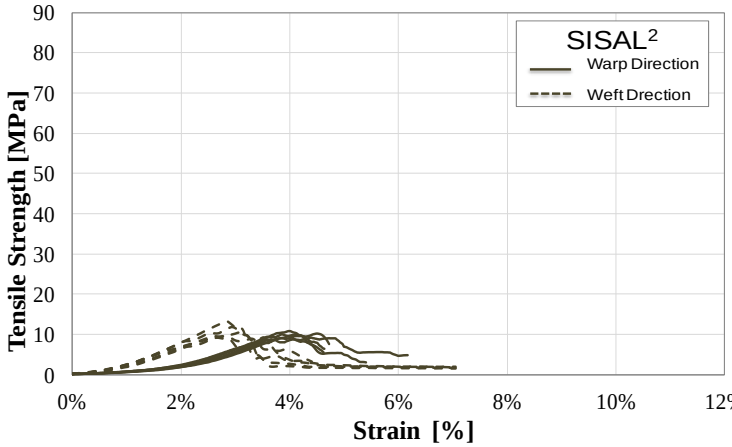

f)

Figure 3.8: Tensile stress - strain diagrams: Flax, Hemp(a); Juta[1](b); Juta[2](c); Juta[3](d); Sisal[1] (e); Sisal[2] (f).

3.2 Matrix

Composite materials are constituted by a dispersed phase that is represent by the reinforced fiber, as stated above, and a continuous phase that corresponds to the matrix, where the reinforced fibers are immersed. Unlike of the fibers, the matrix must instead ensure a uniform distribution of stresses between the single fibers; in many cases it also acts as a bond between the support (surface of the structural element to be reinforced) and the fibers, ensuring the transfer of stresses (adherence). Furthermore, the matrix has protection function from wear for the fiber, as well as that of ensuring a good alignment of them.

Thermosetting resins are the most commonly used matrices for production of FRP materials. The most common thermosetting resins for civil engineering are the epoxy resins and polyester resins. Fiber-reinforced composite materials with thermoplastic polymer matrices are also available but require installation techniques different from thermosetting resin, with the advantage to be bent at any time by means of special thermal treatment.

In the field of structural reinforcement by using composite materials, to common FRP are flanked the FRCM composites(Fiber Reinforced Cementitious Matrix). They exploit both the good properties of fibers (glass, carbon, aramid, etc..) and the properties of the cement-based matrix. The mortar-based matrix presents many differences from traditionally thermosetting resins used, it allows the adhesion to the substrate. The mechanical properties of these matrices are decidedly inferior to those of the fibers but their union achieves a perfect combination of

strength and durability over time, in addition to ensuring the function for which the reinforcement has been conceived. These are materials of most recent entry in the field of composite materials, consisting of a hydraulic binder and pozzolanic specific additives that favor the development of mechanical and physical characteristics different from those typical of FRP with organic polymer-based matrix.

The followed section reports the mechanical characterization of three different types of matrix: two of organic nature, epoxy resin and polyester resin, and a matrix of inorganic nature, cementitious mortar. After a brief description of the preparation specimens and set-up procedure, the properties mechanical achieved from experimental tests on the different matrices are detailed explained .

3.2.1 Mortar

The mortar analyzed as a matrix of fiber-reinforced composites, is a cement-free white masonry mortar made with pozzonala lime and natural siliceous aggregates having a maximum diameter of 2mm. It has high strength and it is used for strengthening masonry structures in many situations such as: reinforced slabs, webbing of vaults, also reinforcements with carbon fiber bars, reinforced joints.

3.2.1.1 Mortar composition and specimens preparation

Concrete, approx 13 kg/m^2 per cm thickness and mortar 17 kg/m^2 per cm thickness, are the components of the mortar used. In order to prepare the specimens, the mortar was mixed with clean water until a lump-free smooth plastic mix was obtained, using a mixer machine (figure 3.9a). To build the specimens for three points bending tests, wood formwork was used, in order to obtain a prism 160mmx40mmx40mm (figure 3.9b). While to build the specimens for compression tests cylindrical steel formwork is considered (figure 3.9c).

Moreover, previously to the laying of mortar, each formwork was treated with a liquid non-stick .The specimens have been placed in a humidity chamber for ≈20 days and were tested only after 28 days.

a) b) c)

Figure 3.9: a) Mixer machine; b) Formwork for 3PBT; c) Formwork for CT

3.2.1.2 Three point bending tests: setup and procedure

Each specimen was weighed and measured (figure 3.10) in order to know the specific weight and the area to calculate the strength; a load of 10N/s was applied in a continuous way until the failure of the specimens, using a machine with two steel supporting rollers of length between 45 mm and 50 mm and 10 mm ± 0,5 mm diameter, spaced 100,0 mm ± 0,5 mm apart, and a third steel roller of the same length and diameter located centrally between the support rollers (see Figure 3.9b). To calculate the flexural strength, f_f, in N/mm the following equation has been used [22]:

$$f_f = 1{,}5 * \frac{Fl}{bd^2} \qquad (3.2)$$

where:

- F is the maximum load applied to the specimen, in Newtons (N);
- l is the distance between the axes of the support rollers, in millimeters (mm).
- b is the width of specimen in millimeters (mm).
- d is the depth of the specimen in millimeters (mm).

a) b) c)

Figure 3.10: a) Laboratory balance; b) Set-up machine; c) Failure mode

3.2.1.3 Compressive tests: setup and procedure

Compressive tests were carried out by using two different sizes of specimens: on cylindrical specimens (figure 3.11b) and on prismatic specimens. in the latter case, half of the twelve specimens, resulting from the three points bending tests on prismatic specimens were subjected to uniaxial compression tests [22], using two metal plates with a size that allowed the execution of the test on specimens with a cubic form (figure 3.11c).

a) b) c)

Figure 3.11: a) Laboratory balance; b) Set-up machine 1; c) Set-up machine 2

3.2.1.4 Test results

The average values of the mechanical and physical characteristics of the mortar achieved from the experimental tests are shown in Table 3.VII, where ρ indicates the specific weight, f_f is the flexural strength and f_t is the tensile strength, calculated as 80% of the flexural strength.

Table 3.VII

Experimental results obtained from three point bending tests on mortar

(CoV is provided inside parentheses)

	Weight [g]	ρ [Kg/m^3]	$\mathbf{F_{max}}$ [N]	$\mathbf{f_{flexural}}$ [MPa]	$\mathbf{f_t}$ [MPa]
Average	467,025	1824,3	1303,66	3,06	2,44
CoV	(8%)	(8%)	(5%)	(5%)	(5%)

In the table 3.VIII the average values obtained from compressive test are shown, in conclusion the mortar has a value of compressive strength equal to12.2 MPa (average of two tests).

Table 3.VIII

Experimental results obtained from compressive tests on half specimens of mortar and on cylindrical specimens of mortar (CoV is provided inside parentheses)

	F_{max} [N]	f_c [MPa]	**Weight** [g]	ρ [Kg/m^3]	F_{max} [N]	$f_{c/cyindric}$ [MPa]
Average	21001,7	13,1	2958,9	46,64	88700	11,3
CoV	(7%)	(7%)	(1%)	(1%)	(5%)	(5%)

Finally, the following figures 3.12-3.13 show the flexural strength-displacement diagram and the compressive strength-displacement diagram obtained from the experimental tests carried out in the laboratory.

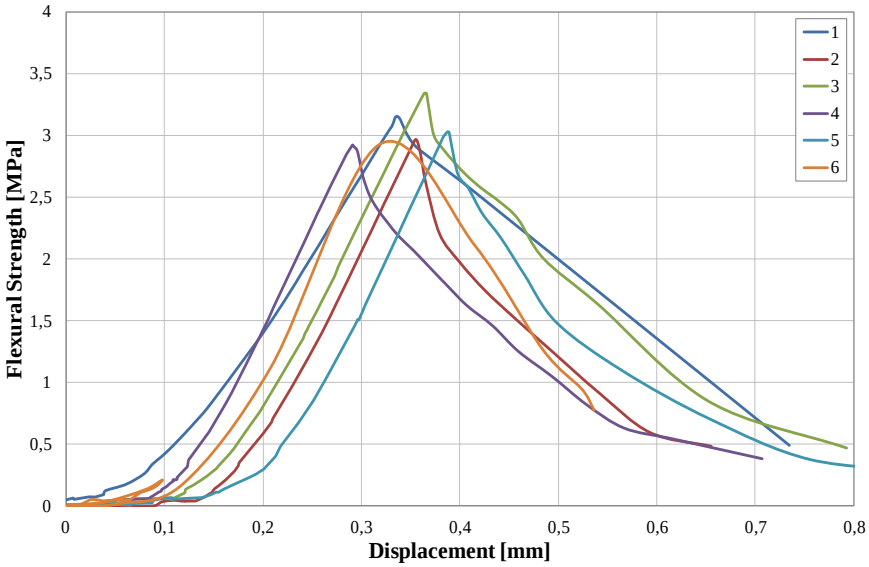

Figure 3.12: Flexural Strength - Displacement Diagram

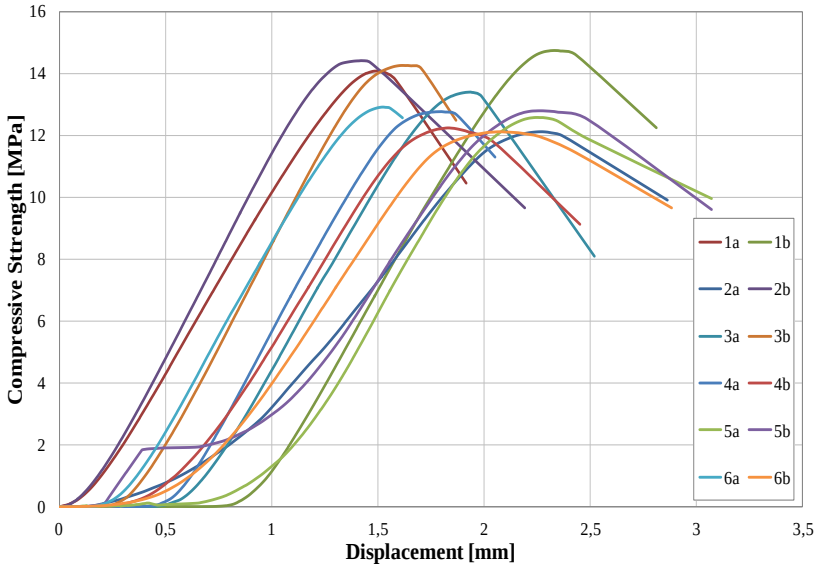

Figure 3.13: Compressive Strength - Displacement Diagram

3.2.2 Resin

In order to manufacture natural fiber-based composite materials, in addition to using of the mortar as a matrix, resin matrices were also taken into consideration, in particular epoxy resin and polyester resin. These types of resin usually are usually used for the impregnation of fabrics, when reinforced elements need to repair or strengthen by using the "dry system". The composition of the resins is made up of two pre-dosed components (Part A = resin and Part B= hardener, with a 4:1 ratio), which have been mixed together before use; once hardened, the matrix has acquired excellent dielectric properties and high mechanical strength.

3.2.2.1 Specimens preparation

The specimens were built in accordance with the specific standard [23], using particular formworks (see figure 3.14) with thickness equal to 4mm (eight specimens, CoV=7%) and width equal to 10 mm (eight specimens, CoV=1%). Moreover, each specimen was weighed obtaining an average value equal to 13g (CoV=5%). The specimens were removed from the formwork after 15 days and cured in room temperature until the time of testing.

a) b) c)

Figure 3.14: a) Formwork of specimens; b) Specimens of Epoxy Resin; c) Specimens of Polyester Resin

3.2.2.2 Tensile tests: setup, procedure and results

Tensile tests on epoxy and polyester resin specimens were carried out using a testing machine (figure 3.15a) conform to the requirements of ISO 7500-1 [24]. The anchorage used was suited to the geometry of the specimens to avoid the slipping of the specimen and to guarantee the only transmission of the tensile force along the longitudinal axis of the specimens. One Extensometer was used to measure the elongation of the specimens under loading; the gauge length of the extensometer was equal to 100mm and the tests length was equal to 200mm (figure 3.15b)

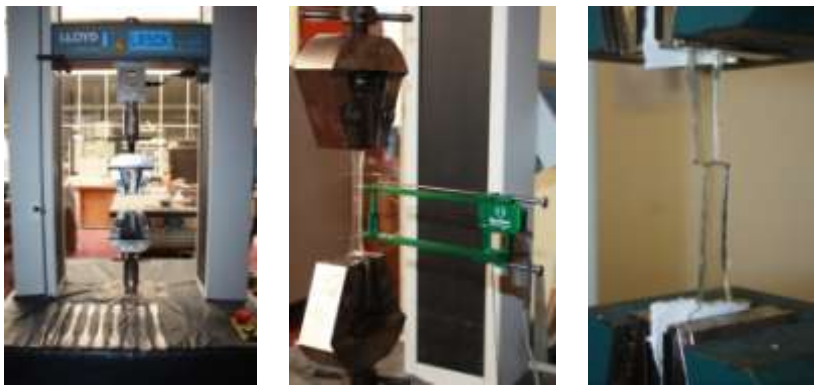

a) b) c)

Figure 3.15: a) Set-up machine; b) Extensometer; c) Failures mode

The tensile strength was calculated using the following equation (3), the Young's modulus was calculated using other equations (4) having measured previously the stress values with the extensometer:

$$f_t = \frac{F_{max}}{A} \qquad (3)$$

$$E = \varepsilon \cdot f_t \qquad (4)$$

The results obtained are summarized in the table 3.IX, while in the figure 3.15, represent the stress-strain diagram obtained from the tensile tests on polyester specimens is represented.

Table 3.IX

Experimental results obtained from tensile tests on polyester resin

(CoV is provided inside parentheses)

	F_{max} [N]	**Area** [mm2]	**f_t** Mpa]	**ε** [%]	**E** [Mpa]
Average	1356,24	41,77	32,47	0,02	2017,92
CoV	(12%)	(6%)	(11%)	(29%)	(19%)

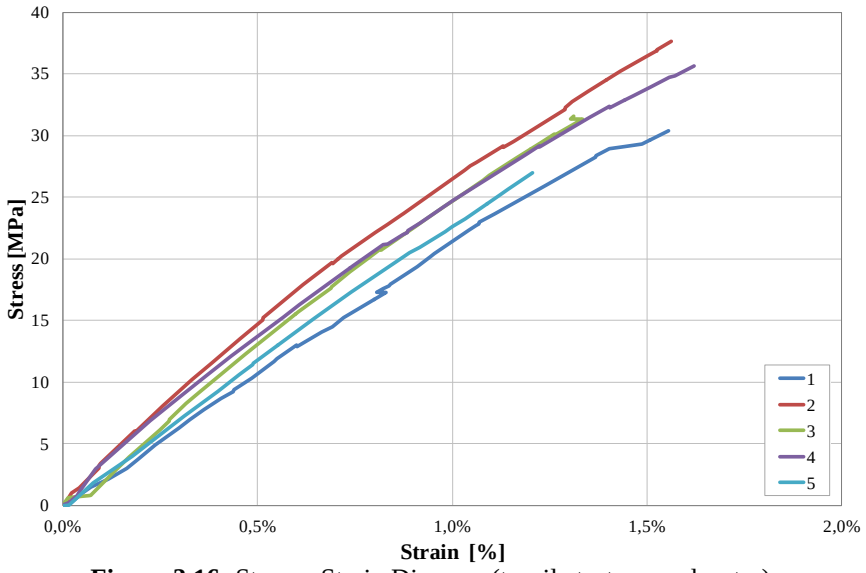

Figure 3.16: Stress - Strain Diagram (tensile tests on polyester)

4

MECHANICAL TESTING AND PERFORMANCE OF NATURAL-FIBER COMPOSITES

4.1 Experimental working plan

Concluded the phase of the mechanical characterization of fibers and matrices, the second part of the research project into two main parts has been divided: the fabrication, in laboratory, of natural fibers-based composite materials followed by characterization tests and the investigation on the adhesion/bond between the masonry system and the composite materials. For this purpose, initially, tensile tests on individual composites were carried out, subsequently, some common bricks usually used in the masonry constructions, were strengthened with composite materials previously produced. The macro-elements built, were subjected to three point bending tests, pull-out tests and single-lap shear bond tests.

Ultimately, two types of composites were produced: *NFRP*, Natural Fiber Reinforced Polymer and *NFRG*, Natural Fibers Reinforced Grout. The natural materials used, are constituted by bidirectional fabrics of flax, hemp, sisal, jute and coir fibers, already analyzed in the chapter 3, whereas the matrices used, are repre-

sented by polymeric matrices and mortar-based matrices. The polymer matrices used are the epoxy resin and the polyester resin. Also in this case, the tests have been performed in the Civil Engineering Laboratory and Fibrous Materials Laboratory at University of Minho.

4.2 Tensile Tests

At the beginning, the tensile tests on NFRP epoxy resin-based matrix have been performed, distinguishing the specimens cut in the warp direction (90°) than those cut in the weft direction (0°). All the seven bidirectional fabrics analyzed in the chapter 3 have been utilized in order to manufacture the composite materials, which have been identified with the acronyms $FFRP_{epoxy}$ (Flax Fiber Reinforced Polymer with epoxy resin), $HFRP_{epoxy}$ (Hemp Fiber Reinforced Polymer with epoxy resin), J^1FRP_{epoxy} (Juta[1] Fiber Reinforced Polymer with epoxy resin), J^2FRP_{epoxy} (Juta[2] Fiber Reinforced Polymer with epoxy resin), J^3FRP_{epoxy} (Juta[3] Fiber Reinforced Polymer with epoxy resin), S^1FRP_{epoxy} (Sisal[1] Fiber Reinforced Polymer with epoxy resin), S^2FRP_{epoxy} (Sisal[2] Fiber Reinforced Polymer with epoxy resin).

By the results obtained from the tests carried out on composites epoxy resin-based matrix (as it will see at the end of the chapter), it is found that the main direction of the fabric, then the warp direction (90°), is the most suitable for the production of natural fibers-based composites, especially in terms of strength. It was also possible to assess the natural materials with higher mechanical properties. Consequently to this, the composite polyester resin-based matrix and composite mortar-based matrix were produced, always in the laboratory, using the four fabrics with the highest performance and in the warp direction only.

In conclusion, flax, hemp, juta[1] and juta[3] (see figure 3.4) were the fabrics used to produce composite materials with polyester resin and mortar as a matrix. In this case, the composite materials have been identified as $FFRP_{polyester}$, $HFRP_{polyester}$, $J^1FRP_{polyester}$, $J^2FRP_{polyester}$ and *FFRG* (Flax Fiber Reinforced Grout), *HFRG* (Hemp Fiber Reinforced Grout), J^1FRG (Juta[1] Fiber Reinforced Grout), J^2FRG (Juta[2] Fiber Reinforced Grout).

To sum up, the schematization of the experimental tensile tests on natural fiber-based composites performed, is shown in Figure 4.1.

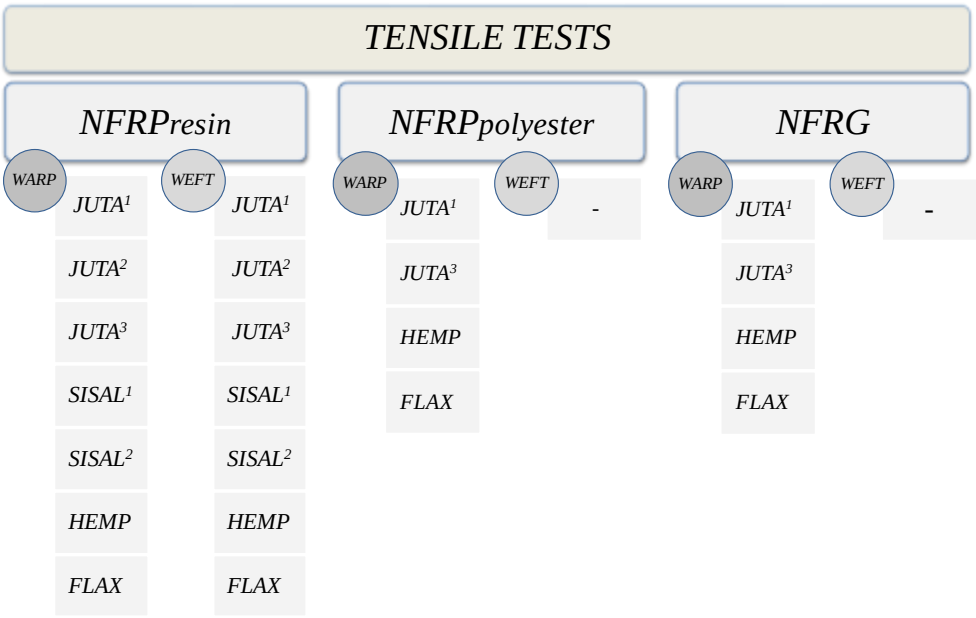

Figure 4.1: Scheduling of experimental working plan for tensile tests

4.2.1 Materials and specimens manufacturing

All the specimens were cut with size equal to 300x50mm^2, being the test length equal to 200mm, in accordance with the standards [20]. Each specimen has been equipped with special steel plates on the edges, in order to ensure a uniform distribution of the load and to avoid the specimen from slipping during the test. Specimens with polymer matrix were tested after 15 days from the preparation in order to guarantee the proper curing of the matrix, while in the case of the mortar, the experimental tests were carried out after 28 days.

In the case of NFRP polyester resin-based matrix, the so called Vacuum Infusion Process (VIP) has been used (figure 4.3). Thanks to this technique it is obtained a constant thickness of the specimens on the contrary to that obtained with the epoxy resin. On the other hand, the NFRP epoxy resin-based matrix were produced with a typical hand lay-up, the fabrics have been manually impregnated using ordinary brushes (figure 4.4).

Vacuum Infusion process

The Vacuum Infusion Process (VIP) is a technique that uses vacuum pressure to drive resin into a laminate. Materials are laid dry into the mold and the vacuum is

applied before resin is introduced. Once a complete vacuum is achieved, resin is literally sucked into the laminate via placed tubing [25-26].

The steps that are performed during the Vacuum Infusion Process are the following: first, the mold and the fabrics were prepared and the vacuum lines were selected. After that, the resin was fed from a standing source (a bucket). Before closing the vacuum bag, the line for getting the resin into the fabric was installed. Both for applying vacuum and for getting the resin in the bag, spiral tubing was used. At this time, it was built the vacuum bag, but before the pump was switched on, the resin line was clamped off, to prevent air bubbles. Once the vacuum bag was closed, the flow regulator to unclamp the resin inlet was remove and the resin quickly was sucked through the tube and into the bag. The resin was visibly moving and this operation has continued until the entire laminate was saturated (figure 4.2).

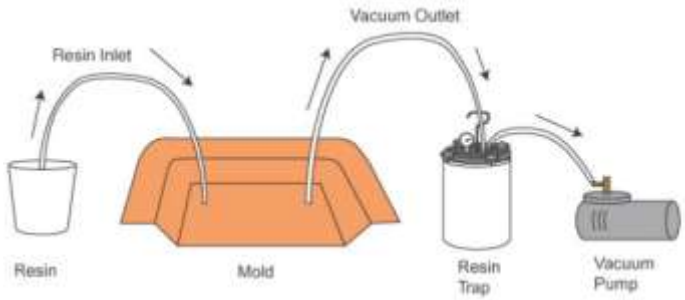

Figure 4.2: Vacuum Infusion sequence illustration

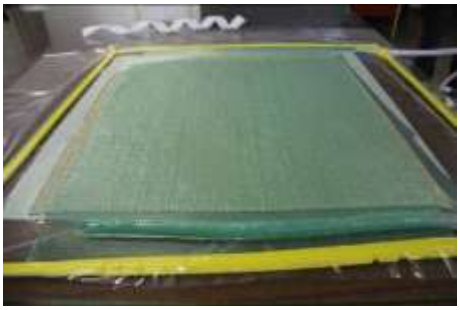

a)

b)

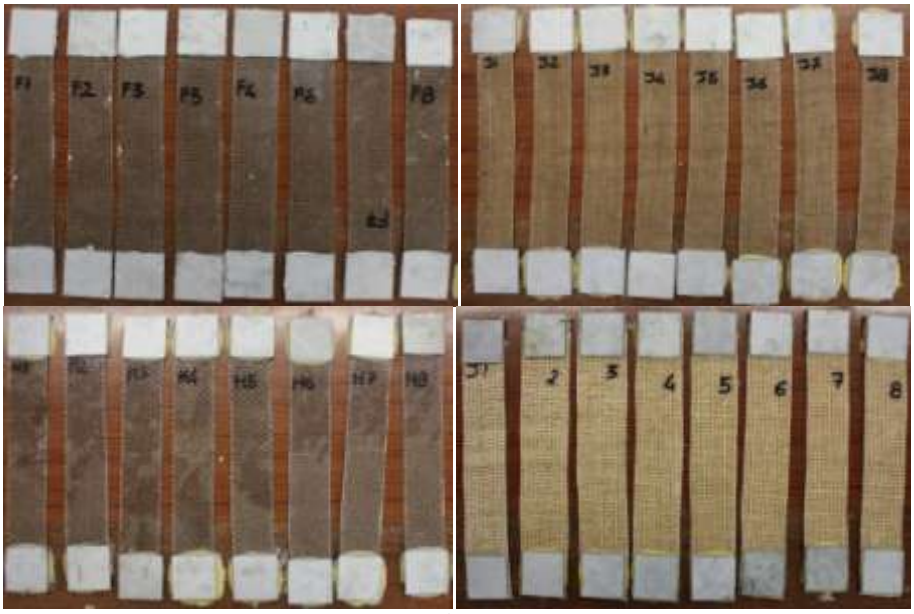

c)

Figure 4.3: Vacuum Infusion technique: (a) preparation of the specimens; (b) Cut of the specimens; c) Specimens with steel plates

Figure 4.4: Preparation of the specimens NFRP with epoxy resins-based matrix

Lastly, to produce NFRG composites, a particular formwork was used in order to obtain a total thickness of the specimen equal to 5 mm: 2 layers of mortar of 2mm each were built plus the layer of the fabric (figure 4.5). Finally, even in this case steel plates in both extremities of the specimen have been glued.

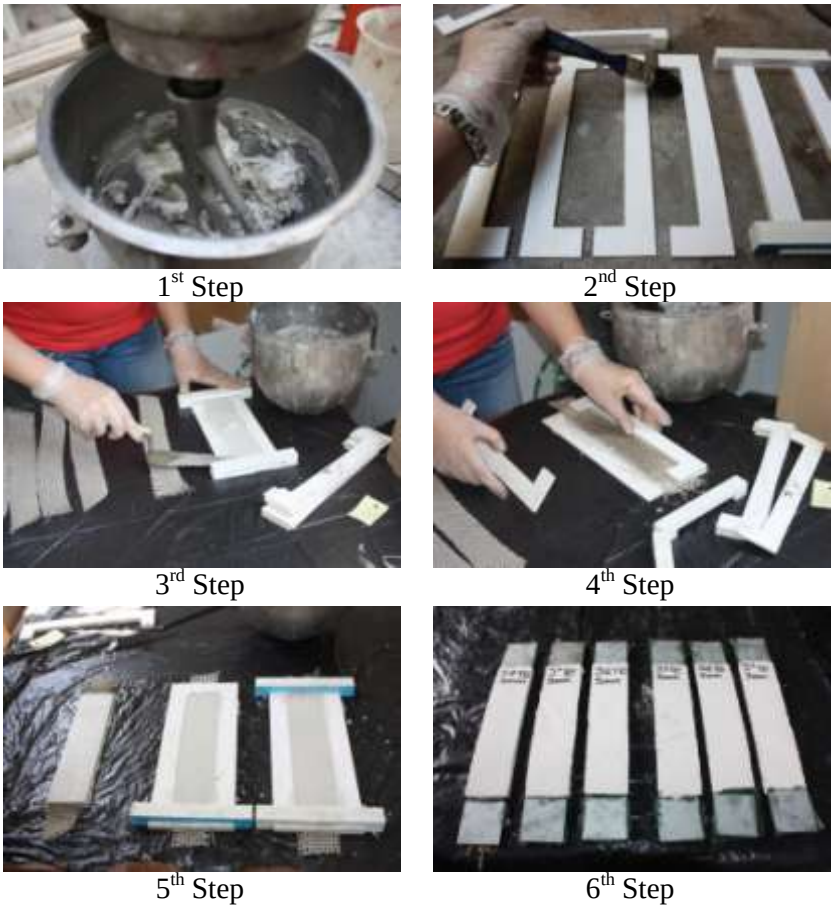

Figure 4.5: Steps carried out to preparation of NFRG

All tensile tests were conducted in a normal atmosphere on specimens previously acclimatized, by means of a high precision universal testing machine, and conducted under displacement control of the crossbar. Before each test, a pre-load of 10N (NFRP) and 1,5N (NFRG) were applied and a crosshead speed equal to 100mm/min (NFRP) and 25mm/min (NFRG) were used.

4.2.2 Results and failure mode

Tensile tests on NFRP and NFRG were carried out to the aim to study the tensile behavior and strength of the natural fiber-based composites previously manufactured, to plot the stress-strains diagram, therefore their constitutive laws.

Substantially, the mechanical properties achieved from the tests are the tensile strength, f_t (MPa), Young's modulus, E (MPa) and the ultimate strain ε (%). To calculate the tensile strength the equation 4.1 was used, whereas the nominal cross-sectional area was calculated taking into account the width of the specimens, mainly the number of the yarns in the specimens. Each specimen was cut with the same number of yarns in the warp direction, so the load direction. Regarding the ultimate strain, which corresponds to ultimate tensile capacity of the composite, it was calculated using equation 4.3, considering the size of the test length in the first (l_i) and in the last step (l_f) of the tests. Finally, the Young's Modulus, it was calculated as a difference between the load stress-strain curve obtained from the load level at 20% and 50% of the tensile capacity (equation 4.4).

$$f_t = \frac{F_{max}}{A} \tag{4.1}$$

$$A = A_{yarn} \cdot n^{\circ}_{yarns} \tag{4.2}$$

$$\varepsilon = \frac{\Delta l}{l_i} = \frac{l_f - l_i}{l_i} \tag{4.3}$$

$$E = \frac{\Delta F}{\Delta \varepsilon \cdot A} = \frac{F_{50\%} - F_{20\%}}{(\varepsilon_{50\%} - \varepsilon_{20\%}) \cdot A} \tag{4.4}$$

Table 4.I

Average values obtained from tensile tests on NFRP epoxy resin-based matrix - warp and weft direction (CoV is provided inside parentheses)

		J^1FRP_{epoxy}	J^2FRP_{epoxy}	J^3FRP_{epoxy}	S^1FRP_{epoxy}	S^2FRP_{epoxy}	$HFRP_{epoxy}$	$FFRP_{epoxy}$
ε_{peak} [%]	*warp*	1%	1,27%	3,38%	2,22%	1%	1,35%	1,91%
		20%	25%	32%	53%	19%	13%	16%
	weft	0,7%	1,0%	3,5%	1,8%	1,1%		
		15%	48%	31%	10%	19%		
***ft* [MPa]**	*warp*	87,32	77,59	73,52	35,21	27,58	63,13	117,37
		31%	10%	15%	25%	6%	12%	17%
	weft	59,42	63,95	37,30	15,95	23,25		
		19%	23%	12%	15%	5%		
***E* [MPa]**	*warp*	1382,24	1430,08	748,10	1272,94	2235,76	1674,7	1866,61
		17%	11%	20%	29%	16%	9%	20%
	weft	3278,67	1157,98	541,89	693,10	1840,65		
		15%	23%	23%	12%	25%		

In the table 4.I, the results achieved from tensile tests on $NFRP_{epoxy}$ are summarized. As expected, following the results obtained for the non-impregnated fabrics, it is observe that flax is the material with higher mechanical properties, followed by jute and hemp; sisal fibers reinforced polymer ($SFRP_{epoxy}$) composites are not suitable as a reinforced fibers due to the lower performance. To confirm what demonstrated during the previously tests carried out (tests on non-impreganted fabrics), also in this case the main direction of the fabric (warp direction) is even the most strong.

Table 4.II
Average values obtained from tensile tests on NFRP polyester resin-based matrix, NFRG (CoV is provided inside parentheses)

Matrix\ Fiber	$NFRP_{Polyester}$			NFRG		
	ε_{peak} [%]	ft [MPa]	E [MPa]	ε_{peak} [%]	ft [MPa]	E [MPa]
JUTE[1]	2% (20%)	80,3 (10%)	4135,3 (20%)	5% (12%)	25,9 (7%)	531,3 (10%)
JUTE [3]	4,48% (11%)	64,3 (21%)	1431,5 (18%)	10,38% (9%)	35,6 (8%)	345,5 (13%)
HEMP	3,84% (18%)	58,2 (13%)	1535 (9%)	3,84% (18%)	33,1 (8%)	268,2 (5%)
FLAX	2,49% (10%)	109,8 (17%)	4393,3 (9%)	7,41% (6%)	57,2 (3%)	774,2 (7%)

Regarding the tensile tests on NFRP polyester resin-based matrix and NFRG, the results achieved are listed in the table 4.II. Impregnated fabrics with polyester resin present tensile strength lowest than those impregnated with epoxy resin. The same applies to the composites based on cement mortar, which show some difficulties related to the water content and to the bond between the water and the fibers reinforcing. So consequently it can be stated that the epoxy resin is most suitable as a matrix of natural fiber composite materials.

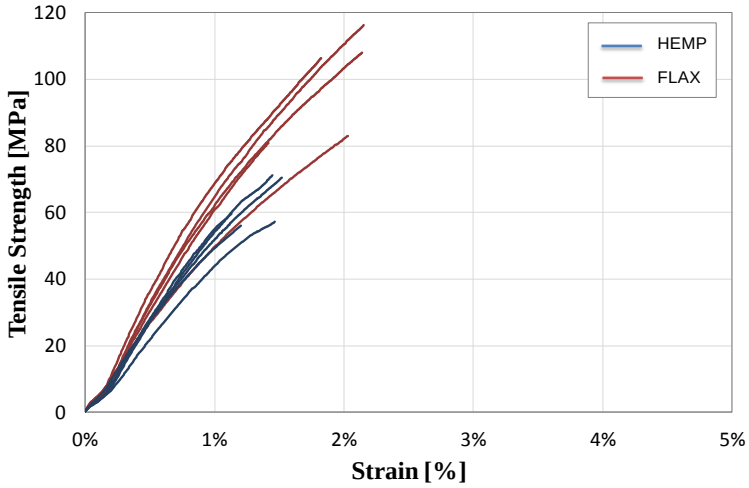
Tensile Strength [MPa]
120
100
80
60
40
20
0
0%
1%
2%
3%
4%
5%
Strain [%]
HEMP
FLAX

a)

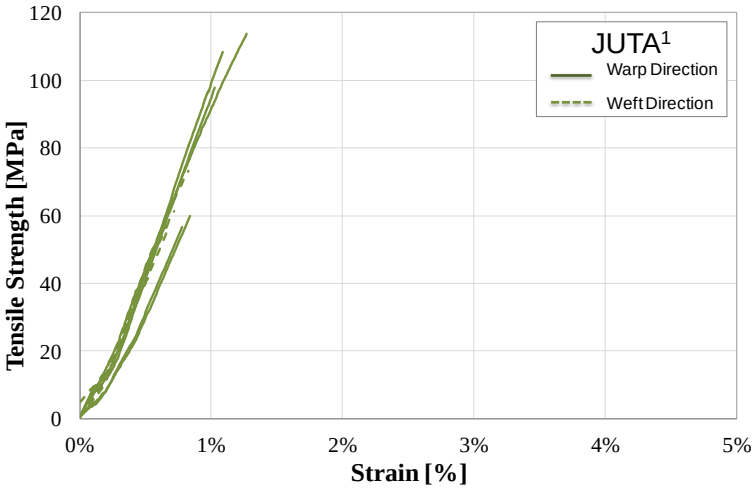
Tensile Strength [MPa]
120
100
80
60
40
20
0
0%
1%
2%
3%
4%
5%
Strain [%]
JUTA1
Warp Direction
Weft Direction

b)

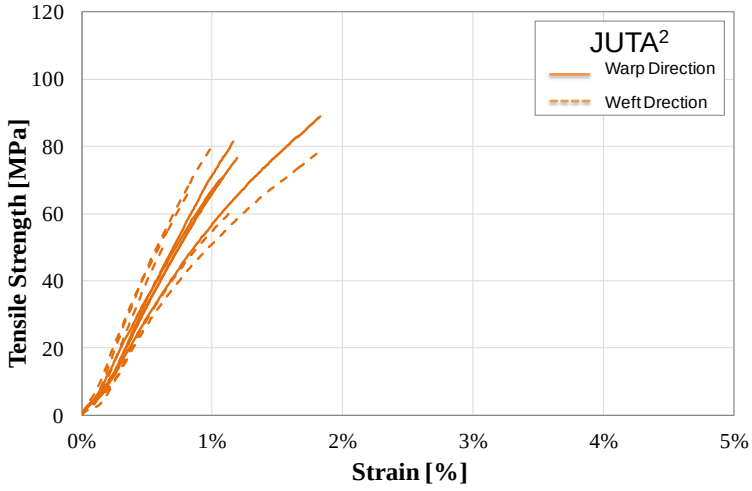
Tensile Strength [MPa]
120
100
80
60
40
20
0
0%
1%
2%
3%
4%
5%
Strain [%]
JUTA2
Warp Direction
Weft Drection

c)

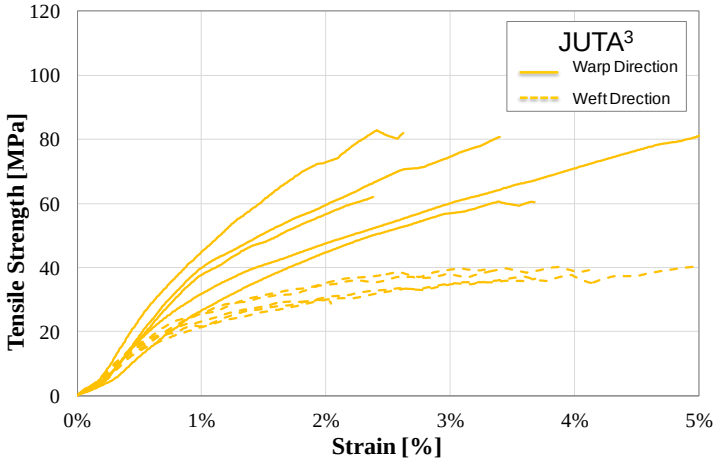

d)

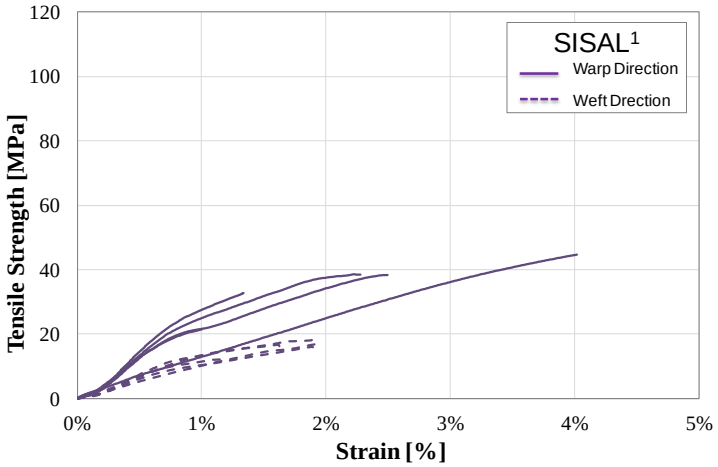

e)

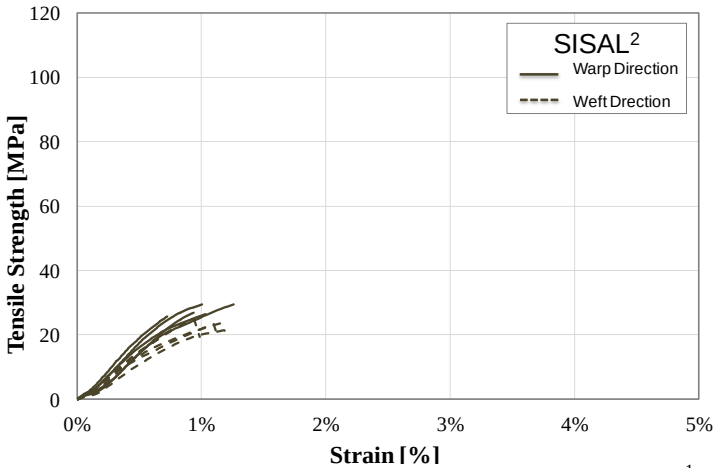

f)

Figure 4.6: Tensile stress - strain diagrams: $FFRP_{resin}$, $HFRP_{resin}$ (a); J^1FRP_{resin} (b); J^2FRP_{resin} (c); J^3FRP_{resin} (d); S^1FRP_{resin} (e); S^2FRP_{resin} (f).

The stress-strain curves of each epoxy resin-based composites (figure 4.6), highlight the brittle behavior of these materials, characterized by a hardening final part, also in the case of tensile tests on NFRP polyester resin-based matrix, the same behavior was observed (figure 4.7). On the other hand, in the case of NFRG the stress-strain curves, for all type of material used, are characterized by a softening final part (figure 4.8), as happens in the case of non-impregnated fabrics (figure 3.8).

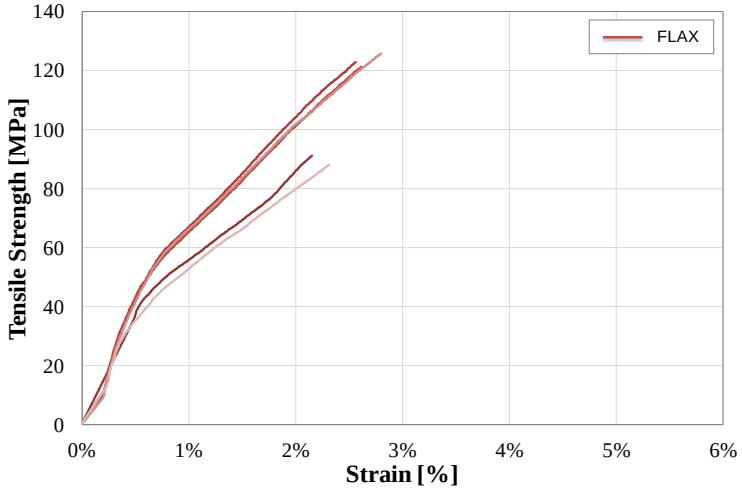

a)

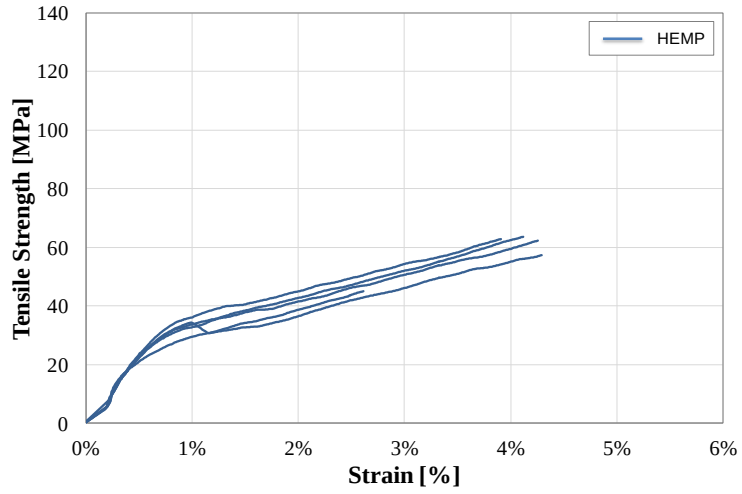

b)

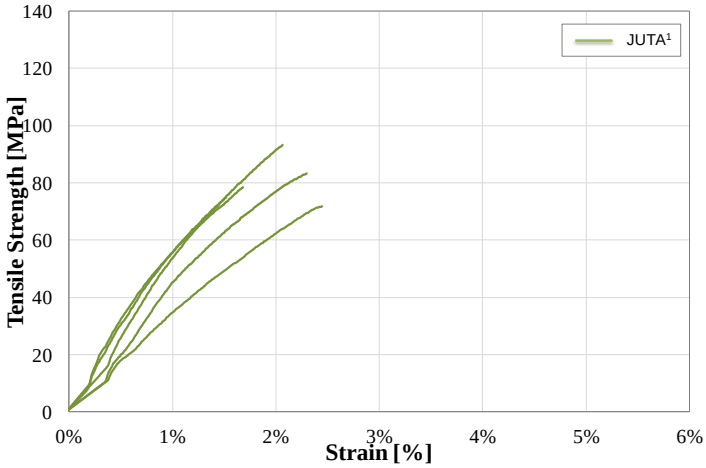

c)

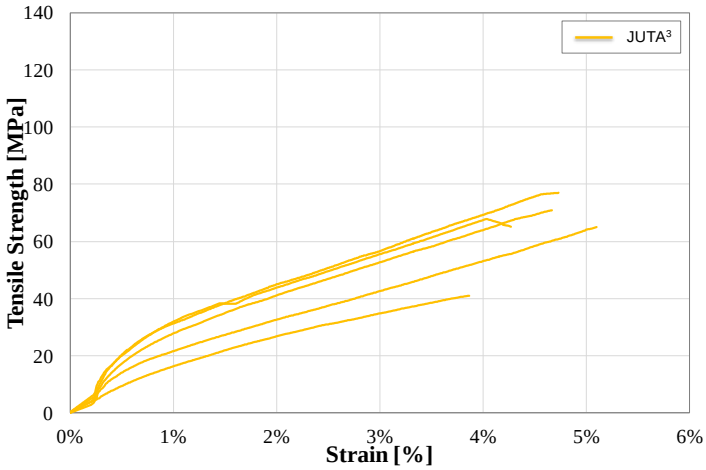

d)

Figure 4.7: Tensile stress - strain diagrams: $FFRP_{polyester}$ (a); $HFRP_{polyester}$ (b); $J^1FRP_{polyester}$ (c); $J^3FRP_{polyester}$ (d).

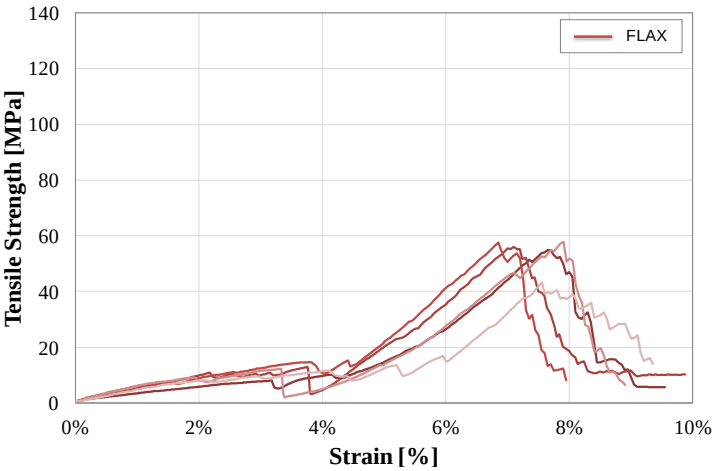

a)

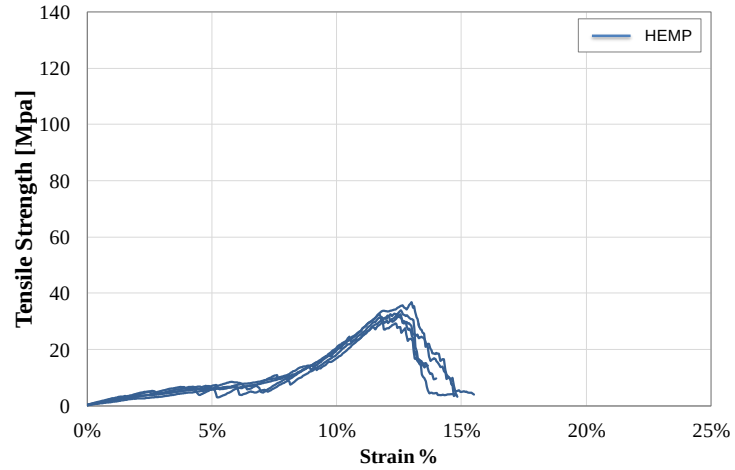

b)

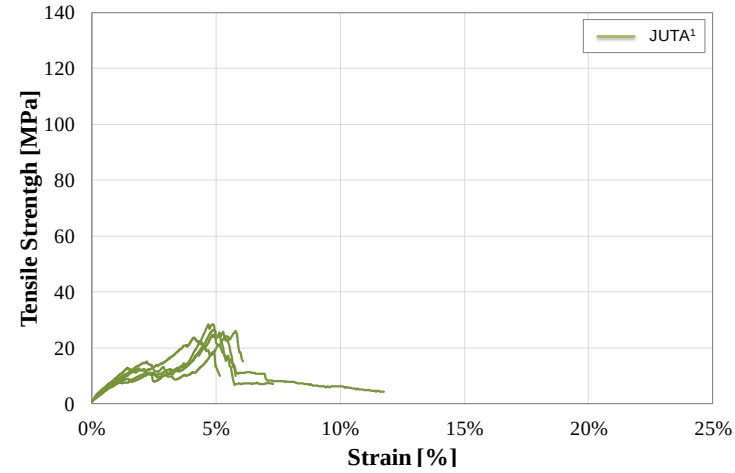

c)

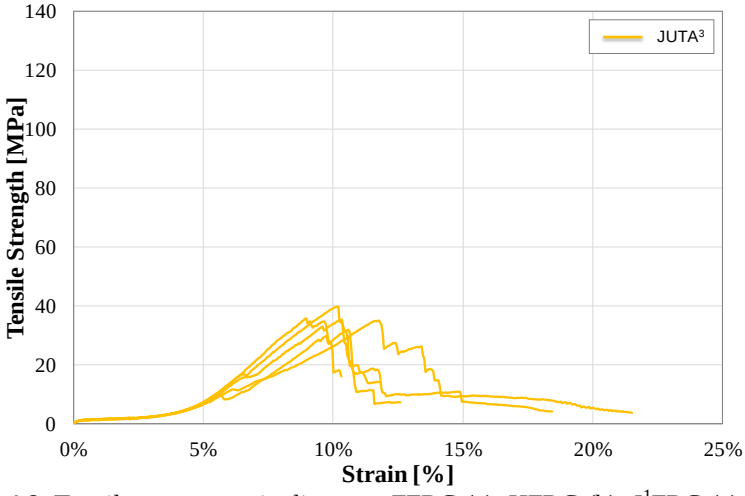

d)

Figure 4.8: Tensile stress - strain diagrams:FFRG (a); HFRG (b); J^1FRG (c); J^3FRG (d).

For the different strengthening systems used, it is of primary importance to discuss of failure modes of the specimens. In the case of non-impregnated specimens there is a reduction of area of the individual yarns that make up the fabric (figure 4.9a), while in the impregnated specimens with the polymer matrix, epoxy (figure 4.9b) and polyester (figure 4.9c), it's possible to notice a instantaneous and uniform break of the specimen. Finally, in the case of cement-based composite, the failure mode occurs slowly marked by the rupture of mortar at the beginning and follow the break/stretching of single yarns that make up the fabric (figure 4.7d). During the tests it was possible to observe a good bond between natural materials and the different types of matrixes.

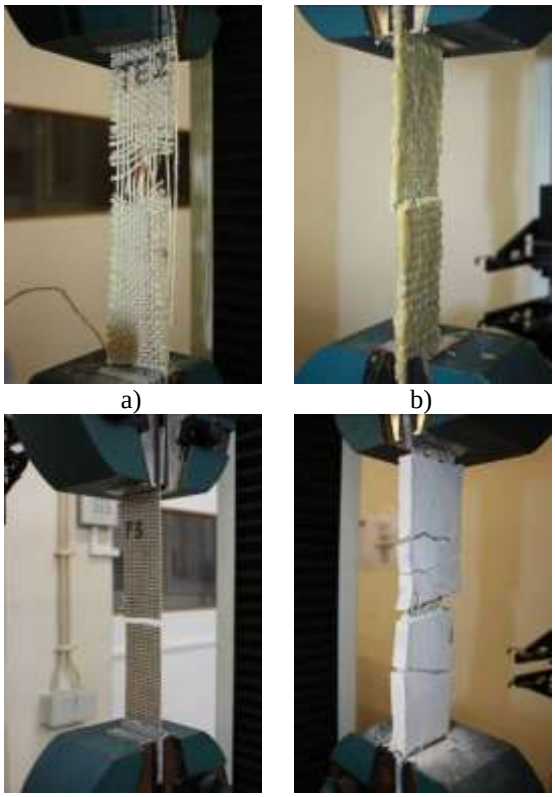

a) b) c) d)

Figure 4.9: Failure mode: Non-impregnated fabrics (a); $NFRP_{epoxy}$ (b); $NFRP_{polyester}$ (c); NFRG (d).

4.3 Pull-out test on strengthened brick

Pull-out tests have been carried out with the aim to evaluate the pull-out strength or commonly called adhesion stress of strengthened masonry bricks. Generally, the execution of test enables to determine the greatest perpendicular force (in tension) that a surface area can bear before a plug of material is detached, or whether the surface remains intact at a prescribed force.

This tests method is a destructive tests, because at the end of the test the maximum force leads to failure of the specimens. Failure usually occurs along the weakest plane within the system comprised of the test fixture, adhesive, composites system and substrate, and is exposed by the fracture surface [27].

4.3.1 Test preparation and procedure

In order to performed pull-out tests, the masonry units used as the substrate were Portuguese traditional solid clay bricks (figure 4.10) with dimension of 200x100x55mm^3, a mean compressive strength of 20MPa (CoV=2,5%), tensile strength of 2,2MPa (CoV=4%) and modulus of elasticity of 5579 MPa. These properties were kindly provided by the University of Minho. Furthermore, flax-based composites and hemp fiber-based composites with epoxy resin-based matrix ($FFRP_{resin}$ and $HFRP_{resin}$) were used to strengthen the bricks and to build the final macro-elements to be tested. In total 5 macro-elements for each type of fiber (flax and hemp) were prepared in laboratory.

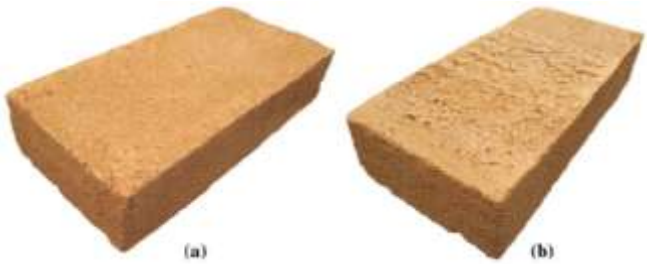

Figure 4.10: Portuguese traditional solid clay bricks:
a) front and b) back sides of brick

The steps that have characterized the preparation of test pieces are divided as so: following the cleaning of the bricks, the composite system was applied. After primer application, a fiber strip of 70 mm width was glued on the brick (Figure 4.11a, plan view). Afterwards, a partial-depth core with 49-mm diameter and 10

mm depth was drilled, see Figure. 4.11a (elevation view), which lead to the creation of circular strengthened areas where rigid steel plates were glued. The testing machine is schematically indicated in Figure 4.11b. In this case only the LVDT control was considered, in correspondence to the load cell.

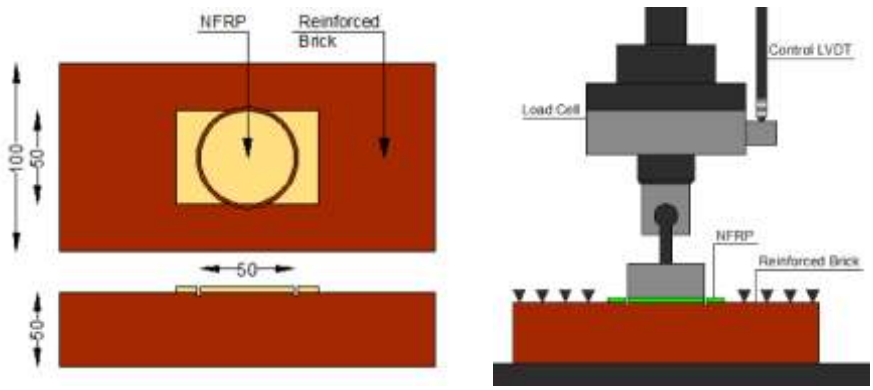

(a) (b)

Figure 4.11: Pull-off tests: (a) Specimen's size (plan view and elevation view); b) Schematic representation.

4.3.2 Calculation of the results and failure modes

Experimental pull-off tests were performed under displacement control. These tests were performed following the guideline ASTM D4541-02 [27]. Table 4.III illustrates the average pull-off test results for the two types of fibers used (flax and hemp). To compute the relative stress applied to each macro-element the following equation was used:

$$f_{pull-out} = \frac{4F}{\pi d^2} \qquad (4.5)$$

where:

- $f_{pull\text{-}out}$ is the pull-off strength achieved at failure of the specimens, in MPa;
- F is tha actual force applied to the tests surface, in Newton (N);
- d is the equivalent diameter of the original surface area stressed, also equal to the diameter of the loading fixture, in millimeters (mm).

Table 4.III
Average of results obtained from pull-off tests (CoV is provided inside parentheses).

	Fiber type	**F_{max}** [kN]	**Pull-out strength** [kPa]
Strengthened	FLAX	2,28 (9%)	1208 (9%)
	HEMP	2,38 (4%)	1265 (4%)

The results indicate that the pull-off strength is practically independent of the fiber, in fact it can be observed the same value of tensile bond strength. This feature can be explained based on the failure behavior registered. For all specimens tested, failure was characterized by the ripping of a thin layer of brick (peeling), as illustrated in Figure 4.12. Indeed, the results show that the tensile strength of the interfaces depends on the tensile strength of the substrate, therefore of the bricks, which is the weakest element of the NFRP-resin-substrate composite system under direct tensile loading.

a) b)

Figure 4.12: a) Schematic failure modes for PT; b) Specimens tested.

In addition, in the figure 4.13 it can be observe the Tensile bond strength – Displacement experimental envelope of unreinforced brick and strengthened brick with $HFRP_{epoxy}$ and $FFRP_{epoxy}$.

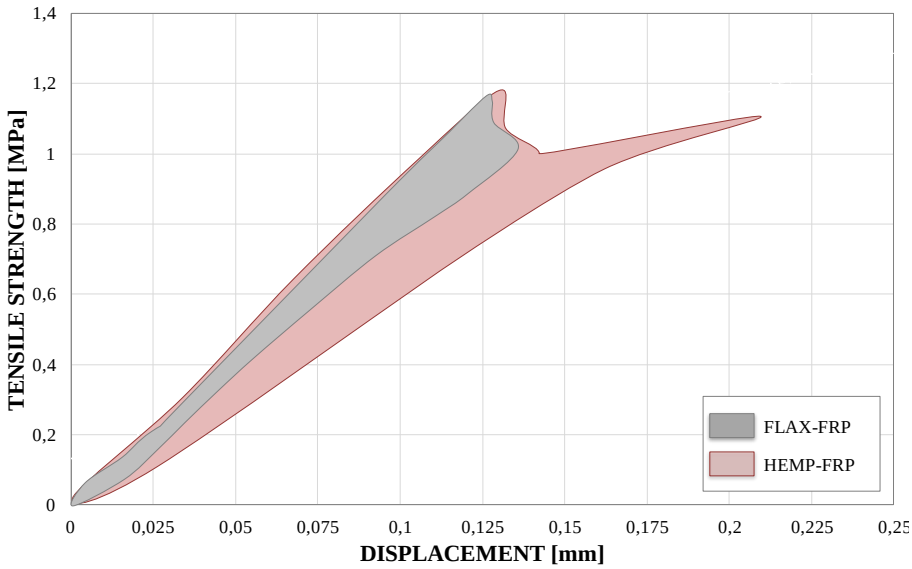

Figure 4.13: Experimental envelope obtained from pull-out tests on Hemp-FFRP and Flax-FFRP strengthened bricks

4.4 Three point bending tests

The flexural failures usually occur on thin panels masonry structures, when they are subjected to horizontal effects, such as wind or earthquake. In this case, the state of stress that occurs in the masonry structures, is typically bending. In this regard, three-point bending tests were performed in order to analyze the bending resistance of macro-elements in masonry reinforced with natural fibers-based composites [28].

4.4.1 Specimens preparation and set-up procedure

To carry out three point bending tests, the same solid clay bricks (figure 4.10) were used as substrate. Also in this case, as for the pull-out tests, flax fiber-based composites and hemp-based composites with a matrix-based thermosetting epoxy resin were selected, to prepare the specimens. The difference compared with the previous tests has been that of be tested both unreinforced and reinforced bricks (figure 4.14). A total of 18 specimens have been built in the laboratory, 6 unreinforced brick and 12 reinforced bricks (6 with $FFRP_{resin}$ and 6 with $HFRP_{resin}$).

a) b)

Figure 4.14: a) Unreinforced brick; d) Reinforced bricks with strain gauges

The testing machine is composed of the fixing of three points (Figure 4.15a); two lower supports and striking edge and the load at midspan, with a radius of 125mm. The sizes of the specimens are schematically indicated in Figure 4.14b. Natural fiber-based composites under study have a thickness t_{fiber}=3mm for flax (six specimens, CoV=16%) and t_{fiber}=2,5mm for hemp (six specimens, CoV=11%). One layer of fabric, previously cut in the warp direction (90° direction) with dimensions equal to 140x50mm^2, for each specimen was applied to the brick, after the cleaning of the substrate and the primer application. To measure the displacements, two LVDT's were applied to the specimen, one in the midpoint of the brick and another, of control, corresponding to the load cell.

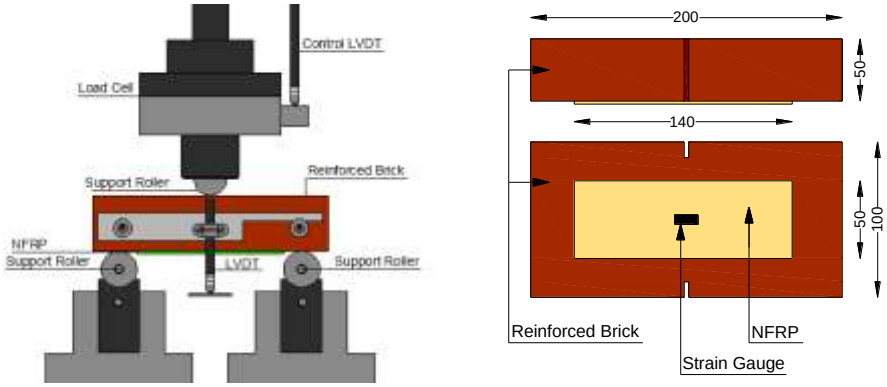

(a) (b)

Figure 4.15: Three points bending test: (a) Schematic representation for TPBT; (b) Specimen's size, plan view and elevation view.

However, to know the value of the strain, one strain gage was bonded at the centerline of the composite (fig. 4.15b).

4.4.2 Results and failure modes

Experimental tests were carried out according to BS EN 1015-11:1999 [22]. However, the tests carried out in this present work differ from the tests described in the standard procedure: in the current test the specimens are bigger (200x100x50mm^3) and they are masonry bricks commonly used in the field of civil applications. Only after 15 days from the preparation of the specimens the tests have been performed, in order to guarantee the proper curing of the matrix applied to the substrate.

To calculate the flexural strength, $f_{flexural}$ (N/mm), it was used the following equation:

$$f_{flexural} = \frac{Fl}{bd^2} \qquad (4.6)$$

where:

- F is the maximum load applied to the specimen, in Newton (N);
- l is the distance between the axes of the support rollers, in millimeters (mm);
- b is the width of specimen in millimeters (mm);
- d is the depth of the specimen in millimeters (mm);

Table 4.IV
Average of results obtained from three point bending tests (CoV is provided inside parentheses).

		d [mm]	**F_{max}** [kN]	**$f_{flexural}$** [kPa]	**ε** [μm/m]
Unstrengthened		0,82 (59%)	4,81 (14%)	800 (14%)	_
Strengthened	HEMP	0,68 (69%)	6,18 (4%)	980 (3%)	1142 (44%)
	FLAX	0,91 (32%)	6,49 (2%)	1050 (3%)	1284 (17%)

The results obtained demonstrate that the reinforced bricks are more resistant when compared to unreinforced bricks, as expected. Indeed, it's possible to note that the reinforced bricks are characterized by an increment of flexural resistance of almost 30% with flax and 28% with hemp (see Table 4.IV).

Also the figure 4.16 shows the maximum Force – Displacement experimental envelope of unreinforced bricks and reinforced bricks (Hemp and Flax). It is possible to note as the reinforced bricks acquire higher ductility than the unreinforced bricks, given the presence of the composite materials, as well as greater resistance in terms of maximum force.

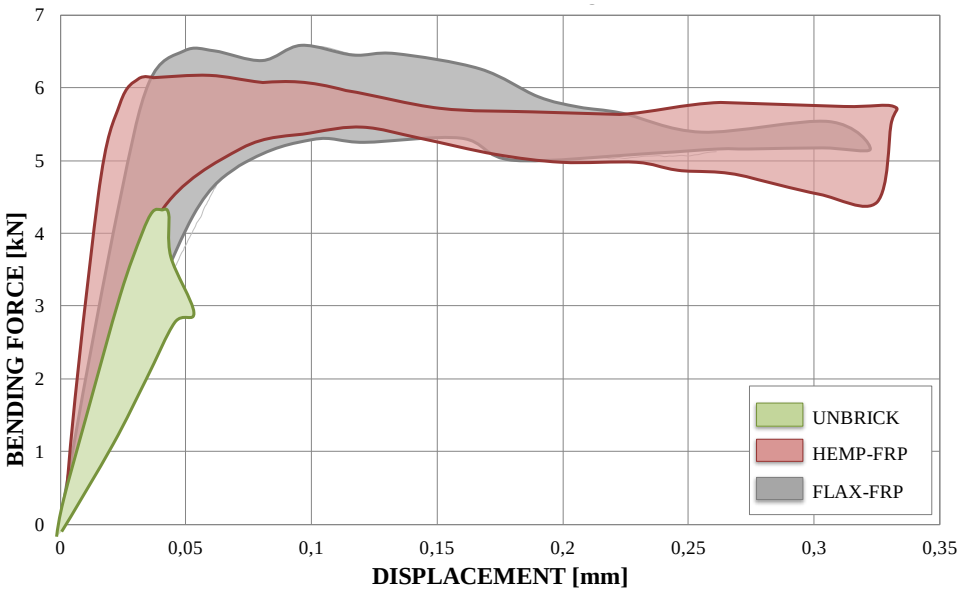

Figure 4.16: Experimental envelope obtained from three point bending tests on unreinforced brick (UNBRICK), Hemp-FFRP and Flax-FFRP strengthened bricks

The failure mode of the specimens is characterized by the breakage of the specimen in the section at the mid-span. This mode is the same for both flax-based reinforced and hemp-based reinforced bricks (Figure 4.17a and 4.17b). Any phenomena of delamination has been not observed, rather it was revealed a strong bond between the composite material and the substrate.

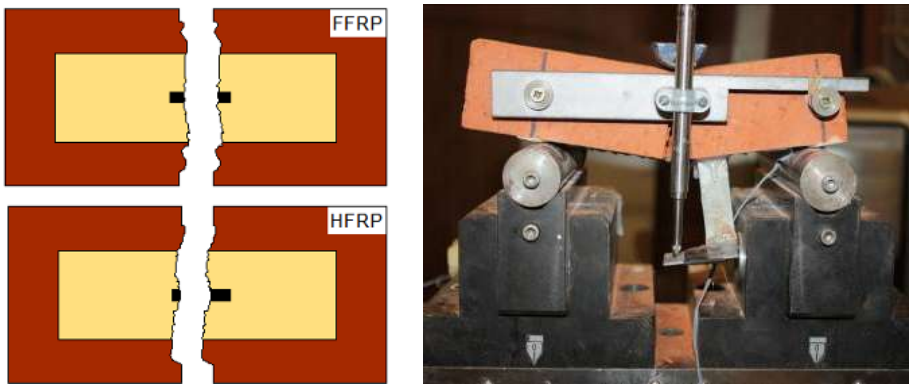

a) b)

Figure 4.17: a) Schematic failure modes for TPBT; b) Testing machine.

4.5 Single-lap shear bond tests

The behavior of structural elements externally reinforced with composite materials has as key mechanism the delamination phenomenon on the composite from the substrate. In the last years, numerous experimental and theoretical studies have investigated the bond behavior in FRP-strengthened concrete. Recently, the scientific research has also focused on the study of the adherence between FRP and masonry substrate. The field of investigation is, however, very extensive due to the heterogeneity of the masonry structures and their low strength substrate.

In (Ceroni et al., 2003), (Aiello and Loose 2005 [29]), and (Accardi, 2006) the results obtained from delamination tests on natural stones are studied. In (Olivito et al. 2007 [30] 2009 [31]) (Panizza et al 2008) and (Briccoli Bati et al. 2009) adherence tests on single clay brick are analyzed. Other experiments aimed to study the phenomenon of masonry are found in (Casareto et al. 2003) and in (Basil et al. 2005) in which the properties of adhesion to the substrate with different size of the bond area are analyzed. Experimental research carried out, highligth that not only the properties of the materials, but also the geometry of the specimens may influence the failure modes to delamination. Other research project (Fedele and Milani 2010), (Faella et al.,2011 [32]) and (Ghiassi et al., 2012 [33]) have conducted empirical formulation and numerical analysis on topic of bond behavior between masonry bricks and composite materials.

On the contrary, single lap shear bond tests on masonry bricks strengthened with cementitious-based matrix composites are less studied. In (Briccoli Bati et al. 2004) bond tests using GRRCM composites are presented and compared with simi-

lar tests on bricks reinforced with CFRCM. Other experimental tests, in (Faella et al. 2009) and (Focacci et al. 2009) can be found, in which specimens of stone and brick are reinforced with CFRCM composites. However, the experimental results on macro-elements of masonry reinforced with FRCM systems, although in number significantly lower than those strengthened with FRP composites, mostly, show failure modes localized on the reinforced layer, rather than in the first layer of the support (see Section 4.5.1). However, the possibility of collapse in the fibers (other very frequent failure modes in the cement-based matrix composites), can be excluded, if it do a careful design that takes account of the non-uniform distribution of the stress in the whole width of the fabric.

4.5.1 Different types of failure modes according with standard

The application of composite materials as structural strengthening requires the use of special adhesives. The choice of the adhesive depends on several factors, one in particular is related to the characteristics of the support (concrete, masonry or wood). Usually the technical data sheet for the FRP-based structural strengthening give specific instructions about the type of adhesive to be used depending on the type of work to be performed. There are many types of natural and synthetic adhesives: the most suitable adhesives for composite materials are based on epoxy resin; adhesive-based on mortar are less used yet.

The well-known problems of debonding, especially in the field of civil engineering, depend precisely from the relationship between the adhesive and the mechanical properties of the substrate [16]. On the basis of the above, the current standards have been identified three types of fracture for adhesive bonding (Figure 4.18):

- *Cohesive fracture*: it takes place inside one of the materials forming the connection. The same material is therefore on both sides of the fracture surface, which may be either smooth or rough. It is the ideal fracture for adhesive.
- *Adhesive fracture*: it takes place at the interface between adhesive and support when the adhesive strength is lower than that of the support. The fracture surface is typically smooth. This type of fracture highlights inaccurate applications.
- *Mixed fracture*: it appears as both cohesive and adhesive failure. The fracture surfaces are very irregular and characterized by coexistence of both

materials. It appears for both weak and non-consolidated support and inaccurate adhesive applications.

Adhesive Fracture Cohesive Fracture Mixed Fracture

Figure 4.18: Comparison between different types of fracture

The bond failure of polymer matrix-based composites usually occurs with detachment of part of the surface, so called "peeling". Consequence of this, the mechanical properties of the support play a role of primary importance, as said: the maximum adhesion stress is, with good approximation, linearly proportional to the tensile strength of the support, and the fracture energy is, linearly proportional to the square root of the tensile strength of the same support. In the case of cement-based matrix composites, as will be seen following, different modes of bond failures occur. For the most part it do not occurs in the support but in the matrix and in the fibers.

4.5.2 Experimental plan ad test preparation

As a result of the importance that the bond performance takes on between composite materials and masonry substrate, also for the purpose of this thesis single-lap shear bond tests have been carried out. In this case, it still does not exist a specific standard that gives recommendation about natural fibers-based composites indicating geometric properties or special configurations regarding the specimens or test machine. Consequently to this, to the typical configuration of test used for masonry substrate reinforced with GFRP or CFRP was made reference, initially (figure 4.19).

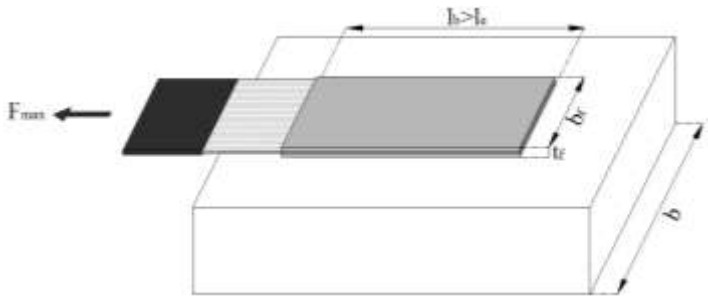

Figure 4.19: Setup scheme of single-lap shear bond test

In view of the results obtained in the previous tests, it was decided to use both epoxy resin-base matrix composites and mortar-based matrix composites; natural fabrics considered were mainly those of flax, hemp and jute. In fact even brick-reinforced with composites based on sisal fibers have been tested, but it has not achieved good results. The organization plan of the single -lap shear bond tests is schematized in the following figure 4.20:

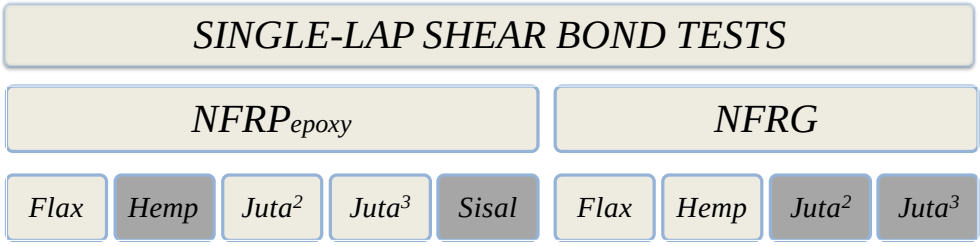

Figure 4.20: Scheduling of experimental working plan for single lap shear bond tests

4.5.2.1 Bricks strengthened with NFRP

To prepare the specimens reinforced with NFRP epoxy resin-based matrix, 6 specimens for each type of fabric were built. To calculate the bond length has been following the provisions of the technical Italian document [16]. The optimal bond length, l_{ed}, can be estimated by the following formula:

$$l_{ed} = min\left\{\frac{1}{\gamma_{Rd} \cdot f_{bd}}\sqrt{\frac{\pi^2 \cdot E_f \cdot t_f \cdot \Gamma_{Fd}}{2}}; 150mm\right\} \qquad (4.7)$$

$$f_{bd} = \frac{2 \cdot \Gamma_{Fd}}{s_u} \qquad (4.8)$$

$$\Gamma_{Fd} = \frac{k_b \cdot k_g}{FC} \cdot \sqrt{f_{bm} \cdot f_{btm}} \qquad (4.9)$$

$$k_b = \sqrt{\frac{3 - b_f/b}{1 + b_f/b}} \geq 1 \qquad (4.10)$$

where:

- E_f e t_f are, respectively, the Young's Modulus in the direction of the force and the thickness of the fiber-reinforced composite;
- Γ_{Fd} is the design value of the specific energy fracture;
- f_{bd} is the design value of the maximum shear stress of adhesion with s_u=0.4mm interface slip at full debonding[1];
- γ_{Rd} is a partial factor for resistance models, equal to 1,5.

The design value of the specific energy fracture is provided by equation (4.9) being:

- f_{bm} e f_{btm} are, respectively, the mean values of masonry elements compressive strength (20MPa) and tensile strength (2MPa);
- FC ia an appropriate confidence factor, equal to 2;
- k_b is a correction geometric factor calculated with equation (4.10) in function of the ratio between b_f/b the width of the reinforcement and that of the reinforced element;
- k_G is an additional corrective coefficient calibrated on the basis of results of experimental tests, assumed equal to 0.031mm in the case of clay brick masonry.

Table 4.V
Geometric characteristic and bond length on NFRP calculated.

Fiber/Properties	**NFRP**					
	b_f [mm]	**t_f [mm]**	**Ef [MPa]**	**l_{ed_1} [mm]**	**l_{ed_2} [mm]**	**l_{ed} [mm]**
FLAX	50	1,3	1867	39,9	150	40
JUTE[2]	50	0,97	1382	29,66	150	40
JUTE[3]	50	2,8	748	37	150	40

From the results obtained (table 4.V), it can infer that, the equations (4.7-4.8-4.9-4.10) actually are not fit to the properties of natural materials, having obtained

[1] Appendix C - CNR DT 200 R1-2012

the values of the bond length equal to 40mm. This is due primarily to the fact that with the natural fibers, the composite is characterized by a Young's Modulus much lower than that of the common carbon or glass fibers (see table 4.I).

At this point, it was decided to build two types of specimens (Figure 4.22): the first configuration with a bond length equal to 150mm and second configuration with a bond length equal to 75mm.

The specimens for the tests have been prepared carrying out a sequence of operations: the bricks, before being reinforced, in the oven for 24 hours at 100C ° C have been put, the brick area to be reinforce along the center line of the front of single clay brick (figure 4.10) with adhesive tape has been demarcated; the first layer of primer was passed in the central part of the brick in order to make clean and uniform the surface; positioned the fabric, with epoxy resin, has been glued manually, using an ordinary brush; finally, to the ends of the NFRP strip, steel plates have been glued, to ensure the fixing to the test machine (figure 4.21).

1st Step

2nd Step

3rd Step

4th Step

5th Step 6th Step

Figure 4.21: Steps carried out to prepare specimens for single-lap shear bond tests: Bricks strengthened with NFRP epoxy resin-based matrix

Moreover, as seen from the preceding figures (figure 4.21), initially the specimens with an un-bonded NFRP strip equal to 150mm have been built. Following the results obtained (see section 4.5.3) configurations I and II (figure 4.22) have been chosen to carry out the tests.

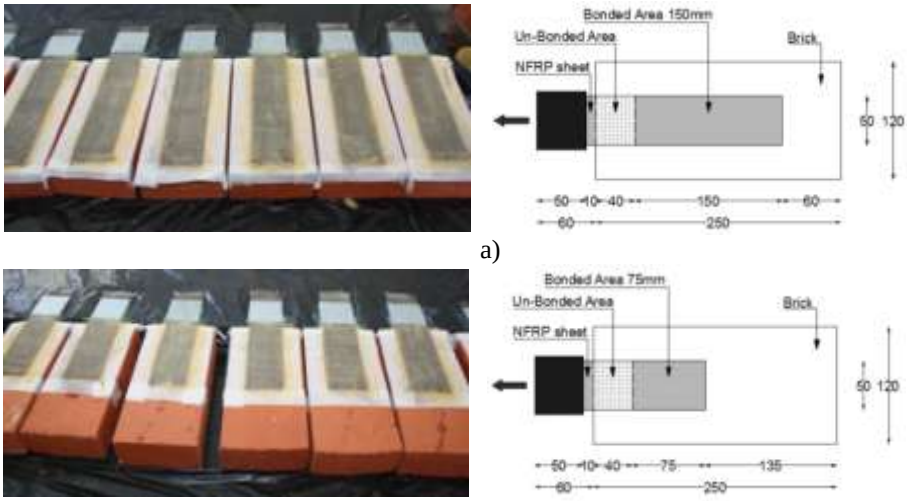

Figure 4.22: Specimens size of bonded area (plane view): a) configuration (I); b) configuration (II).

The testing machine (figure 4.23b) used to perform the tests was characterized by steel device designed and fixed to the rigid steel frame presents in laboratory, where the reinforcement sheet was loaded from above. In particular, the device

is made of a steel profile welded to a rigid plate and stiffened with two diagonal bars (figure 4.23a). The specimen was positioned on the steel device and firmly clamped to it.

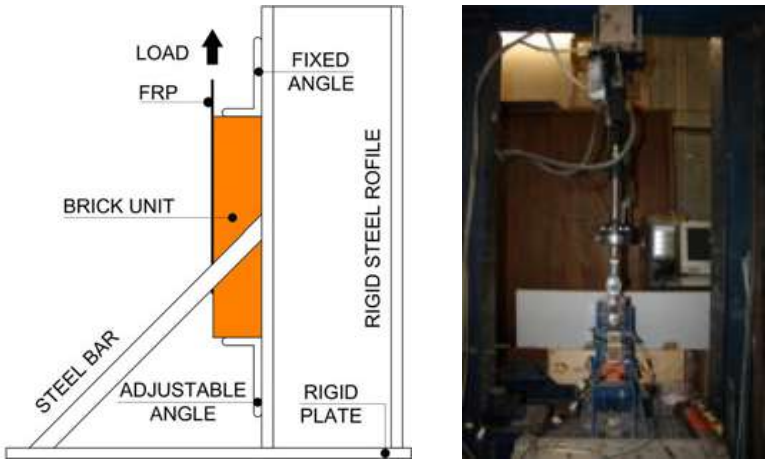

a) b)

Figure 4.23: Schemes of single-lap shear bond tests setups for specimens loaded

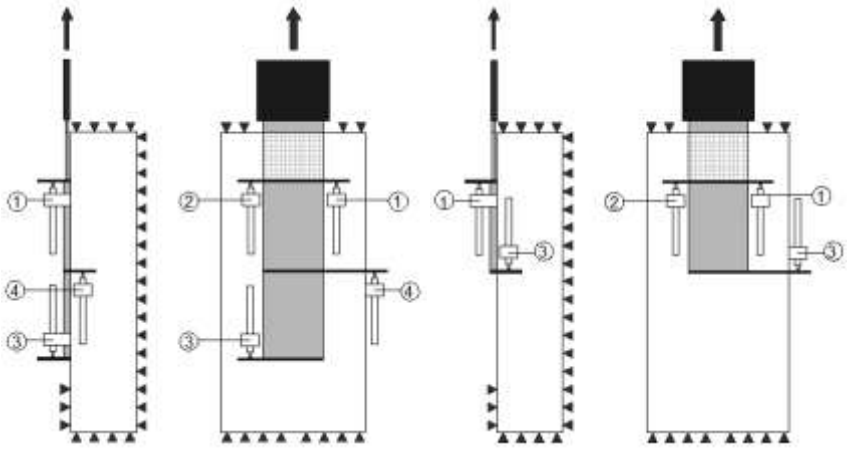

a) b)

Figure 4.24: Schematic representation of single-lap shear bond tests: a) Configuration (I); b) Configuration (II).

The main measurement system consisted of four (configuration I) or three (configuration II) LVDT's placed along the composite strips. The general measurement scheme is shown in figure 4.24.

4.5.2.2 Bricks strengthened with NFRG

To build the specimens reinforced with mortar-based matrix composites, the same previously procedure has been utilized (see section 4.5.2.2). Also in this case, taking into account to the Italian standard, to calculate the bond length, the equations (4.7 - 4.8 - 4.9 - 4.10) have been used. The results obtained are shown in the table 4.VI.

Table 4.VI
Geometric characteristic and bond length on NFRG achieved.

Fiber/Properties	NFRG					
	b_f [mm]	t_f [mm]	Ef [MPa]	l_{ed_1} [mm]	l_{ed_2} [mm]	l_{ed} [mm]
FLAX	50	5	774	50,3	150	50
HEMP	50	5	268	29,6	150	30

It is possible to note that even in this case, lower values of bond length have been obtained (table 4.VI) respect the values usually used for the specimens reinforced with carbon or glass fiber and mortar as a matrix. In this case it is chosen to proceed considering a bond length of 150mm (figure 4.26).

The sequence of operations carried out to build the specimens reinforced with NFRG are summarized in the figures 4.25: the bricks (Figure 4.10), before the preparation, in water for 24 hours have been put; to build the layers of mortar, special metal mold have been used, a first mold of 2mm thickness and a second mold of a thickness of 5mm, so as to contain both the first layer of mortar (2mm), the layer of the fabric and the last layer of mortar. Even in this case at the edges of the NFRG special steel plates have been glued.

1st Step

2nd Step

3rd Step

4th Step

5th Step

6th Step

7th Step 8th Step

Figure 4.25: Steps carried out to prepare specimens for single-lap shear bond tests: Bricks strengthened with NFRG

To measure the displacements, four LVDT's have been glued to the specimens: two on the edges of the NFRG strip and one in the center line the bond area. To avoid that the specimen would break in un-bonded area, the NFRP strip with epoxy resin has been impregnated.

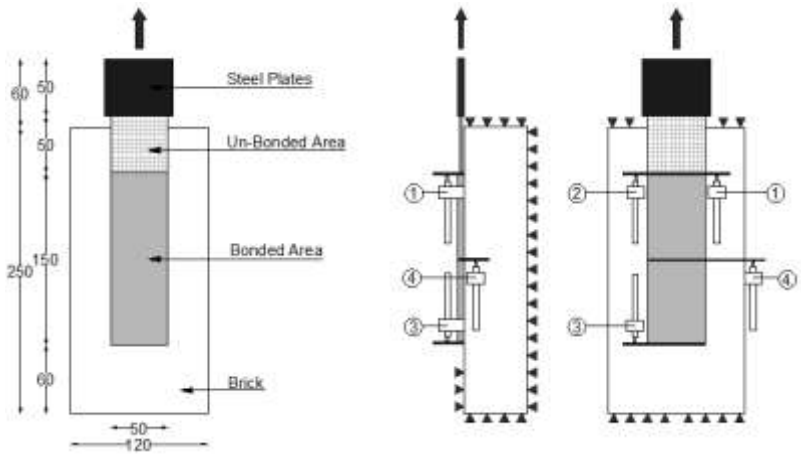

a) b)

Figure 4.26: a) Specimens size (plane view); b) Schematic configuration.

Also for the performance of single-lap shear bond tests on the bricks reinforced with NFRG the same device shown in figure 4.23a has been used, while the set-up machine used is represented in figure 4.27.

Figure 4.27: Set-up machine used in the case of brick-strengthened with NFRG

4.5.3 Experimental results and failure modes

4.5.3.1 Bricks strengthened with NFRP

Single-lap shear bond tests carried out on the bricks reinforced with NFRP epoxy resin-based matrix did not provide good results. The main causes that led to this, are the following:

I. The length of the un-bonded area, originally adopted, was much larger than the actual purpose of the test. In fact, from the first tests conducted, it is deduced as the break of the specimen occurred in correspondence of this area (figure 4.28b). The test was transformed, then, in a tensile test on composite, confirming what was obtained from the previous tests (figure 4.29). The bond between the composite and the brick is result much stronger than the tensile strength of the fabric.

II. In order to prepare the specimens and to calculate the bond length, the Italian code[1] has been followed. This standard was drawn up on the basis of experimental results achieved using FRP composites (carbon and glass). From the results obtained using NFRP composites, it is clear that the formulations suggested in current standard are not adapted to the characteristics of composites based on natural fibers.

[1] Italian standard: CNR DT 200 R1-2012

a) b)

Figure 4.28: a) Set-up machine; b) Failure modes.

Considering the first configuration I (figure 4.24a), from the specimens reinforced with flax, juta2 and juta3, the results shown in Figure 4.29 have been obtained, in terms of maximum force. The failure mode, for all five specimens tested and for each type of fabric, has occurred in an instantaneous way and it localized in the un-bonded area (Figure 4.28b). Moreover, It can be noted that the maximum values of the strength, both for tensile tests on $NFRP_{epoxy}$ that for single-lap shear bond tests, have the same order of magnitude. To confirm what it previously stated, in relation to current legislation.

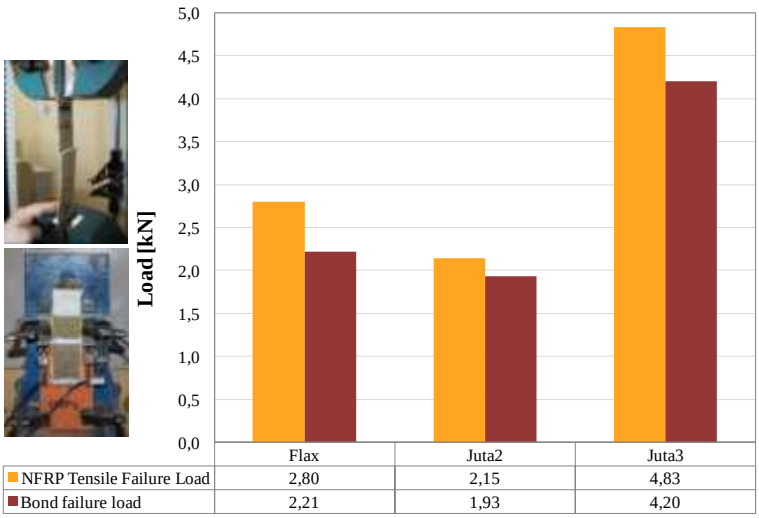

Figure 4.29: Comparison between NFRP epoxy-based matrix failure load and debonding failure load

In the case of the configuration II (Figure 4.24b) different results have been obtained. In this case only bricks reinforced with hemp fibers were prepared. The maximum bond failure load (3541N) was higher than the maximum tensile load reached (1973N). This is due to the fact that there has been a little phenomenon of delamination on the brick (figure 4.30), not to be considered, however, acceptable and suitable to the end of the study the bond adhesion between the masonry system and composite materials.

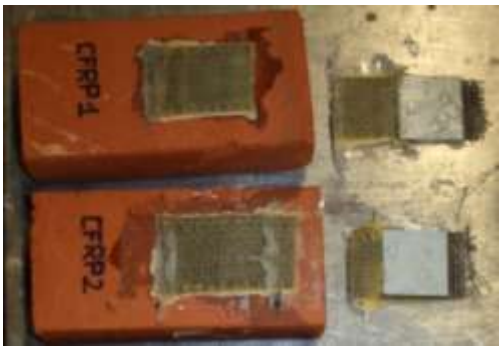

Figure 4.30: Failure mode configuration II on brick strengthened with $HFRP_{epoxy}$

4.5.3.2 Bricks strengthened NFRG

The results obtained from the tests carried out on bricks reinforced with NFRG have been shown a better behavior during the performance of the tests in respect the tests described in 4.5.3.2 section. In this case it was possible to make a classification of the failure mode of the specimens. They are basically divided in 4 different ways:

- Failure of the composite, in the interface between matrix (mortar) and fabric (Mode A);
- Delamination of the support (brick) (Mode B);
- Failure in the matrix (mortar) in the interface between support and bonded area (Mode C);
- Failure in the NFRP sheet (mode D).

The different types of failure modes are schematized in figure 4.31.

A comparison between the maximum tensile failure Load and the maximum bond failure load has been the first operation performed, after carrying out the tests, in order to validate the effectiveness of the tests (figure 4.32). As expected,

the maximum tensile failure load was higher than that obtained for the case of the maximum bond failure load, except in the case of the brick reinforced with HFRG in which it is obtained a value almost equal in both cases.

In terms of percentage on a total number of 6 specimens tested for each type of fiber has been obtained: 11% fracture in the composite (Mode A); 6% cohesive fracture in the brick (Mode B); 61% cohesive fracture in the matrix (Mode C) 22% NFRG fracture in the fabric NFRG sheet (Mode D).

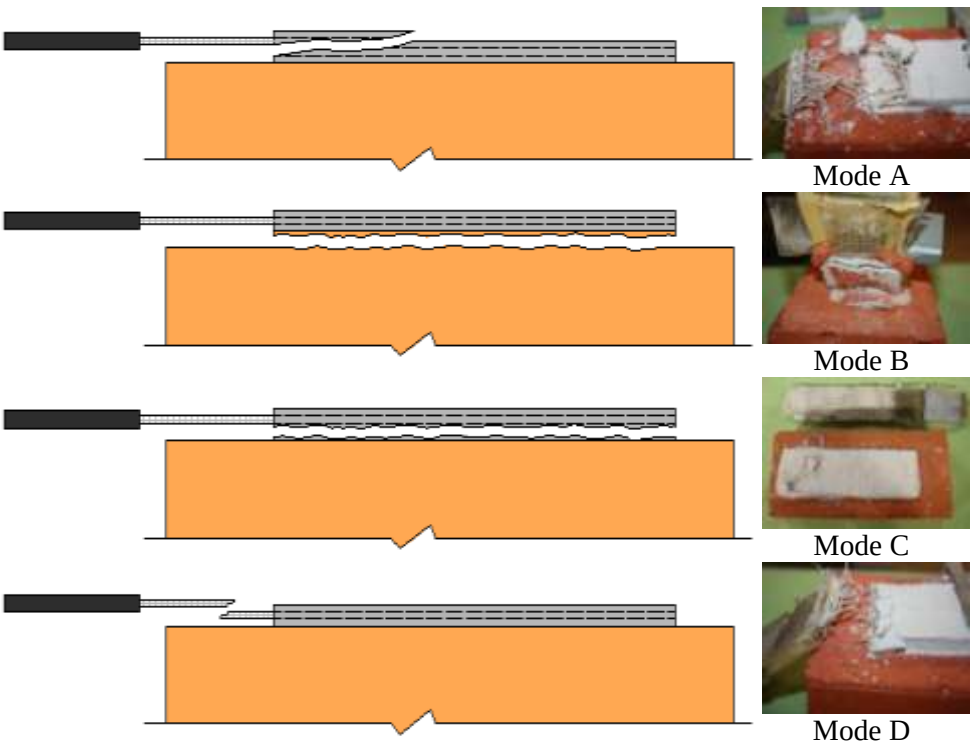

Figure 4.31: Different failure mode obtained from single-lap shear bond tests

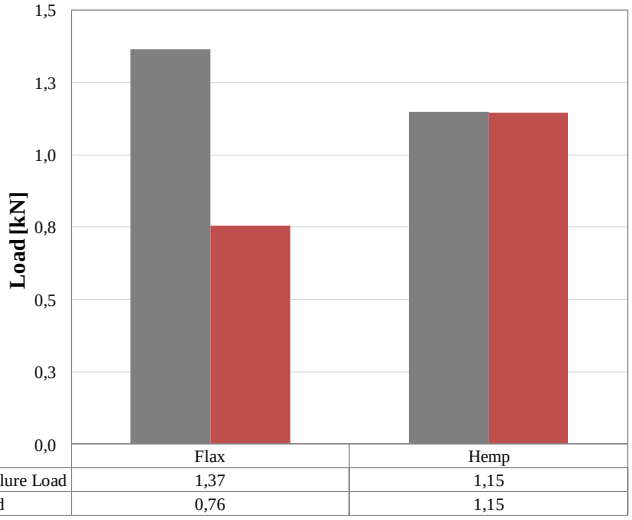

Figure 4.32: Comparison between NFRG tensile failure load and debonding failure load

During the performance of the tests, it was not used strange gauges to compute the deformation during the tests. The value of bond stress was calculated taking into account of the maximum force and bonded area. The envelopes of the local bond-displacement behavior near the loaded end is shown in figure 4.33 for each composite material used. From some observation it can be noted that a similar behavior has been found for the different composite materials; the experimental values obtained from the tests are summarized in the table 4.VII, in terms of maximum force, F_{max}, maximum displacement, *Slip*, and bond stress, f_b.

Table 4.VII
Average of the experimental values obtained from single-lap shear bond tests on NFRG.

	F_{max} [N]	*Slip* [mm]	f_b [MPa]
FFRG	756,67	4,01	0,96
	27%	26%	27%
HFRG	1145,83	2,36	1,46
	25%	9%	25%

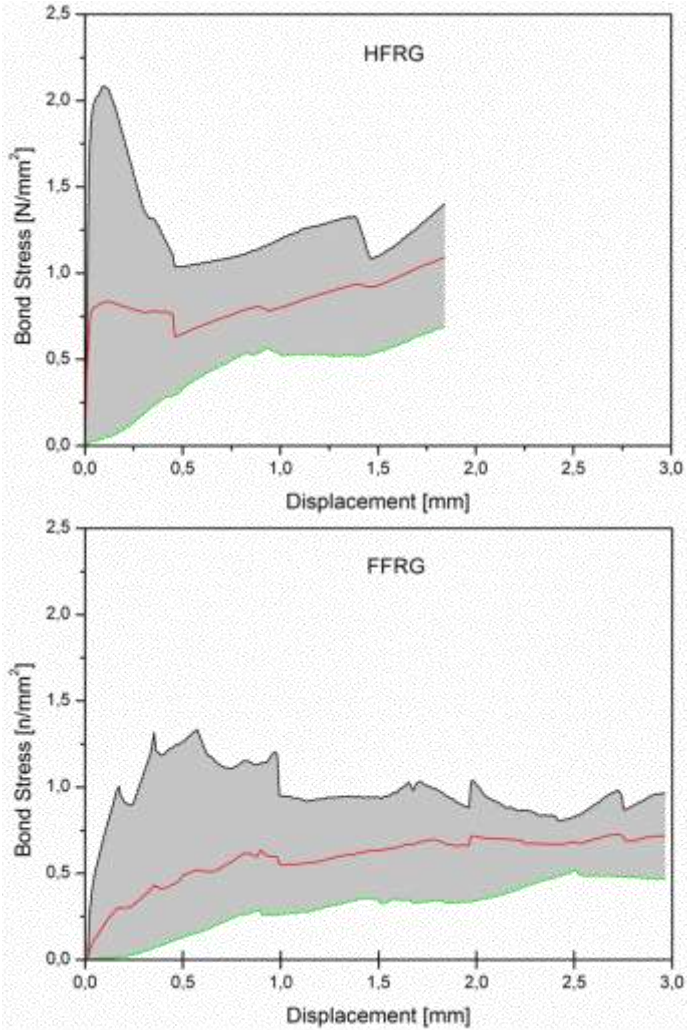

Figure 4.33: Local bond-stress slip curves (the envelopes of six tests are shown): a) HFRG strengthened specimens; b) FFRG strengthened specimens.

4.5.4 Comparison with the guidelines CNR-DT 200/2004 s.m.i.

At the end of the experimental tests, it has been done a comparison between the results obtained experimentally and theoretical results proposed by the Italian code CNR-DT 200/2004, which currently represents the Italian normative reference on design and construction of externally bonded FRP systems for strengthening existing structures.

With reference to the typical adhesion test, shown schematically in the figure 4.19, the maximum force supported by the FRP, before it occurs the phenomenon of delamination, depends on the geometry of the reinforcement, in particular from the bond length of the composite on the support. This length grows with l_b up to draw a maximum corresponding to a precise length, l_e: additional lengthening of the bonded area do not increase the force transmitted. The maximum force in accordance with the standard can be expressed as:

$$F_{max} = b_f \sqrt{2 \cdot E_f \cdot t_f \cdot \Gamma_f} \qquad (4.7)$$

where:

- t_f, b_f, E_f are the thickness, the width and the modulus of elasticity of the reinforcement in the force direction;
- Γ_f is the specific fracture energy.

To calculate the fracture energy, it is possible to follow two approach, according with the standard:

- 1st approach:

$$\Gamma_f = k_b \cdot k_G \cdot \sqrt{f_{bm} \cdot f_{btm}} \qquad (4.8)$$

- 2nd approach:

$$\Gamma_f = k_b k_G \tau_{b,\max} = k_b k_G \frac{f_{bm} \cdot f_{btm}}{f_{bm} + f_{btm}} \qquad (4.9)$$

$$k_b = \sqrt{\frac{2 - b_f/b}{1 + b_f/b}} \geq 1 \;\; with \;\; \frac{b_f}{b} \geq 0{,}25 \qquad (4.10)$$

where:

- k_b is a dimensionless correction factor given by (4.10), depending on the reinforcement width and the reinforced element;
- k_G is a further corrective factor calibrated on the basis of experimental results, expressed in millimeters (mm) and dependent on the type of masonry. In this specific case, this parameter is equal to 0.031 mm, having used clay bricks[1].

[1] The coefficient k_G has been calibrated on the basis of a large population of experimental results available in the nationally and internationally literature. A part of the experimental database collects the results of tests of adher-

- f_{bm} is average compressive strength of the blocks that constitute the masonry, expressed in N/mm^2;
- f_{btm} is the average tensile strength of the blocks that constitute the masonry, expressed in N/mm^2.

Considering what has been described up to now and distinguishing between the two approaches to the calculation of the fracture energy, the theoretical values of the bond stress and maximum force have been calculated, which have been compared with the data obtained experimentally (table 4.VIII - first approach and table 4.IX - second approach).

Table 4.VIII
Comparison between experimental and theoretical results (1st approach)

			Theoretical		**Experimental**	
	k_b	Γ_f	$F_{max,d}$	f_{bd}	$F_{max,mean}$	$F_{b,mean}$
FFRG	1,36	0,134	1191,12	0,668	756,67	0,96
HFRG	1,36	0,134	701,01	0,668	1145,83	1,46

Table 4.IX
Comparison between experimental and theoretical results (2nd approach)

			Theoretical		**Experimental**	
	k_b	Γ_f	$F_{max,d}$	f_{bd}	$F_{max,mean}$	$F_{b,mean}$
FFRG	1,36	0,077	903,18	0,384	756,67	0,96
HFRG	1,36	0,077	531,55	0,384	1145,83	1,46

The experimental results are not substantially in agreement with those obtained by applying the equations suggested by the current standard concerning composite materials and according to the two approaches. It can be noted, however, that the formulations contained in the CNR-DT 200 R1/2012 are explicitly re-

ence composite-concrete carried out within Task 8.2 of the Project ReLUIS-DPC 2005-2008. The calibration of the average values and the characteristic of the coefficient kG was performed in accordance with the approach suggested in EN1990 - Annex D (Design assisted by testing), considering as random variables also the mechanical characteristics of the materials.

lated to polymer-based matrix composites and synthetic fibers-based composites. For which the technical document does not take into account the relevant thickness of the mortar-based matrix (5mm) and especially the delamination that occurs inside of the matrix, rather than in the support. Based on the foregoing, it is understood as the analytical representation and the study on delamination using natural fiber-based composites to strengthened masonry bricks is currently a problem for researchers in the field.

4.6 Determination of density of NFRP

In order to determinate the *specific gravity* or *density* of the composite materials, in accordance with the specific standards [34], it is possible to used two methods: *test method A or B*. In this specific case, *test method A* have been considered. The test specimens were cut with dimension equal to 150x150mm and thickness approximately equal to 1mm. A total number of 10 specimens, for each types of composite has been prepared (figure 4.34). To calculated the density, an analytical balance (figure 4.35a) with a precision 0.1mg, equipped with a stationary support for the immersion vessel above the balance pan, has been used. The water, contained in the vessel, was substantially air-free and distilled (figure 4.35b).

a)

b)

Figure 4.34: a) Specimens of NFRP-epoxy; b) Specimens of NFRP-polyester

First of all, it has been weighted and recorded the water temperature. Each dry specimens was weighted obtaining the value of *w(g)* (figure 4.35c), afterwards the immersion vessel has been mounted on the support. At this step, the specimens was completely immersed in the water at temperature of 23°C (figure 4.35d) and

weighted; this weight is the mass of the specimens holder in liquid, marked *G(gcm^{-3})*. The procedure has been repeated for all number of specimens.

a) b) c) d)

Figure 4.35: a) Analytical Balance; b) Immersion vessel; c) Dry specimen; d) Full immersion of the specimen in the liquid.

Finally, the density has been calculated, according with the standards[34], using the following equation:

$$\rho = \frac{w \cdot [\rho(H_2 0) - 0{,}0012]}{0{,}99983 \cdot G} + 0{,}0012 \qquad (4.11)$$

The results have been summarized in the table X, marking out between NFRP- based resin and NFRP-based polyester.

Table 4.X

Density of the natural fiber reinforced polymer (CoV is provided inside parentheses)

		JUTE[1]	**JUTE[2]**	**JUTE[3]**	**SISAL[1]**	**SISAL[2]**	**HEMP**	**FLAX**
NFRP-Resin	ρ g/cm^3	1,27 (0,7%)	1,28 (0,7%)	1,09 (8%)	1,09 (0,4%)	1,14 (0,5%)	1,15 (1,2%)	1,16 (5%)
NFRP-Polyester	ρ g/cm^3	1,23 (0,7%)	_	2,26 (5%)	_	_	2,07 0(,4%)	1,35 (4%)

5

MODELLING OF NFRP-STRENGTHENED MASONRY CLAY BRICK

Virtually every phenomenon in nature, whether biological, geological, or mechanical, can be described with the aid of the laws of physics, in terms of algebraic, differential, or integral equation relating various quantities of interest. But is true too that the representation of physical phenomena can be accomplished graphically, experimentally and not only mathematically [35].

The use of numerical models becomes a reliable solution when an interpretation of real situations is sought. There are several approaches that take into account material nonlinearities, like the masonry material [36]:

- *Continuous Methods*: it concerns the Finite Difference Method (FDM), the Finite Element Method (FEM) and Boundary Element Method (BEM);
- *Discrete Method*: it concerns a Discrete Element Method (DEM) and the Discrete systems of Fracture Method (DFN);
- *Hybrid methods*: Continuous or Discrete.

Mostly, very common numerical technique applicable to problems with arbitrary geometry and boundary condition is the finite element model (FEM).

This Chapter, a numerical analysis of clay brick reinforced with natural fiber-based composites using epoxy based-matrix is presented. The goal has been to provide model able to describe the flexural behavior of unreinforced and reinforced brick on the basis of experimental response observed during laboratory tests. The numerical analysis has been performed with a finite element model in the FE code DIANA.

The Chapter into two sections is organized: the first part concerns a brief description of the formulation of the finite element method and advances procedures used to perform the numerical models and a second part concerns the numerical results achieved, which they were compared with the experimental envelope experimental results.

5.1 Non-linear finite element formulation

In this section, the finite element method is adopted to simulate the structural behavior of the masonry macroelements. In a nonlinear structural analysis, given a structure, the material properties (geometrical, physical and mechanical), play a truly important role. Also important it is the spatial discretization of the geometry into elements. Each element is connected in the domain by nodal points at the inter-element boundaries. In order to obtain the unknown nodal displacement in each element, it is necessary to solve a system of equation, between all elements of the structure and loads and boundary condition applied to the same structure, that it will ensure the global equilibrium of the structure studied.

The system of equation to be solved, for each type of element, is usually expressed as the relation between generalized stress and strain vectors (eq. 5.1), where $\boldsymbol{K}$ is the system stiffness matrix, $\boldsymbol{s}$ is the stress vector and $\boldsymbol{e}$ is strain vector. In the present study, the assumption of plane stress element is adopted, they are characterized by the fact that the stress components perpendicular to the face are zero ($\sigma_{zz} = 0$). For plane continuum plane stress element, the stress vector $\boldsymbol{s}$ and strain vector $\boldsymbol{e}$ are defined respectively, as:

$$s = Ke \tag{5.1}$$

$$s = \begin{Bmatrix} \sigma_x \\ \sigma_y \\ \tau_{xy} \end{Bmatrix} \qquad e = \begin{Bmatrix} \varepsilon_x \\ \varepsilon_y \\ \gamma_{xy} \end{Bmatrix} \tag{5.2}$$

In this specific case, the elements are integrated using the standard reduced Gauss scheme (2x2-point Gauss quadrature) in the case of the brick (fig. 5.1a), on the other hand in the case of the composites the element is a two-node directly integrated (1-point) truss elements (fig. 5.1b).

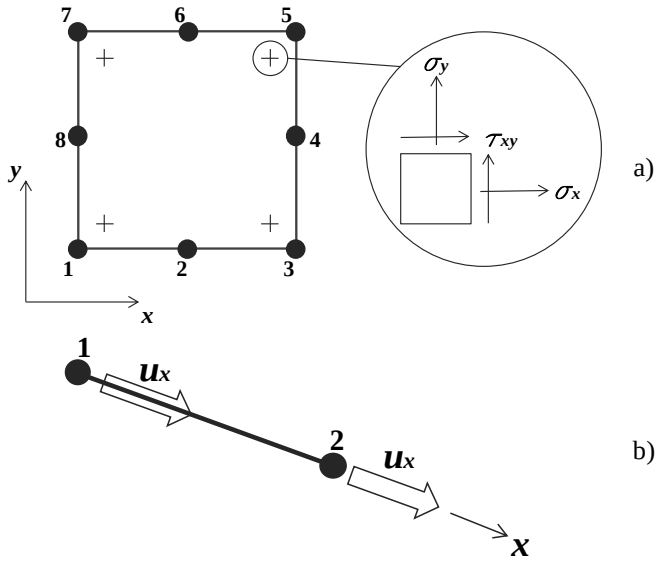

Figure 5.1: Type of finite element employed in this study: a) eight-node continuum plane stress element; b) two-node truss elements

5.1.1 Solution procedures for non-linear problems

In linear and nonlinear finite element analysis the required memory and analysis time is strongly depending on the chose procedure for solving the set of linear equations. The main parameters considered for explicit equations are force vector ($\boldsymbol{f}_{internal}$ and $\boldsymbol{f}_{external}$) and nodal displacement vector $\boldsymbol{u}$. The relation between these two parameters generally leads to a non-linear relation between force vector and nodal displacement vector, which implies that displacement often depend on the

displacements at previous stages. In the linear analysis, the nodal displacement vector is easily calculated as the equilibrium between the internal and external forces, on the contrary in the non linear case it is not possible. To achieve equilibrium at the end of the increment, it can be used an *iterative* solution algorithm, where the load is applied into a finite number of increments (discretization in space). These increments can also be associated to time steps, which a pseudo-time variable could be introduced to describe the loading progression The combination of both is called an *incremental-iterative solution procedure*. The general iterations process is usually carried out in the following schematic flow diagram:

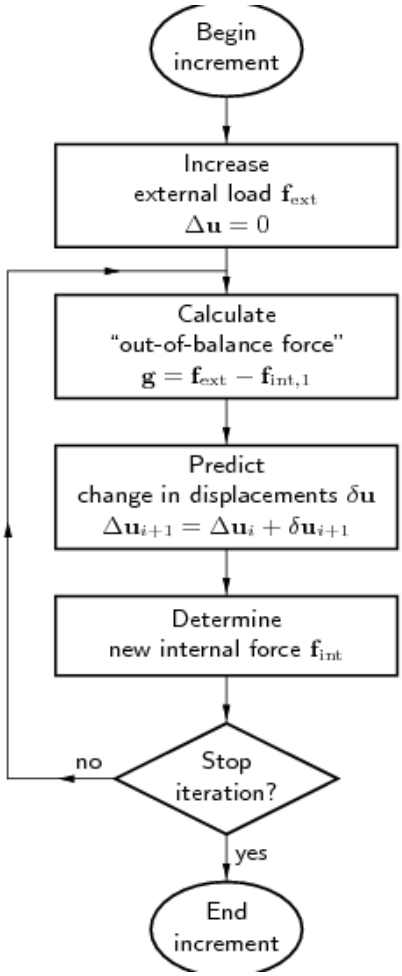

Figure 5.2: Incremental-iterative solution procedure

The total displacement increment $\boldsymbol{\Delta u}$ is calculated iteratively by iterative increments $\boldsymbol{\delta u}$ until equilibrium is reached, up to a prescribed tolerance. Indicating the iteration number with a right subscript, the incremental displacements at iteration *i + 1* are calculated using the follow equation:

$$\Delta u_{i+1} = \Delta u_i + \delta u_{i+1} \quad (5.3)$$

There are several iterative procedures for the calculation of $\boldsymbol{u}$, in each of these is considered the "stiffness matrix" $\boldsymbol{K}$ to calculate the increments iterative. It represents the linearized form of the relation between the force vector and displacement vector. For each iteration the matrix $\boldsymbol{K}$ will take on a different value, and that is why it is indicated as $\boldsymbol{K_i}$. A direct approach to determine the iterative increments is the following:

$$\delta u_i = K_i^{-1} \cdot g_i \quad (5.4)$$

where $\boldsymbol{g_i}$ is the out-of-balance force vector at the start of iteration *i*. In linear case a set of equations is solved at every iteration.

The iterative procedures most commonly used are: the Newton-Raphson method, the Quasi-Newton method and the Constant Stiffness method.

5.1.2 Advanced solution procedures

Some advanced solution procedures are briefly presented in this section, used to analyzed the model proposed later in order to compare and to evaluate the results obtained experimentally.

Newton-Raphson methods

Newton-Raphson methods, generally two subclasses is possible to distinguish: the Regular and the Modified Newton-Raphson method. Both methods use (eq. 5.5) to determine the iterative increment of the displacement vector. In a Newton-Raphson method, the stiffness matrix $\boldsymbol{K_i}$ represents the tangential stiffness of the structure:

$$K_i = \frac{\partial g}{\partial \Delta u} \quad (5.5)$$

The difference between the Regular and the Modified Newton-Raphson method is the point at which the stiffness matrix is evaluated.

In order to improve the convergence of the iterative scheme and to pass limit points, Modified Newton-Raphson method has been used in the analyses performed with the numerical model proposed later on this Chapter.

The Modified Newton-Raphson method only evaluates the stiffness relation (eq. 5.5) at the start of the increment (fig. 5.3) always based on a converged equilibrium state. For every iteration only the prediction of the iterative incremental displacements and the internal force vector is calculated, it is not necessary to set up a new stiffness matrix.

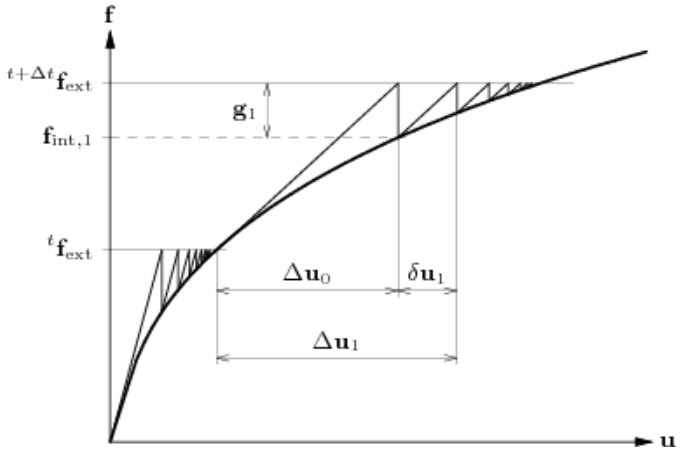

Figure 5.3: Modified Newton-Raphson iteration

To sum up, given a system of external forces (eq. 5.6), the respective displacements are obtained (eq. 5.7), such that the internal force, function of the displacement, is equal to the external force (eq. 5.8):

$$\bar{f}_{ext}^{(1)} \; ; \; \bar{f}_{ext}^{(2)} \; ; \; \bar{f}_{ext}^{(2)} \; ; \ldots \qquad (5.6)$$

$$u^{(1)} \; ; \; u^{(2)} \; ; \; u^{(3)} \; ; \ldots \qquad (5.7)$$

$$f_{int}\left(d^{(n)}\right) = \bar{f}_{ext}^{(n)} \quad n = 1,2,3 \ldots \qquad (5.8)$$

Finally the set of equations to solve for every iteration are summarized in equation 5.9 and 5.10:

$$K^{(n,0)}\delta u^{(n,i)} = \bar{f}_{ext}^{(n)} - f_{int}^{(n,i-1)} \quad i = 1,2,3 \ldots \quad (5.9)$$

$$u^{(n,i)} = u^{(n,i-1)} + \delta u^{(n,i)} \quad (5.10)$$

Line search technique

In the case of irregular structures or in the case of cracking of a structure, the iteration process does not converge easily to the "exact" numerical solution. There are so called *line search algorithms* that help to increase the convergence rate leading to a convergence solution correct. Basically, the line search algorithms can be regarded as a minimization of the total potential energy of the system, which is a function of the total displacements *u*, in the direction of the iterative incremental displacement vector Δu_{i+1}, which is calculated from a scaled iterative increment:

$$\Delta u_{i+1} = \Delta u_i + \eta \cdot \delta u_{i+1} \quad (5.11)$$

where η is the line search factor scales the iterative displacement ad is calculated making the projection of the projection of the unbalance forces in the search direction equal to zero. To further information and detailed see Crisfield [44].

Arch-length Control

Regarding the incremental part of the solution procedures, there are various method: load control displacement control and arch-length control. In this specific case arch-length control method has been used to achieve numerical results. It is a method that can adapt the step size depending on the results in the current step. The initial choice of the step size for every increment is an important factor in the incremental-iterative process. This method, is basically used when the displacement increments can become very large, for instance when the load-displacement curve is almost horizontal.

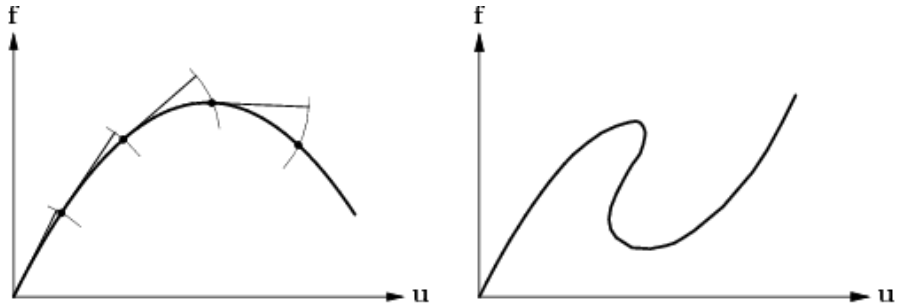

a) b)

Figure 5.4: Arc-length control; structural behavior: a) Snap-through; b) Snap-back

It is possible to consider two structural behaviors: snap-through and snap-back behavior. In the first case (fig. 5.4a), to compute the response beyond maximum load points, a special solution procedure that allows for a decrease in load and an increase in displacement is used. this approach cannot be applied to all structural problems and is incapable of properly handling strong localizations, for this reason is more useful to consider the second approach (fig. 5.4b).

5.2 Numerical modeling

Complementary to the experimental research described above, a numerical simulation of the three point bending test is presented in this Section to further assess and compare the experimental results. The numerical analysis has been performed with a plane stress finite element model in the FE code DIANA [36], see figure 5.6, distinguishing two different cases: unreinforced bricks and Natural Fiber Reinforced Polymer (NFRP) strengthened masonry clay bricks.

Initially, the model assumes that the NFRP strips behave in an elastic fashion whereas non-linear behavior is concentrated in the brick units (Case 1). In a second part of the modeling both brick units and NFRP strips are assume as non-linear behavior (Case 2). In particular, the numerical part was organized into two sections: preliminary linear analysis of the specimens (UNBRICK and REBRICK) and non-linear analysis. In the second case, quasi-brittle behavior has been the constitute model used for the brick and for FFRP and HFRP strips. It is characterized by tensile cracking and compressive crushing; in particular the so called “Total Strain crack models”, which describes the tensile and compressive behavior of a material with one stress-strain relationship evaluated in the principal directions of the strain vector, was adopted. The stress –strain diagram considered during the non-linear

static analysis is represented in figure 5.5 and it is characterized by exponential tension softening diagram in tension and parabolic diagram in compression. To take into account the possible lateral cracking, due to the reduction of the strength of the brick along the principal compressive direction, the relationship of the model Vecchio & Collins has been taken [38].

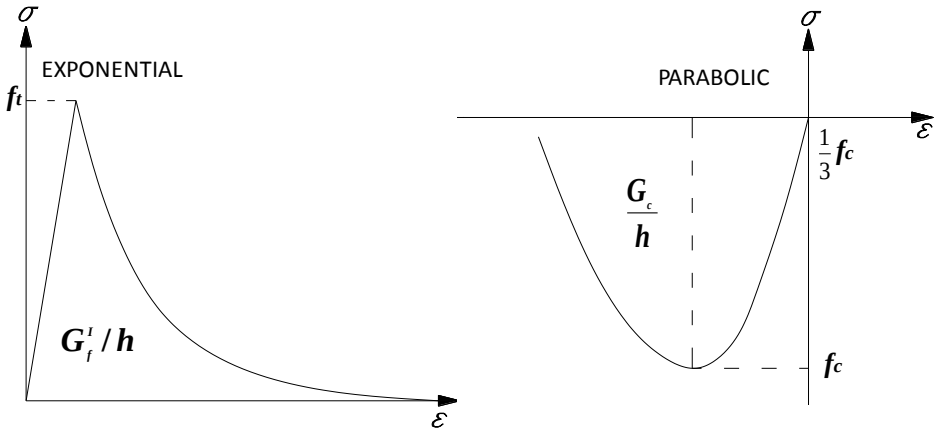

a) b)

Figure 5.5: Constitutive model: a) Compression behavior; b) Tension behavior

In these simulations, the brick were modeled using eight-node continuum plane stress elements (fig. 5.6a) and, for the NFRP strips, two-node truss elements were used (fig. 5.6b). The boundary conditions and the load application method were defined in accordance with the experimental arrangement, as shown in figure 5.7. An incremental force was applied in the top center of the brick, which is in the plane of the element, in order to simulate the bending conditions.

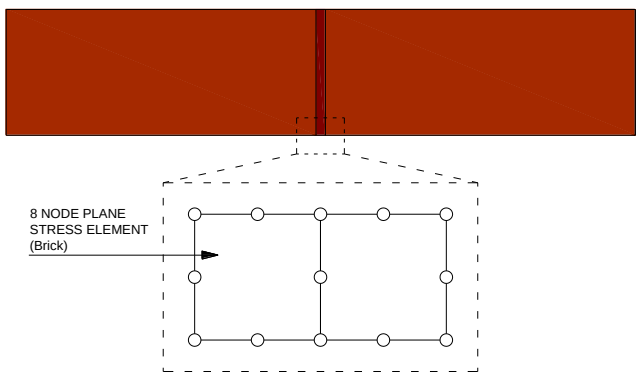

a)

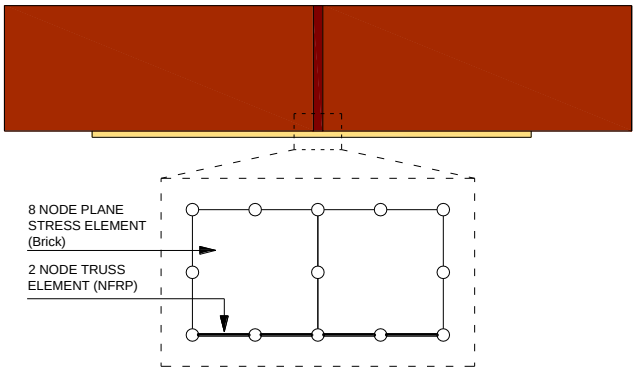

b)

Figure 5.6: Finite element model: a) Unreinforced brick, b) Reinforced brick

Two different element sizes were used for representing the brick, Element 1(5x5mm) for the edges of the brick and Element 2 (3x5mm) for the central area, subjected to a higher stress state variation, see figure 5.7. Two different meshes were modeled, Mesh 1 for the unreinforced bricks and Mesh 2 for reinforced bricks, in order to compare the two behaviors. The total number of elements and the total number of nodes for each mesh are shown in table 5.I.

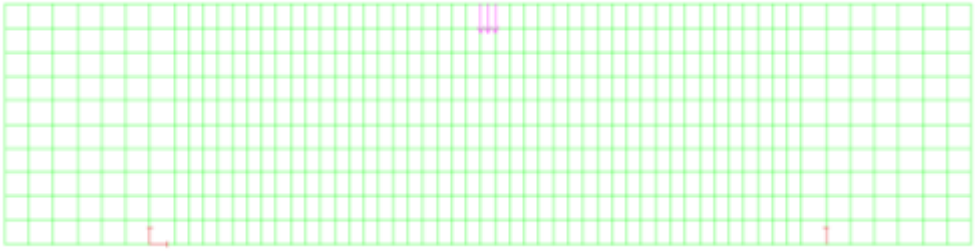

Figure 5.7: Full mesh with loads and boundary constrains

Table 5.I
Adopted mesh types

Mesh type	Total n. of elements	Total n. of nodes
Mesh 1	570	1845
Mesh 2	656	1845

5.2.1 Material models

Isotropic elastic material models are used for NFRP strips and brick; the mechanical properties of the brick and NFRP strips are shown in the table 5.II, in terms of modulus of elasticity, E_f, tensile strength, f_t, Poisson's ratio, ν, composite thickness, t_f, and cross-section area, A_f, obtained from experimental tests (see chapters 3 and 4). Regarding the physical properties of the materials used, two different cases have been considered: one for the brick (100mm) and another for the cross section on the middle of the brick (80mm), so called crack section (see fig. 4.15). In addition, for the non-linear analysis, the mode-I tensile fracture energy of the brick has been selected equal to G_f =0,08 N/mm and compressive fracture energy equal to 20 N/mm [39], whereas the mode-I tensile fracture energy of the NFRP strips has been considered equal to G_f =0,14 N/mm (see section 4.5.4) as calculated in accordance with DT 200/2012.

Table 5.II
Mechanical Characteristics of the materials

Materials	E_f **[MPa]**	f_t **[MPa]**	ν	t_f **[mm]**	A_f **[mm^2]**
Bricks	9579	2,2	0,15	-	-
FFRP	1866	118	0,15	2,9	1,2
HFRP	1674	64	0,15	2,6	1,7

5.2.2 Preliminary linear analysis

First of all, it was performed a linear analysis in order to check the validity of the model, both for unreinforced brick and reinforced brick. In this first step, the deformed mesh and the principal Cauchy stresses have been analyzed in order to better understanding of the behavior of the model.

Compared to those described in the previous section 5.2, two types of models have been considered. In both cases (case 1, case 2) the trend of the deformed and the relative nodal displacement in the load direction, DTY, has been displayed (fig. 5.8-5.9). In the case of unreinforced brick, values of the maximum nodal displacement DTY_{max} equal to 0,779E-2 and minimum DTY_{min} equal to 0,317E-1 have been obtained; in the case of the reinforced brick, with both flax and hemp fibers, a maximum value of the nodal displacement DTY_{max} equal to 0.117 E-1mm, in corre-

spondence of the two top ends of the model, and a minimum nodal displacement DTY_{min} equal to -0.475 E-1mm, in correspondence of the bottom central area of the model have been obtained. Same results, for both case 1 and for case 2, with flax and hemp fibers have been obtained in terms of the principal stresses (fig. 5.10): maximum value of the compressive stress equal to 4,34MPa and minimum value of the tensile stress 13,9MPa, whereas in the case of unreinforced brick maximum value of the compressive stress equal to 2,89MPa and minimum value of the tensile stress 9,28MPa have been achieved.

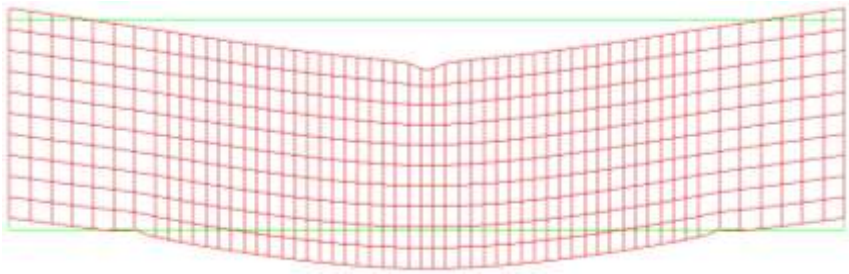

Figure 5.8: Deformed shape of the mesh

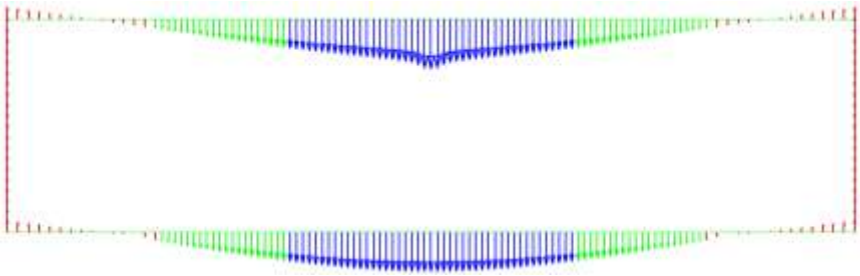

Figure 5.9: Total displacement: nodal results component DTY

Figure 5.10: Principal Cauchy stresses (σ_{xx})

5.2.3 Load-displacement diagrams UNBRICK

The numerical results obtained from nonlinear analysis on the unreinforced brick, are compared with the experimental ones in figure 5.11, in order to assess the reliability of the proposed model. Two different types of results have been obtained depending on the value assumed for the crack bandwidth. In the first model it was assumed a default value by the numerical program used, in the second model it was used the maximum values of the crack reported to the maximum load reached during the experimental tests and measured with the LVDT placed in the specimens. It's possible to note that the numerical global force-relative displacement curve fits the envelope of the experimental results with reasonable accuracy, especially in terms of stiffness and maximum load: in the first case (crack bandwidth by default) the numerical curve is characterized by a softening final part (fig. 5.11a), on the contrary, in the second case (crack bandwidth equal to 0,05mm) the numerical model fits the experimental results catching the brittle behavior of unreinforced brick (fig. 5.11b).

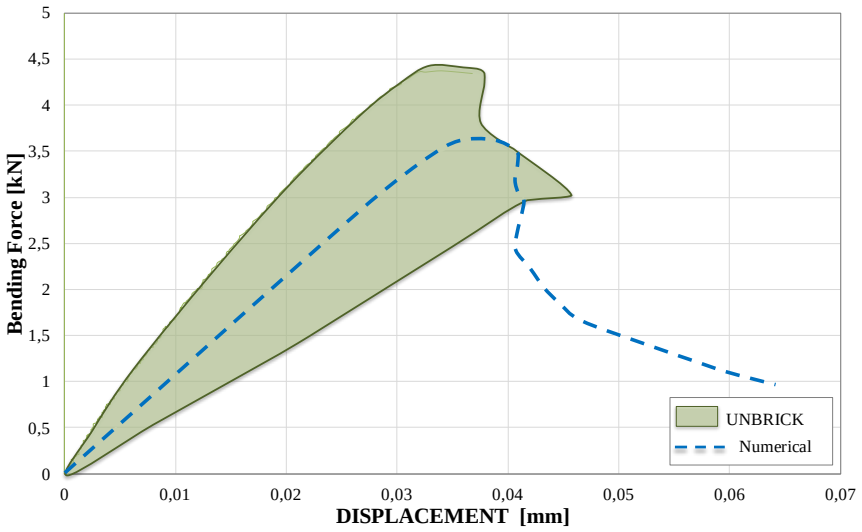

a)

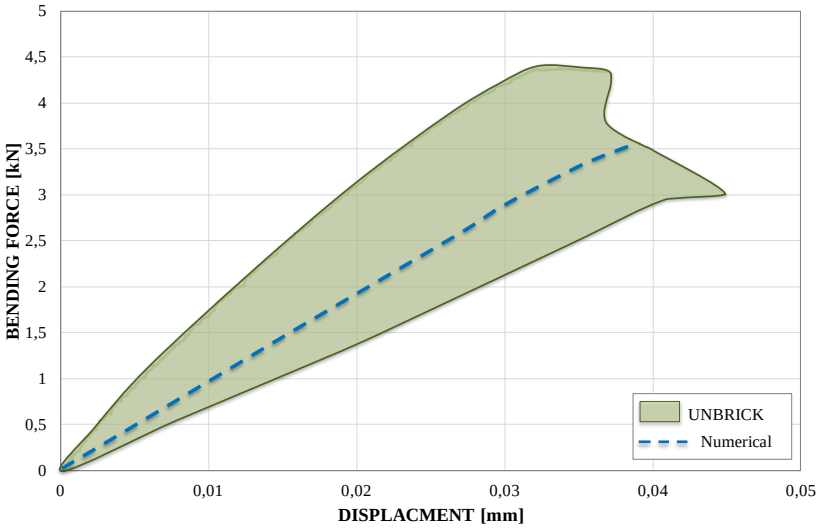

b)

Figure 5.11: Comparison of numerical and experimental force-relative displacement envelopes of unreinforced brick: a) crack bandwidth by default; b) crack bandwidth equal to 0,05mm

5.2.4 Load-displacement diagrams REBRICK

The numerical results obtained from nonlinear analysis on the reinforced brick, as specified previously, have been distinguished with respect the two different models used: Case 1 and Case 2.

Figure 5.12 shows the comparison between the numerical results obtained and the with the experimental ones, using flax fibers (fig. 5.12a) and hemp fibers (fig.5.12b) like a strengthening of the bricks using Case 1. As expected the curve represents the only mechanical behavior of the brick with a maximum value of force equal to 5,7 kN for the bricks strengthened with flax and 5,6 kN for the bricks strengthened with hemp, respect the maximum values achieved from experimental tests (6,5 kN for flax and 6,2 kN for hemp). The model is able to capture the pre-peak behavior and the load capacity, but the ductility exhibited during experiments was not reproduced numerically, also due to the fact that it was considered a crack bandwidth by default.

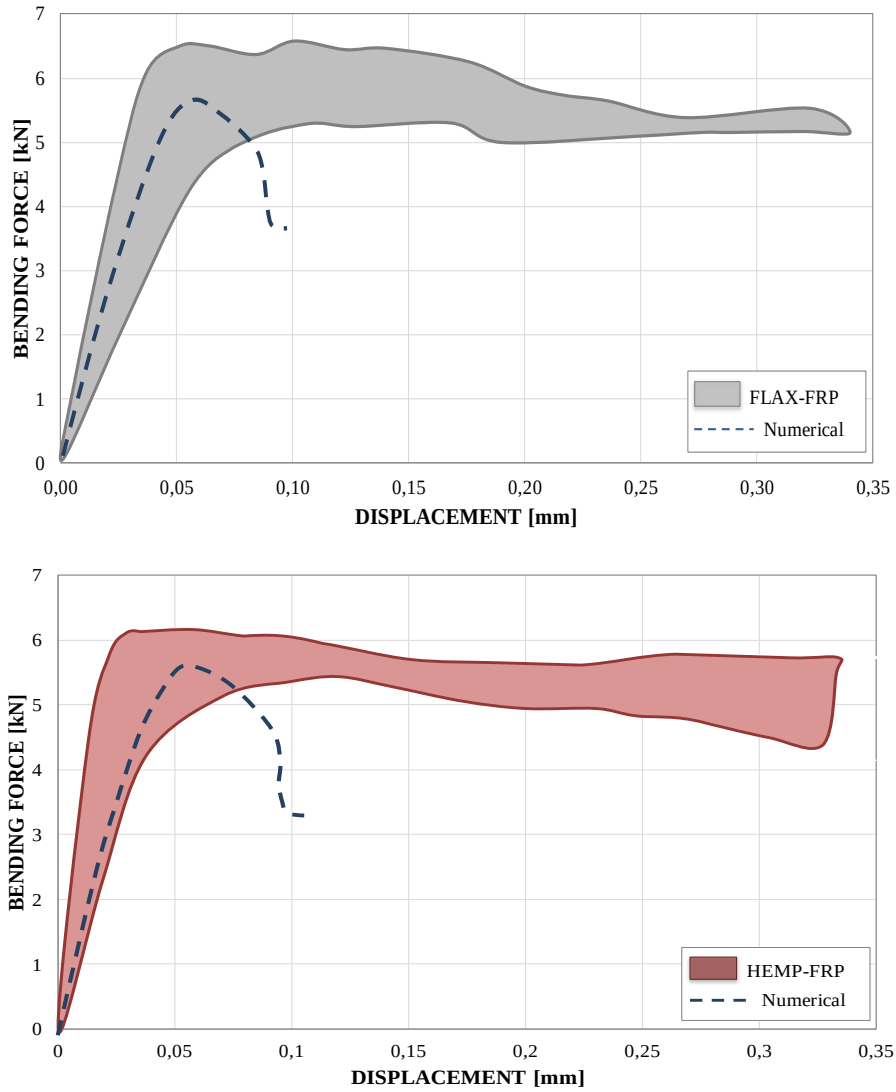

Figure 5.12: Comparison of numerical (CASE 1)and experimental bending force-relative displacement envelopes of reinforced brick: a) Flax fiber; b) Hemp fiber

Following the results obtained by considering the Case 1, was considered the Case 2. Figure 5.13 shows the comparison between the numerical and experimental results: flax fibers (fig. 5.13a) and hemp fibers (fig.5.13b). In this case, due to non-linear behavior assumed for both the materials used, the agreement between experimental and numerical responses can be considered satisfactory. On balance, it seems that the model is able to capture both the stiffness of the material, but also

the ductile behavior of the reinforced brick. A maximum value of the force equal to 5,8 kN for the bricks strengthened with flax and 5,7 kN for the bricks strengthened with hemp.

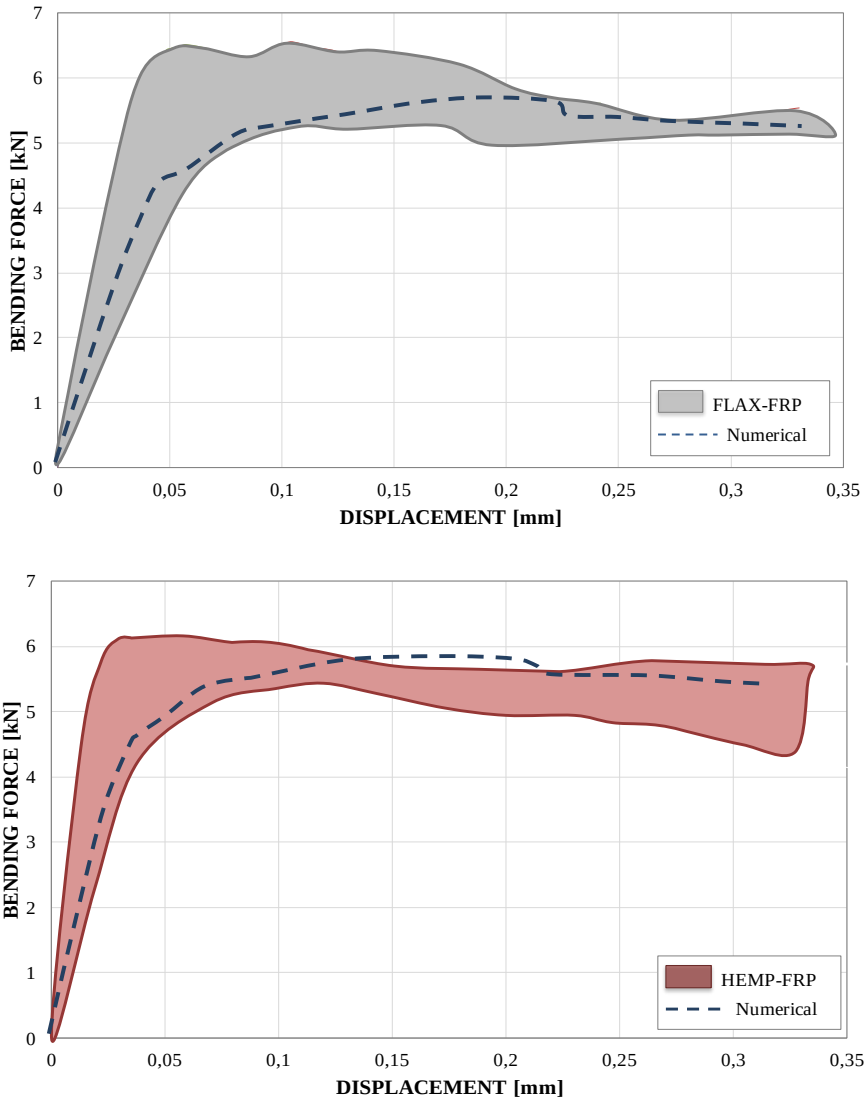

Figure 5.13: Comparison of numerical (CASE 2)and experimental bending force-relative displacement envelopes of reinforced brick: a) Flax fiber; b) Hemp fiber

5.2.5 Failure modes

Together with the global load-displacement response, a comparison in terms of the deformed mesh and failure pattern has been analyzed in order to appraise the quality of the numerical results: figure 5.14 show crack pattern near the Ultimate Limit State, both unreinforced brick (fig 5.14a) and reinforced brick (fig. 5.14b-Case1; fig. 5.14c-Case2), whereas figure 5.15 show the development of the stress for increasing deformation for the first and the last load step.

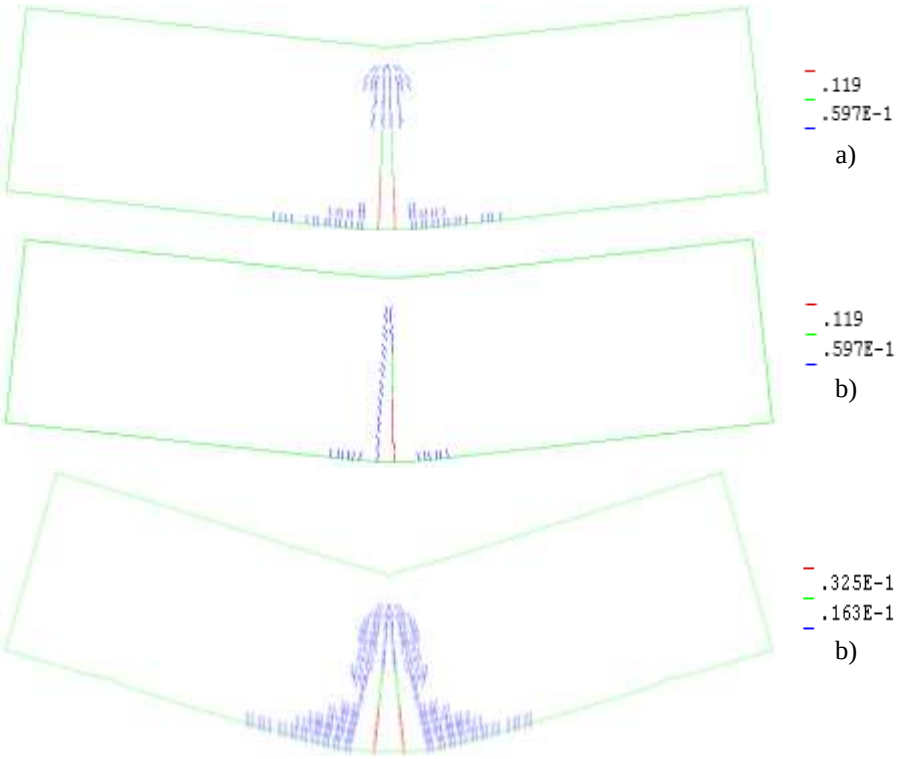

Figure 5.14: Crack pattern near the Ultimate Limit State:
a) Unreinforced brick; b) Reinforced brick, Case 1; c) Reinforced brick, Case 2

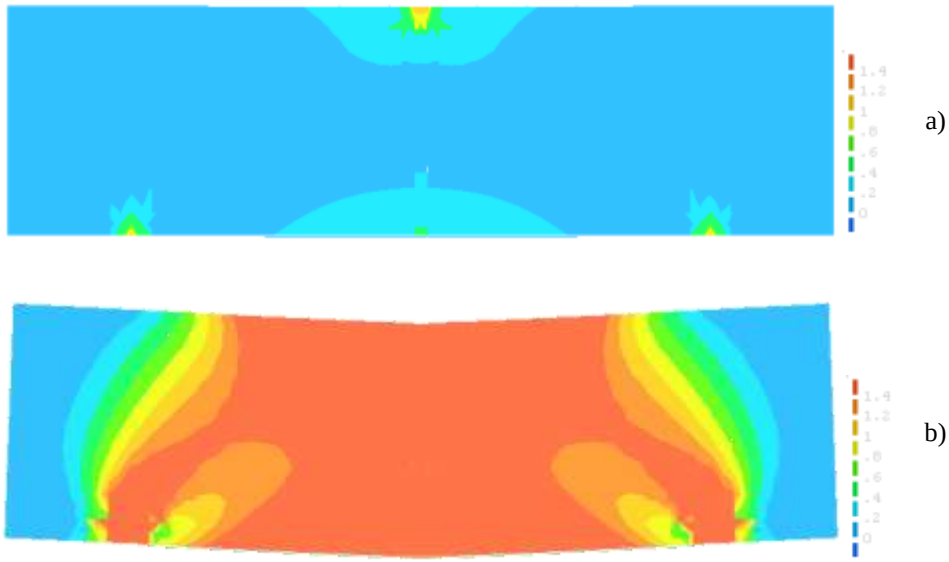

Figure 5.15: Nonlinear analysis: Von Mises equivalent stress on reinforced brick: a) First load step, b) Max load step

It is noticed that, in Case 1 the model is characterized by a lesser deformation than Case 2, due to the resistance of the NFRP strip and the assumption of its linear behavior; it follows a crack pattern more widespread in Case 2 than in Case 1, which involves into a reduced central portion of the brick. On the contrary in case of reinforced brick the crack pattern is concentrated in the central axis of the brick at the point of application of load.

6

CONCLUDING REMARKS

The present chapter reports a summary and a conclusion of the work done. The most significant contributions of this Phd thesis are the study of natural-fiber reinforced composites (NFRP or NFRG) and the new strengthening system for the ancient masonry using advance and innovative composites.

For the aim of this thesis, natural materials have been used like flax, hemp, jute, sisal and coir. All of these materials have been analyzed carrying out experimental tests. In the first part of the experimental program, tensile tests have been carried out in the laboratory on single yarns and non-impregnated fabrics. Each single yarn was measured and weighed in order to compute the linear density (Tex) and tenacity (N/tex) of the different materials. Analyzing the first results on the single yarns, it was possible to observe that flax and hemp are the materials that present higher values in terms of tensile strength, followed by sisal, jute and coir (fig. 6.1). Moreover, it was observed that the tensile strength of the fiber is inversely proportional to the linear density, in fact the coir fibers with a linear density equal to 2887 Tex is characterized by a tensile strength of 52MPa, as opposed to

198MPa of flax fibers (fig. 6.1). The failure mode of the yarns, was observed non homogeneous; this is due to the fact that the specimens are characterized by non-uniform diameters and above all they are natural materials. Consequently, in order to obtain 5 good results, with a failure mode in the middle of the specimens, a number between 10-15 specimens, for each type of material, were tested.

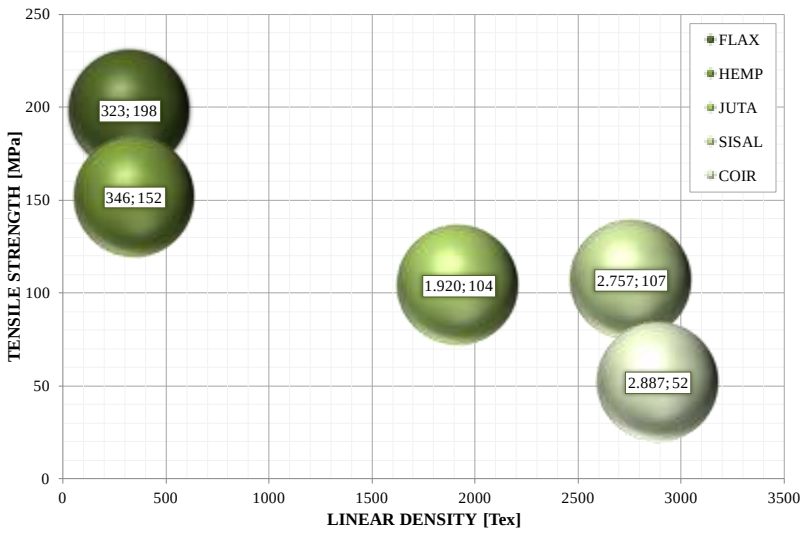

Figure 6.1: Linear density-Tensile strength diagram of single yarns of natural materials

From the results obtained from the tensile tests of non-impregnated fabrics it was possible to see that flax is, also in that case, confirming the results previously obtained, the material with higher mechanical properties, followed by jute and sisal. In this part of the experimental program, a total of seven bi-directional woven fabrics have been analyzed, two of these were mixed fabrics with the presence of different type of materials in warp or weft direction. Non-impregnated fabrics were studied both in warp and weft direction, in order to research the most resistant direction of the fabrics. The results showed that the stronger direction of the fabrics is the warp (90°) for all types of materials (fig. 6.2).

In the second part of the experimental program natural fiber-based composites (NFRP-NFRG) have been manufactured and tested. Three manufacturing methods were used to produce NFRP or NFRG: manual lay-up, vacuum infusion process and traditional technique with the use of steel formworks. The vacuum infusion process is the best manufacturing method for composites materials, especially because it is possible to achieve a uniform thickness of the composite and a uni-

form distribution of the matrix into the fibers. The manual lay-up is, most probably, the easier and faster method, but it is more difficult to obtain a uniform configuration of the composite. Regarding, instead, the composite materials mortar-based matrix, the use of the steel formworks represents the manufacturing method mostly used in civil engineering field.

From the results achieved from tensile tests on the three typologies of composites produced, it is clear that (fig. 6.2): impregnated fabrics with epoxy resin (NFRP) increase considerably the mechanical properties of composite systems based on natural fibers, presenting a tensile strength greater than the polyester resin, so consequently it can be stated that the epoxy resin is most suitable as a matrix of natural fiber composite materials. Concerning the fabrics with the mortar-based matrix (NFRG) further studies are still needed, especially regarding the thickness of the mortar that has to be applied to the specimen and the quantities of the water to consider in the composition of the mortar. However, during the tests it was possible to observe a good bond between natural materials and the different types of matrixes.

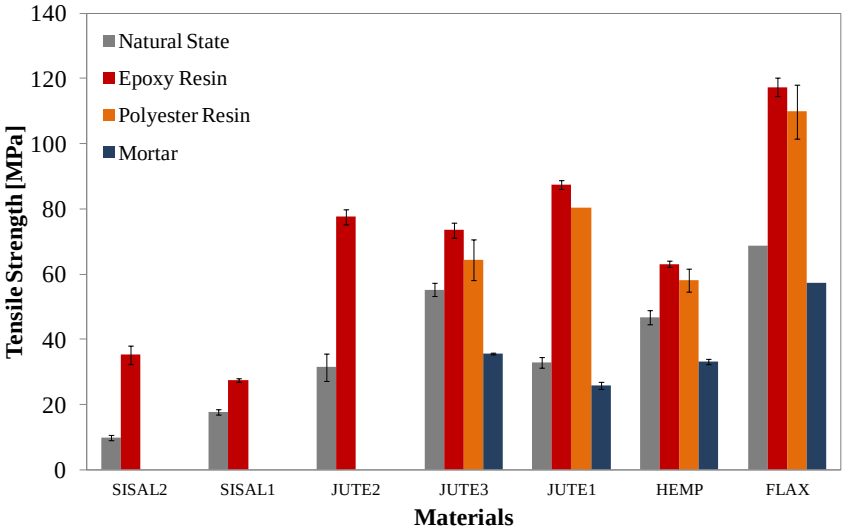

Figure 6.2: Tensile strength - Materials diagram

In addition, it is possible to say that natural fiber-based composite materials have a wide variety of mechanical properties. This is a consequence of the fact that the properties of natural materials are influenced by several variables, as the type of fiber, the diameter of the fibers, the environmental conditions and possible methods of fiber treatment. This is also confirmed by the variety of the results obtained and

shown in this work, especially in the case of tensile tests (fig. 6.2). However, the first data obtained, confirms the significant development that the natural materials are acquiring in function of their biodegradability, low cost, low relative density, adequate specific resistance and renewable nature.

To sum up, figure 6.2 highlights all the results achieved from the tensile tests carried out on the fabrics and composites cut in the warp direction. Initially all seven fabrics are tested in their non-impregnated configuration and with epoxy resin-based matrix, both in warp and weft direction. Afterwards, analyzing the results obtained and having prepared a list depending on the more resistant material, in terms of maximum load capacity and tensile strength, the composites based on the mortar and polyester resin were only produced with the four strongest materials. that is why in the figure sisal and jute fabrics were not considered in the second part of the experimental plan.

In the last part of the experimental plan, the bond behavior and adhesion between natural-fiber-based composites and masonry substrate have been researched, being the primary problem always present in case of masonry structures and thoroughly studied by many researchers. In particular, three point bending tests, pull-off result tests and single-lap shear bond tests have been carried out.

Three point bending tests on unreinforced solid clay bricks and on bricks externally strengthened with natural fiber reinforced polymer (NFRP) sheets have been carried out. Two different natural fibers have been used to strengthen the bricks: flax and hemp; and one type of matrix: epoxy resin. From the results achieved, it is clear that the reinforced bricks present more resistance, compared with unreinforced bricks, than expected. There is an increase of resistance of 30% in the case of NFRP flax-based fibers and of 28% in that of NFRP hemp-based fibers. In both cases, the same bond behavior and failure mode was observed; indeed, failure has occurred in a uniform way in the middle of the brick and of the fiber, ensuring a strong bond between the two materials.

Pull-out tests on bricks also externally reinforced with natural fiber reinforced polymer (NFRP) sheets have been carried out. In this case, the results indicate that the pull-out strength is practically independent from the fiber, in fact the same value of tensile bond strength can be observed. For all specimens tested, failure was characterized by the ripping of a thin layer of brick (peeling). Actually, the results show that the tensile strength of the interfaces depends on the tensile strength of the substrate, made of bricks, which is the weakest element of the composite system under direct tensile loading.

Single-lap shear bond tests on brick externally strengthened with composites mortar-base matrix and epoxy resin-based matrix. In order to build the specimens, the Italian standard has been considered. It is a technical document that was drawn up in accordance with the mechanical properties of carbon/glass fiber. This has led to some difficulties in the preparation of test specimens, having obtained a bond length much lower than what was usually obtained for the performance of these experimental tests. However, it was decided to carry out the tests using two different configurations in the case of NFRP based epoxy resin: the first with a bond length equal to 150mm and the second with a bond length equal to 75mm. In case of bricks reinforced with NFRG only one configuration (bond length = 150mm) has been used, due to practical problems related to laboratory. The results obtained from the tests carried out on specimens reinforced with resin, indicate that the design of the specimen is not suitable for natural materials. In fact the single-lap shear bond test has turned into a tensile test because in the specimen the failure occurred in un-bonded area, mainly in the composite. To confirm the validity of the tensile tests, previously carried out, a comparison in terms of maximum load has been made. The comparison gave a positive result, being the bond failure load lower than the tensile failure load. In case of bricks strengthened with NFRG, better results have been obtained, both in terms of failure modes and bond stress. The bond stress obtained is quite comparable with the values usually achieved from experimental tests carried out on bricks reinforced with carbon or glass based composites. Indeed, using flax and hemp fibers, a value of bond stress between 1-1.5 MPa has been reached, while in the case of carbon fibers, a value between 2-2.5 Mpa is usually obtained. The failure modes were divided into four typologies, that were achieved: 11% of rupture in the composite, 6% of cohesive failure in the brick, 61% cohesive fracture in the mortar and finally also in this case 22% of rupture into the fibers. Definitely a more detailed study should be done about this type of test, especially linked to the drafting of standards on natural fibers.

Finally, complementary to the experimental research described above, a numerical simulation of the three point bending test has been performed in order to further assess and compare the experimental results. The numerical analysis, based on plane stress conditions, was developed for the aim to investigate the bending behavior of unreinforced bricks and of composite materials (Hemp-FRP and Flax-FRP) applied to solid clay bricks. In particular a numerical simulation of the global behavior (bending force-relative displacement) has been researched. The proposed model, for the unreinforced brick, has been found in good agreement with the ex-

perimental results, both in terms of stiffness of the model and in terms of maximum force and cracking development. Regarding the reinforced brick, two numerical models have been considered: a model where the nonlinear properties were only applied to the brick, while for NFRP, a isotropic elastic behavior has been used; a model where the nonlinear properties have been applied both for brick and NFRP. The first model is proved to be suitable especially in terms of stiffness and maximum load, but the ductility behavior of the reinforced brick could not be captured. The second model, instead, due to nonlinear behavior assumed for both the materials used, the agreement between experimental and numerical responses can be considered satisfactory. Basically it seems that the model is able to capture both the stiffness of the material, but also the ductile behavior of the reinforced brick. Furthermore, also regarding the cracking development, the numerical model has reproduced the same crack progress as obtained from the experimental point of view, characterizing the central part of the specimen. Overall, comparable results have been achieved from numerical and experimental studies performed.

Furthermore, in appendix, a new fiber placement technology has been explained, the so-called "braiding technology". Braiding technique was used to produce natural fiber axially reinforced fibrous structures. This technique showed good mechanical properties of the single braids compared with the strength values obtained from single yarns or NFRP. Consequently, from the tensile test results obtained on fabrics produced with this technology, it is possible to say that braiding technology could ensure the resistance values greater than the common natural fiber fabrics.

References

[1] H. Ku , H. Wang, N. Pattarachaiyakoop, M. Trada, "A review on the tensile properties of natural fiber reinforced polymer composites", Composites: Part B, Volume 42, Issue 4, June 2011, Pages 856–873.

[2] Li X., Tabil L.G., Panigrahi S., Crerar WJ., "The influence of fiber content on properties of injection molded flax fiber-HDPE biocomposites", Can Biosyst Eng 2009;08–148:1–10.

[3] Malkapuram R, Kumar V., Yuvraj S.N., "Recent development in natural fibre reinforced polypropylene composites", J Reinf Plast Compos 2008;28:1169–89.

[4] P. Wambua, J. Ivens, I. Verpoest, *Natural fibres: can they replece glass in fibre reinforced plastics?*, ELSEVIER Composites Science and Technology, 63, 1259-1264 (2003).

[5] D. Foulk, D.E. Akin, R.B. Dodd, *New low cost flax fibers for composites*, SAE Technical paper number 2000-01-1133, SAE 2000 World Congress, Detroit, March 6-9 (2000).

[6] Ahmad I, Baharum A, Abdullah I., "Effect of extrusion rate and fiber loading on mechanical properties of Twaron fiber-thermoplastic natural rubber (TPNR) composites", J Reinf Plast Compos 2006;25:957–65.

[7] Xue Li, Lope G. Tabil, Satyanarayan Panigrahi, "Chemical Treatments of Natural Fiber for Use in Natural Fiber-Reinforced Composites: A Review", Journal of Polymers and the Environment, 04/2012; 15(1):25-33. doi:10.1007/s10924-006-0042-3.

[8] Omar Faruk, Andrzej K. Bledzki, Hans-Peter Fink, Mohini Sain, "Biocomposites reinforced with natural fibers: 2000–2010", Progress in Polymer Science, Volume 37, Issue 11, November 2012, Pages 1552–1596.

[9] D. Chandramohan, K. Marimuthu, "A review on natural fibers", International Journal of Research and Reviews in Applied Sciences, Vol. 8, Issue 2, Agosto 2011.

[10] Hoi-yan Cheung, Mei-po Ho, Kin-tak Lau, Francisco Cardona, David Hui, "Natural fibre-reinforced composites for bioengineering and environmental engineering applications", Composites: Part B, Volume 40, Aprile 2009, pag. 655-663.

[11] R. Fangueiro and F. Soutinho, "Textile structures", Fibrous and composite materials for civil engineering applications, Woodhead Publishing Series in Textiles: Number 104, Edited by R. Fangueiro, 2011.

[12] A. Carpintieri, "Meccanica dei materiali e della frattura", Ingegneria strutturale, Pitagora Editrice Bologna, 1992, IBSN 88-371-0543-6.

[13] Ben Brahim S, Ben Cheikh R., "Influence of fibre orientation and volume fraction on the tensile properties of unidirectional Alfa-polyester composite", Composites Science and Technology, 2007;67:140–7.

[14] Jacob M, Thomas S, Varughese KT, "Mechanical properties of sisal/oil palm hybrid fiber reinforced natural rubber composites", Composites Science and Technology 2004;64:955–65.

[15] Torulf Nilsson, "Flax and hemp fibres and their composites – A literature study of structure and mechanical properties", Report TVSM- 7139, Division of Structural Mechanics, Lund University, (2005).

[16] CNR, 2012. CNR-DT 200 R1/2012, Istruzioni per la Progettazione, l'Esecuzione ed il Controllo di Interventi di Consolidamento Statico mediante l'utilizzo di Compositi Fibrorinforzati – Materiali, Strutture di c.a. e di c.a.p., Strutture murarie, Consiglio Nazionale delle Ricerche.

[17] R. M. Rowell, "Natural fibers:types and properties", Properties and performance of natural-fiber composites, Edited by Kim L. Pickering, 2008, IBSN 978-1-85573-739-6.

[18] M. De Araújo, " Natural and man-made fi bres: Physical and mechanical properties", Fibrous and composite materials for civil engineering applica-

tions, Woodhead Publishing Series in Textiles: Number 104, Edited by R. Fangueiro, 2011.

[19] NP EN ISO 2062 "Textile yarn winding in the form of determination of strength of break and elongation at break".

[20] EN ISO 13934-1 and EN ISO 13934-2:1999, "Tensile properties of fabrics, Part 1: Determination of maximum force and elongation at maximum force using the strip method, Part 2: Determination of maximum force using the grab method".

[21] ISO 3374- 2000, Reinforcement products — Mats and fabrics — Determination of mass per unit area.

[22] BS EN 1015-11:1999 "Methods of test for mortar for masonry - Part 11: Determination of flexural and compressive strength of hardened mortar".

[23] ISO TC 71/SC 6 N - 2003, "Non-traditional reinforcing materials for concrete structures", Testing methods for fibre-reinforced cementitious composites/FRP reinforcement material specifications.

[24] UNI EN ISO 7500-1:2005, Materiali metallici - Verifica delle macchine di prova statica uniassiale - Parte 1: Macchine di prova a trazione/ compressione - Verifica e taratura del sistema di misurazione delle forze.

[25] W.D Brouwer, E.C.F.C van Herpt, M Labordus, "Vacuum injection moulding for large structural applications", Composites Part A: Applied Science and Manufacturing, Volume 34, Issue 6, June 2003, Pages 551‑558.

[26] Liubing Donga, Feng Houa, Yang Lib, Lei Wanga, Hongxu Gaoa, Yanlong Tanga, "Preparation of continuous carbon nanotube networks in carbon fiber/epoxy composite, "Composites Part A: Applied Science and Manufacturing", Volume 56, January 2014, Pages 248‑255.

[27] ASTM D4541-02 "Standard Test Method for Pull-Off Strength of Coatings Using Portable Adhesion Testers".

[28] A. Emami, E. Fehling, and M. Schlimmer, "External strengthening of masonry structures with natural fibers", XXXVII IAHS, Octobre 26-28, 2010, Santander (Cantabria). Spain.

[29] M.A. Aiello, S.M. Sciolti, "Bond Analysis of masonry structures strengthened with CFRP sheets", Construction and Building Material, Elsevier, Vol. 20, pp. 90-100, (2006).

[30] R.S. Olivito, F.A. Zuccarello, E. Milani, A. Tralli, "FRP reinforced bricks: delamination tests", Atti del Convegno IPMM 2007, Salerno, 25-29 Giugno (2007).

[31] R.S. Olivito, A. Venneri, F.A. Zuccarello, "An experimental equipment for delamination tests of FRP reinforced bricks", III Convegno Nazionale Meccanica delle Strutture in Muratura Rinforzate con Compositi (MURICO3), Venezia, 22-24 Aprile (2009).

[32] Bahman Ghiassi, Giancarlo Marcari, Daniel V. Oliveira, Paulo B. Lourenço, "Numerical study of the role of mortar joints in the bond behavior of FRP-strengthened masonry", Composites Part B: Engineering, Volume 46, March 2013, Pages 21–30.

[33] Bahman Ghiassi, Giancarlo Marcari, Daniel V. Oliveira, Paulo B. Lourenço, "Numerical analysis of bond behavior between masonry bricks and composite materials", Engineering Structures, Volume 43, 2012, pag. 210-220.

[34] ASTM D 792 – 98, Standard Test Methods for Density and Specific Gravity (Relative Density) of Plastics by Displacement.

[35] J. N. Reddy, "An introduction to the finite element method", McGraw-Hill Book Company, 1986.

[36] A. Rafiee, M. Vinches, C. Bohatier, Application of the NSCD method to analyse the dynamic behaviour of stone arched structures, International Journal of Solids and Structures, 45, 6269-6283 (2008).

[37] DIANA, Displacement analysis finite element software. V. 9.4, TNO Building Division, Delft, The Netherlands, 2009.

[38] Vecchio, F. J., and Collins, M. P."Compression response of cracked reinforced concrete" J. Str. Eng., ASCE 119, 12 (1993), 3590-3610.

[39] Lourenço, P.B., Almeida, J.C., Barros, J.A., "Experimental investigation of bricks under uniaxial tensile testing", Masonry International, 18(1), p.11-20 (2005).

[40] R. Fangueiro, *Textile structures. Fibrous and composite materials for civil engineering applications*. s.l. : Woodhead Publishing, (2011).

[41] R. Fangueiro, C. Gonilho Pereira, S. Jalali, M. Araujo, P. Marques, *Braided reinforced composite rods for the internal reinforcement of concrete,* Mechanics of Composite Materials, Vol. 44, No. 3, 2008.

[42] R. S. Olivito, R. Codispoti, F. A. Zuccarello, *Applicazione di materiali compositi in fibre naturali e malta cementizia a strutture murarie,* Atti del XX Congresso Nazionale Associazione Italiana di Maccanica Teorica ed Applicata (AIMETA), Bologna, Italia, (2011).

[43] F. Cunha, S. Rana, G. Vasconcelos, R. Fangueiro, S. Abreu, *Retrofitting masonry infill walls with novel fibrous structures,* ICDS12-International Conference Durable Structures: from construction to rehabilitation Lisbon, Portugal.

[44] Crisfiled M. A. "Non-linear finite element analysis of solid and structures", Volume 1, John Wiley & Sons, 1991.

---

[45] D.V. Oliveira, I. Basilio, I., P.B. Lourenço, *Experimental behavior of FRP strengthened masonry arches*, J. Compos. for Constr., 14(3), pp. 312-322 (2010).

[46] D.V. Oliveira, I. Basilio, P.B. Lourenço, *Experimental bond behavior of FRP sheets glued on brick masonry*, J. Compos. for Constr., 15(1), pp. 32-41 (2011).

[47] R. S. Olivito, R. Codispoti, F. A. Zuccarello, Applicazione di materiali compositi in fibre naturali e malta cementizia a strutture murarie, Atti del XX Congresso Nazionale Associazione Italiana di Maccanica Teorica ed Applicata (AIMETA), Bologna, Italia, (2011).

[48] R.Codispoti, D.V. Oliveira, R. Fangueiro, R.S. Olivito, P.B. Lourenço, Study on natural fiber based composites for strengthening of masonry structures, AIAS12- Conferenza nazionale analisi delle sollecitazioni, Vicenza, Italia, (2012).

[49] M. Giglio, A. Gilioli, A. Manes, Numerical investigation of a three point bending test on sandwich panels with aluminum skins and Nomex™ honeycomb core, Computational Materials Science 56 (2012) 69–78.

[50] R. Codispoti, D.V. Oliveira, R. Fangueiro, R.S. Olivito, P.B. Lourenço, "Experimental behavior of natural fiber-based composites used for strengthening masonry structures", International Conference on Natural Fibers, Guimaraes, Portugal, (2013).

[51] Rosamaria Codispoti, Daniel V. Oliveira, Renato S. Olivito, " Natural fibers based composites applied to masonry structures: experimental and numerical analysis", Atti del XX Congresso Nazionale Associazione Italiana di Maccanica Teorica ed Applicata (AIMETA), Torino, Italia, (2013).

[52] RILEM TECHNICAL COMMITTEE, "Round Robin Test for composite-to-brick shear bond characterization", Materials and Structures, Volume45, 2012, pag. 1761–1791, DOI 10.1617/s11527-012-9883-5

[53] D. V. Oliveira - Phd Thesis: "Experimenal and numerical analysis of blocky masonry structures under cyclic loading", Civil Engineering Department of University of Minho, January 2003.

[54] I. B. Sànchez - Phd Thesis: "Strengthening of arched masonry structures with composite materials", Civil Engineering Department of University of Minho, July 2003.

[55] W. Van Paepegem, K. De Geyter, P. Vanhooymissen, J. Degrieck, " Effect of friction on the hysteresis loops from three-point bending fatigue tests of fibre-reinforced composites", Composite Structures, Volume 72, 2006, pag. 212–217

[56] R. Capozzucca, " Experimental FRP/SRP–historic masonry delamination", Composite Structures, Volume 92, 2010, pag 891–903.

[57] M.R. Valluzzi*, D. Tinazzi, C. Modena, "Shear behavior of masonry panels strengthened by FRP laminates", Construction and Building Materials, Volume 16, 2002, pag. 409–416.

[58] Ernesto Grande, Maura Imbimbo, Elio Sacco, "Bond behaviour of CFRP laminates glued on clay bricks: Experimental and numerical study", Composites: Part B, Volume 42, 2011, pag. 330–340.

[59] M. Ramesh, K. Palanikumar , K. Hemachandra Reddy, "Mechanical property evaluation of sisal–jute–glass fiber reinforced polyester composites", Composites: Part B, Volume 48, 2013, pag. 1–9.

[60] A. D'Ambrisi, L. Feo, F. Focacci, "Experimental and analytical investigation on bond between carbon-FRCM materials and masonry", Composites: Part B, Volume 46, 2013, pag. 15–20.

[61] R. S. Ying Wong - PhD thesis, " Towards modelling of reinforced concrete members with externally-bonded fibre reinforced polymer (frp) composites", Department of Civil Engineering, University of Toronto, 2001.

APPENDIX

BRAIDING TECHNOLOGY

Braiding technique was used to produce natural fiber axially reinforced fibrous structures [40-41]. This technique has been used for two centuries and is being increasingly used in technical applications. The braided architecture has greater ability of twisting, shearing and impact than woven fabrics, combined with low cost fabrication routes. The technique consists in the braiding in the transverse and longitudinal directions forming a tubular structure. The external yarns rotate in two opposite orientations, anticlockwise and clockwise direction. The stability of the braided structure depends on the detailed fiber architecture and above all on the angle formed between the longitudinal axis and the direction of insertion of the braiding yarns; its dimension can be different according to the braiding yarn diameter, diameter of the axial structures and of the circulation velocity.

A.1 Testing procedure and results

The braided fibrous structures were produced in a vertical braiding machine (figure A.2). The machine worked with 16 bobbins of cotton braiding and the braids obtained have a regular structure (triaxial braid), in a tubular form of biaxial yarn direction. In the centre of the tubular braid additional fibers (axial yarns) were inlaid. In particular braids with 1-2-4-8 axial yarns were produced (figure A.3) and tensile tests were carried out [42-43]. Two different types of sisal fibers were used,

later on called Sisal_1 and Sisal_2 (fig. A.1), with different values of linear density (TEX). Before to manufacture the specimens braids in laboratory, mechanical characterization tests have been carried out on the single yarns, in order to calculate the tensile strength and Young's modulus (table A.I). A total of 7 specimens for each number of axial yarns were tested. Before each test, a pre-load of 1,5N was applied and a crosshead speed equal to 250mm/min was used. Table A.II summarizes the results obtained.

a) b)

Figure A.1: Different types of material used to produce braids: a) Sisal_1; b)Sisal_2

Table A.I

Average values obtained from tensile tests on single yarns

		Linear Density	**A**	**ft**	**E**
		[Tex]	[mm^2]	[MPa]	[Mpa]
Sisal_1	*Average*	377,72	0,54	203,54	2979,2
	CoV	11%	9%	11%	20%
Sisal_2	*Average*	1856,95	2,25	167,26	3131,9
	CoV	19%	21%	16%	9%

a) b) c)

Figure A.2: (a) Braiding yarns; (b) Axial yarns; (c) Braiding process

The breaking load of produced braided yarns increases linearly with the number of axial sisal yarns as well as with the linear density of braids. Therefore, it is quite easy to produce a braded yarn with required tensile strength by adjusting the number of axial sisal yarns (figure A.4-A.5).

Figure A.3: Braiding process

Table A.II
Average values obtained from tensile tests on braids

Material	n° axial yarns	Linear Density [Tex]	ft [MPa]	Tenacity [N/Tex]	ε_{peak} [%]	E [MPa]
Sisal_1	1	310,5	175,38	0,2702	4,82	3650,39
	2	621	81,74	0,2607	5,47	1493,42
	4	1242	19,18	0,2613	6,27	306,29
	8	2484	11,89	0,1942	6,530	182,002
Sisal_2	1	2910,8	105,65	0,1847	6,44	1655,08
	2	4383,5	71,13	0,1604	5,44	1312,07
	4	8719,5	22,74	0,1436	6,05	376,76
	8	16904,2	10,24	0,1246	5,86	174,91

The technique of braiding technology showed good mechanical properties of the single braids compared with the strength values obtained from NFRP. Consequently fabrics produced with this technology could ensure the resistance values greater than the common natural fiber fabrics.

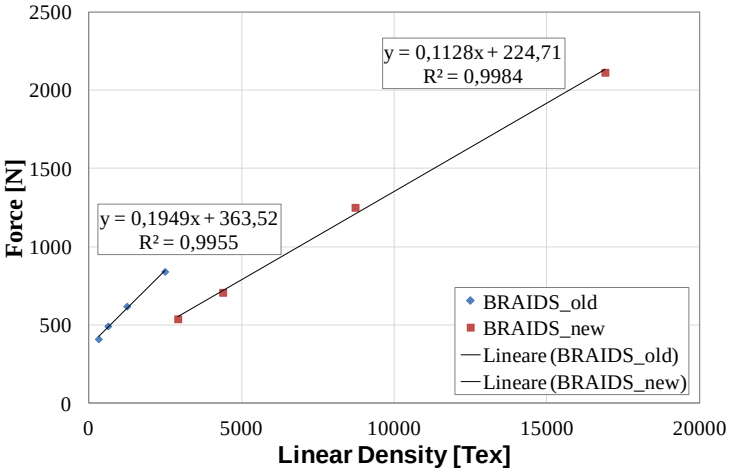

Figure A.4: Linear Density - Force Diagram on Braids

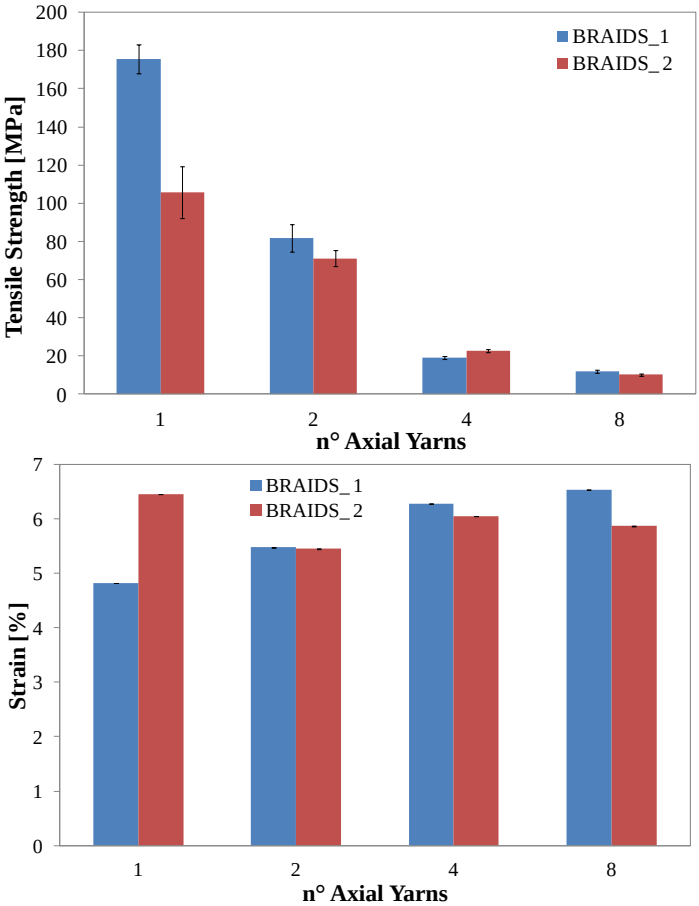

Figure A.5: Tensile strength/Strain - n° Axial Yarns Diagr